



**Calhoun: The NPS Institutional Archive**  
**DSpace Repository**

---

Theses and Dissertations

1. Thesis and Dissertation Collection, all items

---

1990

# Validation of the Schwartz and Hon algorithm at low grazing angles

Lawler, Gregory M.

Monterey, California. Naval Postgraduate School

---

<http://hdl.handle.net/10945/37564>

*Downloaded from NPS Archive: Calhoun*



Calhoun is a project of the Dudley Knox Library at NPS, furthering the precepts and goals of open government and government transparency. All information contained herein has been approved for release by the NPS Public Affairs Officer.

**Dudley Knox Library / Naval Postgraduate School**  
**411 Dyer Road / 1 University Circle**  
**Monterey, California USA 93943**

<http://www.nps.edu/library>

NPS-61-90-006

# NAVAL POSTGRADUATE SCHOOL

## Monterey, California

AD-A238 162



DTIC  
ELECTE  
JUL 15 1991  
S B D

## THESIS

VALIDATION OF THE SCHWARTZ AND HON ALGORITHM  
AT LOW GRAZING ANGLES

by

Gregory M. Lawler

September 1990

Thesis Advisor: Alfred W. Cooper

Approved for public release; distribution is unlimited

Prepared for:

NOARL - Atmospheric Directorate

Monterey, California 93943-5000

91-04976



91 / 104

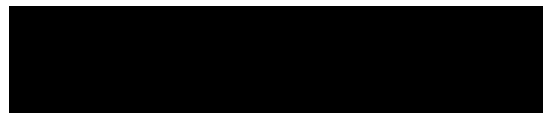
Rear Admiral R. W. West  
Superintendent

Harrison Schull  
Provost

This thesis is prepared in conjunction with research sponsored in part by the Naval Oceanographic & Atmospheric Research Laboratory (NOARL) under funding document N6846290WR00013 assigned to the Naval Academic Center for Infrared Technology (NACIT).

Reproduction of all or part of this report is authorized.

Released by:



Gordon E. Schacher  
Dean of Faculty and  
Graduate Studies

UNCLASSIFIED

SECURITY CLASSIFICATION OF THIS PAGE

REPORT DOCUMENTATION PAGE				Form Approved OMB No. 0704-0188	
1a. REPORT SECURITY CLASSIFICATION <b>UNCLASSIFIED</b>			1b. RESTRICTIVE MARKINGS		
2a. SECURITY CLASSIFICATION AUTHORITY			3. DISTRIBUTION/AVAILABILITY OF REPORT Approved for public release; Distribution is unlimited		
2b. DECLASSIFICATION/DOWNGRADING SCHEDULE					
4. PERFORMING ORGANIZATION REPORT NUMBER(S) <b>NPS-61-90-006</b>			5. MONITORING ORGANIZATION REPORT NUMBER(S)		
6a. NAME OF PERFORMING ORGANIZATION <b>Naval Postgraduate School</b>		6b. OFFICE SYMBOL (If applicable) <b>PH</b>	7a. NAME OF MONITORING ORGANIZATION <b>NOARL-Atmospheric Directorate</b>		
6c. ADDRESS (City, State, and ZIP Code) <b>Monterey, California 93943-5000</b>			7b. ADDRESS (City, State, and ZIP Code) <b>Monterey, California 93943-5000</b>		
8a. NAME OF FUNDING/SPONSORING ORGANIZATION		8b. OFFICE SYMBOL (If applicable)	9. PROCUREMENT INSTRUMENT IDENTIFICATION NUMBER		
8c. ADDRESS (City, State, and ZIP Code)			10. SOURCE OF FUNDING NUMBERS		
			PROGRAM ELEMENT NO.	PROJECT NO.	TASK NO.
11. TITLE (Include Security Classification) <b>VALIDATION OF THE SCHWARTZ-HON ALGORITHM AT LOW GRAZING ANGLES</b>					
12. PERSONAL AUTHOR(S) <b>Lawler, Gregory M.</b>					
13a. TYPE OF REPORT <b>Master's Thesis</b>		13b. TIME COVERED FROM _____ TO _____		14. DATE OF REPORT (Year, Month, Day) <b>1990, September 15</b>	
15. PAGE COUNT <b>118</b>					
16. SUPPLEMENTARY NOTATION This work was supported by the Naval Oceanographic & Atmospheric Research Laboratory (NOARL) and carried out at the Academic Center for Infrared Technology under Naval Postgraduate School Direct Funding					
17. COSATI CODES			18. SUBJECT TERMS (Continue on reverse if necessary and identify by block number) thermal radiation, emissivity, blackbody radiators, background radiance, computer code, LOWTRAN 6, computer code PC-TRAN, AGA 780 system, Schwartz-Hon model, Fortran code, AGACAT program		
FIELD	GROUP	SUB-GROUP			
19. ABSTRACT (Continue on reverse if necessary and identify by block number)  An experimental validation of the Schwartz-Hon computer code for emissivity of the rough sea surface in the grazing angle region was carried out using an AGEMA 780 thermovision radiometric sensor. The experimental measurements were made in Monterey Bay using a meteorological suite mounted on the Research Vessel <i>Point Sur</i> , with coordinated radiosonde launches. Predicted sea surface radiance was computed from reflected sky radiance and thermal sea emission, using the Schwartz-Hon algorithm for sea emissivity and equivalent specular incidence angle. PC-TRAN in radiance mode was used to compute the sky radiance, and compared with AGEMA measurements. AGEMA sea radiance measurements were compared with the model predictions as a function of observation angle and were found to agree within 8% for elevation angles from zero to 5 degrees. PC-TRAN sky radiance computations for the grazing angle region agreed with AGEMA measurements within approximately 12%.					
20. DISTRIBUTION/AVAILABILITY OF ABSTRACT <input checked="" type="checkbox"/> UNCLASSIFIED/UNLIMITED <input type="checkbox"/> SAME AS RPT <input type="checkbox"/> DTIC USERS			21. ABSTRACT SECURITY CLASSIFICATION <b>UNCLASSIFIED</b>		
22a. NAME OF RESPONSIBLE INDIVIDUAL <b>Alfred W. Cooper</b>			22b. TELEPHONE (Include Area Code) <b>646-3008</b>		22c. OFFICE SYMBOL <b>PHCr</b>

DD Form 1473, JUN 86

Previous editions are obsolete.

SECURITY CLASSIFICATION OF THIS PAGE

S/N 0102-LF-014-6603

UNCLASSIFIED

# Validation of the Schwartz and Hon Algorithm at Low Grazing Angles

by

Gregory M. Lawler  
Lieutenant, U.S. Navy  
B. A., United States Naval Academy, 1982

Submitted in partial fulfillment of the  
requirements for the degree of

MASTER OF SCIENCE IN SYSTEMS ENGINEERING

from the


NAVAL POSTGRADUATE SCHOOL


September, 1990


Author:

  
Gregory M. Lawler

Approved by:

  
Alfred W. Cooper, Thesis Advisor

  
E. A. Milne, Second Reader

  
Joseph Sternberg, Chairman  
Electronic Warfare Academic Group

# ABSTRACT

An experimental validation of the Schwartz-Hon computer code for emissivity of the rough sea surface in the grazing angle region was carried out using an AGEMA 780 thermovision radiometric sensor. The experimental measurements were made in Monterey Bay using a meteorological suite mounted on the Research Vessel *Point Sur*, with coordinated radiosonde launches. Predicted sea surface radiance was computed from reflected sky radiance and thermal sea emission, using the Schwartz-Hon algorithm for sea emissivity and equivalent specular incidence angle. PC-TRAN in radiance mode was used to compute the sky radiance, and compared with AGEMA measurements. AGEMA sea radiance measurements were compared with the model predictions as a function of observation angle and were found to agree within 8% for elevation angles from zero to 5 degrees. PC-TRAN sky radiance computations for the grazing angle region agreed with AGEMA measurements within approximately 12%.

<b>Accession For</b>	
NTIS GRA&I	<input checked="checked" type="checkbox"/>
DTIC TAB	<input type="checkbox"/>
Unannounced	<input type="checkbox"/>
Justification	
By	
Distribution/	
Availability Codes	
Dist	Avail and/or Special
A-1	



# TABLE OF CONTENTS

I.	INTRODUCTION . . . . .	1
	A. GENERAL . . . . .	1
	B. RELATED WORK . . . . .	2
	C. ORIGINAL AREA OF THESIS RESEARCH . . . . .	2
	D. PURPOSE AND ORGANIZATION OF THESIS . . . . .	3
II.	THEORY AND BACKGROUND . . . . .	4
	A. THE INFRARED SPECTRUM . . . . .	4
	B. RADIATION QUANTITIES-LAWS . . . . .	5
	1. Planck's Blackbody Radiation Law . . . . .	5
	2. Stefan-Boltzmann Relation . . . . .	6
	3. Lambert-Beer Law . . . . .	6
	4. Absorption and Scattering . . . . .	6
	5. Radiation Contrast . . . . .	7
	6. Effective Sea Surface Radiance . . . . .	9
III.	AGA 780 THERMOVISION SCANNER . . . . .	11
	A. INTRODUCTION . . . . .	11
	B. DESCRIPTION OF THE SYSTEM . . . . .	11
	1. Electro-Optic Scanning Mechanism . . . . .	11
	2. Optics . . . . .	12
	3. Black and White Monitor Chassis and Color Monitor . . . . .	12
	4. Computer and Software Package . . . . .	13
	C. THERMAL MEASUREMENT TECHNIQUES . . . . .	15
	1. Relative Measurement . . . . .	15
	2. Direct Measurement . . . . .	15

IV.	VALIDATION OF THE SCHWARTZ-HON MODEL . . . . .	17
A.	SCHWARTZ-HON MODEL . . . . .	17
1.	Computer Program-EMISS (Schwartz-Hon) . . . . .	18
2.	Shapiro Algorithm in EMISS . . . . .	19
3.	PC-TRAN and LOWTRAN 6 . . . . .	20
B.	EXPERIMENTAL VALIDATION OF THE SCHWARTZ-HON SEA RADIANCE MODEL . . . . .	21
1.	Introduction . . . . .	21
2.	Meteorological Conditions . . . . .	21
C.	EXPERIMENTAL PROCEDURE . . . . .	21
1.	Correlation of Physical Horizon with the Computer Display .	22
2.	Measurements . . . . .	23
D.	DATA COLLECTION . . . . .	24
1.	Meteorological Data . . . . .	24
2.	$\theta_V$ : View Angle Measurement . . . . .	24
3.	$\theta_i$ and $\theta_R$ View Angle Measurement . . . . .	25
4.	$S_{sky}$ and $L_{SST}$ Measurement . . . . .	25
5.	$L_{SSE}$ and $T_{BR}$ Measurement . . . . .	26
6.	In-Band Blackbody Temperature ( $T_{BB}$ ) . . . . .	26
7.	$L_{SSC}$ and $L_{SSM}$ Measurement . . . . .	27
8.	$T_{SSC}$ and $T_{SSM}$ Measurement . . . . .	28
V.	DATA ANALYSIS, RECOMMENDATIONS AND CONCLUSIONS . .	29
A.	INTRODUCTION . . . . .	29
1.	PC-TRAN Inputs . . . . .	29
2.	Validation of the Schwartz-Hon Model . . . . .	29
B.	DATA ANALYSIS AND RESULTS . . . . .	30



1. Sky Radiance Comparison . . . . .	31
2. Schwartz-Hon Validation . . . . .	31
3. Shapiro Validation . . . . .	32
4. Recommendations and Conclusions . . . . .	33
APPENDIX A - FIGURES . . . . .	34
APPENDIX B - TABLES . . . . .	55
APPENDIX C - ATTEMPTED COMPARISON OF OPERATIONAL FLIR RANGE WITH TDA PREDICTIONS . . . . .	82
APPENDIX D - LISTING OF MICROSOFT FORTRAN PROGRAM: AGACATS . . . . .	85
APPENDIX E - EMISSIVITY MEASUREMENTS OF THE RESEARCH VESSEL <i>POINT SUR</i> . . . . .	99
LIST OF REFERENCES . . . . .	105
INITIAL DISTRIBUTION LIST . . . . .	106

## ACKNOWLEDGEMENTS

The work on this thesis was sponsored by the Naval Oceanographic & Atmospheric Research Laboratory (NOARL) in conjunction with SPAWAR and the Naval Postgraduate School. The technical assistance of Mr. Mike Sierchio and the operational assistance of Mr. John Cook of NOARL is greatly acknowledged. I wish to thank Professor A. W. Cooper of the Naval Academic Center for Infrared Training (NACIT), who took time out of his busy schedule to provide me with individual tutoring and background for this thesis. I would also like to acknowledge the technical assistance provided by Mr. Eric Moore, Mr. Bob Sanders, Dr. Phil Walker, Capt Joseph Murray, USMC, and the Naval Postgraduate School Meteorology Department. I deeply appreciate the assistance of Professor E. Milne on the subject of computer programming as well as his assistance in proofreading this work.

# I. INTRODUCTION

## A. GENERAL

In recent years, the United States Navy has developed and deployed a large number of optical and infrared devices for use on surface ships and aircraft. These systems are used for target detection, recognition, intelligence gathering, and weapon deployment. Performance of these systems may be degraded significantly by signal attenuation due to atmospheric absorption, precipitation, aerosols, fog, and clouds. System design is further complicated by the fact that potential targets interact with the environment so that the expected infrared contrast of the target relative to its background may be difficult to measure. To predict performance of any infrared detection system, it is necessary to know not only something of the target's signature but also the background.

An infrared system model can be divided into three major areas. The first describes the difference between target temperature and the ambient temperature surrounding it. From performance runs on actual targets, differences between target and ambient temperatures are compared and a resulting temperature difference is determined ( $\Delta T$ ). The second component of the system describes the varied effects the atmosphere has on infrared transmission. These effects include reflection, refraction, absorption, and scattering. The third and final component describes the performance characteristics of the actual infrared measuring device. These include system parameters such as spectral bandwidth and minimum resolvable temperature difference. Within each of these components, complex computer algorithms have been developed to simulate and accurately describe atmospheric effects on sensor performance [Ref. 2: p. 1-8].

## **B. RELATED WORK**

Currently, there is a great deal of work being done to improve computer algorithms used for predicting infrared performance. Previous work in this area at the Naval Postgraduate School includes LT Mark Ridgeway's look at sea surface emissivity models for use in forward looking infrared (FLIR) tactical decision aids [Ref 3] and Maj Panagiotis Psihogios' studies of thermal imaging of sky and sea surface background infrared radiation [Ref. 4].

This thesis will deal with the results of a computer model (The Ira B. Schwartz and David Hon Model) used to generate a synthetic surface as a function of wind speed and viewing angle and compute its effect on the average emissivity of the ocean surface. Of particular importance is the fact that ocean surface roughness is a function of wind speed and this determines the emissivity of the ocean surface [Ref. 1: p. 1]. Since the emissivity of a water surface is angle dependent, one needs to know the geometry of the ocean surface at any given time. The Schwartz-Hon model predicts average emissivity at specific view angles and wind speeds; however, the capacity of the model to predict emissivity at low grazing angles is still unproven.

## **C. ORIGINAL AREA OF THESIS RESEARCH**

The original area of this thesis research effort was to be the experimental validation of FLIR tactical decision aids for use by patrol aircraft. Equipment failure and weather constraints hampered this effort and newly acquired data will instead be applied to existing algorithms where suspected deficiencies exist in modeling. The experimental plan devised and the difficulties encountered are described in Appendix C.

## D. PURPOSE AND ORGANIZATION OF THESIS

This thesis will describe an experiment to validate the Schwartz-Hon algorithm for sea surface emissivity and sky radiance incident on the ocean surface at low grazing angles beyond the previously validated range of the model. Thermal images of sky and sea background radiance were taken with an AGEMA 780 Thermovision Imaging System and were compared to apparent sky radiance predicted by the propagation/radiance code LOWTRAN 6. In order to simulate the viewing angle of a patrolling aircraft flight path or a surface ship sensor, grazing angles on the order of  $1^{\circ}$ – $5^{\circ}$  were used.

The present work consists of five chapters including the introduction. The thesis is organized as follows:

- A. Chapter I - Introduction
- B. Chapter II - Theory and Background: Thermal radiation theory, equations used in validation of model and experimental background.
- C. Chapter III - Equipment: Describes equipment and measurement techniques.
- D. Chapter IV - The Schwartz-Hon Model: Describes the procedure for validation of the Schwartz-Hon model.
- E. Chapter V - Summary, conclusions, and recommendations for further study in this area.
- F. Appendixes A and B are figures and tables.
- G. Appendix C is a description of the original area of thesis research.
- H. Appendix D is a listing of the computer program AGACATS, written in FORTRAN and compiled with microsoft FORTRAN V.
- I. Appendix E describes an experimental measurement of the emissivity of the R/V *Point Sur*.

## II. THEORY AND BACKGROUND

### A. THE INFRARED SPECTRUM

Every object with a temperature other than absolute zero emits what is known as thermal radiation. A thermal radiator emits energy due to its temperature and for objects at ambient temperatures this emission is concentrated mainly in the infrared region of the electromagnetic spectrum. This band is bounded on one side by the visible region at a wavelength of approximately  $.7 \mu\text{m}$  and on the other by the millimeter waveband at  $1000 \mu\text{m}$ . The infrared spectrum is broken down into the near infrared ( $.70\text{--}3 \mu\text{m}$ ), middle infrared ( $3\text{--}6 \mu\text{m}$ ) and the far infrared ( $6\text{--}15 \mu\text{m}$ ) region.

The ability of an infrared system to detect a target is dependent on many factors affecting the apparent target to background temperature difference. The atmosphere is characterized by transmitting windows whose spectral location restricts the choice of detector and optical material. Figure 2.1 shows the relationship between wavelength and transmittance in the  $.3$  to  $14 \mu\text{m}$  wavelength region for a 6000 ft horizontal path at sea level [Ref. 5: p. 115]. IR imaging systems can be severely degraded by high humidity or poor visibility. The  $3\text{--}5 \mu\text{m}$  window is superior in transmittance on clear, humid days while hazy, dry days favor the  $8\text{--}12 \mu\text{m}$  [Ref. 5: p. 114–141]. The AGA 780 Thermovision camera used to collect data in this experiment is able to detect IR radiation in both windows. This section is devoted to the basic concepts and mathematical relations used to describe and analyze thermal imaging systems.

## B. RADIATION QUANTITIES – LAWS

The following thermal radiation laws and equations are used in validating the Schwartz-Hon algorithm. All equations are taken from Hudson [Ref. 5: p. 35–64] and Lloyd [Ref. 6: p. 1–55].

### 1. Planck's Blackbody Radiation Law

Planck's Law describes the spectral distribution with which all objects with a temperature above 0° Kelvin radiate or emit energy in the electro-magnetic spectrum. The intensity with which a body radiates at each wavelength in the electromagnetic spectrum is the spectral brightness of the blackbody. The blackbody emits and absorbs the maximum theoretically available amount of thermal radiation at a given temperature. The spectral radiant emittance is a function of the temperature and wavelength and is shown in the following equation:

$$B_{\lambda} = (2hc^2)/(\lambda^5[\exp(hc/kT\lambda)] - 1) \text{ Watts}/m^3 \quad (2.1)$$

$\lambda$  = Wavelength (m)

$k$  = Boltzmann's constant ( $J \cdot K^{-1}$ )

$c$  = Speed of light (m/s)

$h$  = Planck's constant ( $J \cdot s^{-1}$ )

$T$  = Temperature (K)

Planck's Law is fundamental for all forward looking infrared systems and holds throughout the entire electromagnetic spectrum. Figure 2.2 shows the spectral radiant emittance of a blackbody at various temperatures, ranging from 500° to 900° Kelvin [Ref. 5: p. 36].

## 2. Stefan-Boltzmann Relation

The Stefan-Boltzmann relationship expresses the total radiant emittance,  $B$ , by integrating  $B_\lambda$  over all the wavelengths in Equation (2.1). The relationship that remains after integration is:

$$B = \sigma T^4 \quad (2.2)$$

$B$  = Radiant emittance (Watts/m<sup>2</sup>)

$\sigma$  = Stefan-Boltzmann constant ( $5.67 * 10^{-8}$ ) (Watts/m<sup>2</sup>K<sup>4</sup>)  
=  $(2\pi^5 k^4)/(15c^2 h^3)$

## 3. Lambert-Beer Law

Every object with a temperature greater than absolute zero emits thermal energy. Atmospheric transmittance at a specific wavelength for a specific set of atmospheric conditions can be described by an equation known as the Lambert-Beer Law:

$$\tau_A(\lambda) = \exp(-\mu(\lambda)R) \quad (2.3)$$

$R$  = Range or path length

$\mu$  = Extinction coefficient

$\lambda$  = Specific wavelength

For the purposes of these experiments, we will primarily be interested in a narrow range of wavelengths in the infrared region of the electromagnetic spectrum from 8 to 12  $\mu\text{m}$ .

## 4. Absorption and Scattering

Two processes which attenuate infrared energy as it propagates through the atmosphere are absorption and scattering. Thermal radiation is attenuated in



the atmosphere by absorption by gas molecules, scattering by molecular clusters (aerosols), aerosol absorption and molecular scattering. The total extinction coefficient is the sum of the coefficients for total absorption and total non-forward scattering. Water, carbon dioxide, and ozone are the most significant absorbers of this radiation and are described in the following equations:

$$\mu = \mu_A + \mu_S \quad (2.4)$$

$\mu$  = Total extinction coefficient

$\mu_A$  = Extinction coefficient for total absorption

$\mu_S$  = Extinction coefficient for scattering

Scattering and absorption may further be broken down into categories according to their causes:

$$\mu_A = k_m + k_A \quad (2.5)$$

$$\mu_S = \sigma_m + \sigma_A \quad (2.6)$$

$k_m$  = Molecular absorption coefficient

$k_n$  = Aerosol absorption coefficient

$\sigma_m$  = Molecular scattering coefficient

$\sigma_A$  = Aerosol scattering coefficient

## 5. Radiation Contrast

The AGA Thermovision camera operates on the concept of radiation contrast which is defined as the ratio of the difference between target and background radiant emittance to their sum [Ref. 7: p. 10.1].

$$C_R = (W_T - W_B)/(W_T + W_B) \quad (2.7)$$

$C_A$  = Radiation contrast

$W_T$  = Target radiant emittance

$W_B$  = Background radiant emittance

Figure 2.3 shows the radiation contrast for the 8–14  $\mu\text{m}$  band as a function of target to background temperature difference for four background temperatures [Ref. 6: p. 29]. In-band radiant emittance for the target ( $T$ ) or background ( $B$ ) may be found by integrating Equation (2.1) over the wavelength range of interest. The area between the two wavelengths of interest (minus absorption and scattering) represents the power available for the thermal imaging system. It is this contrast in radiant emittance that allows a target to be detected.

$$W_T = \int_{\lambda_1}^{\lambda_2} B_\lambda(T_T) d\lambda \quad (2.8)$$

$$W_B = \int_{\lambda_1}^{\lambda_2} B_\lambda(T_B) d\lambda \quad (2.9)$$

Differentiating with respect to temperature yields the following equations:

$$\frac{\partial W_T}{\partial T} = \int_{\lambda_1}^{\lambda_2} \frac{\partial B_\lambda(T_T)}{\partial T} d\lambda \quad (2.10)$$

$$\frac{\partial W_B}{\partial T} = \int_{\lambda_1}^{\lambda_2} \frac{\partial B_\lambda(T_B)}{\partial T} d\lambda \quad (2.11)$$

The spectral radiant emittance,  $B_\lambda$ , is plotted as a function of wavelength at several interesting temperatures in Figure 2.4 [Ref. 6: p. 23]. Table 2.1 [Ref. 6: p. 29] shows the integrated thermal derivative of Planck's law for wavelengths from 3 to 14  $\mu\text{m}$  at several background temperatures ( $T_B$ ). The majority of scenes taken in this experiment do not have apparent temperature differences in excess of  $\pm 20^\circ\text{K}$  from the ambient so we will confine reference to that range. According to Lloyd

[Ref. 6: p. 22], for small differences between target and background temperature, the target radiant emittance may be expressed as:

$$W_T = W_B + \frac{\partial W}{\partial T} \Delta T \quad (2.12)$$

from which:

$$\Delta T = \frac{W_T - W_B}{\left. \frac{\partial W}{\partial T} \right|_{T=T_B}} \quad (2.13)$$

with the partial derivative:

$$\left. \frac{\partial W}{\partial T} \right|_{T=T_B} \quad \text{from the values of the spectral integral of the thermal derivative of Planck's law shown in Table 2.1.}$$

The parameter  $\Delta T$  is the temperature difference between blackbody sources with equivalent radiance difference and will be referred to in this paper as the radiometric  $\Delta T$ . It represents the difference between the radiance of the target ( $L_T$ ) and the radiance of the sea surface ( $L_{SSE}$ ).

## 6. Effective Sea Surface Radiance

The total radiance from the sea surface consists of the radiance due to the sea surface temperature, sea surface emissivity, and sky radiance reflected from the sea surface [Ref. 8: p. 843]. This total radiance at a given view angle from the sensor to the target is shown in the following formula [Ref. 3: p. 14]:

$$L_{SSE} = (\epsilon_{SS} * L_{SST}) + (\rho_{SS} * L_{SKY}) \quad (2.14)$$

$L_{SSE}$  = Total in-band surface radiance (Watts/cm<sup>2</sup> - sr as measured using the AGA camera).

$L_{SKY}$  = In-band sky radiance incident on the sea surface (measured using LOWTRAN 6, Watts/cm<sup>2</sup> - sr).

$\epsilon_{SS}$  = Sea surface emissivity (calculated using the FORTRAN program EMISS).

$L_{SST}$  = Blackbody in-band radiance due to sea surface temp.

$\rho_{SS}$  = sea surface reflectivity

In fact, the total reflected sky radiance is an integral over the total hemisphere and wave slope spectrum.

### **III. AGA 780 THERMOVISION SCANNER**

#### **A. INTRODUCTION**

The AGA 780 Thermovision scanner with the CATS E program is a dual selectable channel, nitrogen cooled thermographic scanner consisting of a standard shortwave (SW) scanner, which covers the 3 to 5.6  $\mu\text{m}$  spectral band, and the longwave (LW), which covers the 8 to 14  $\mu\text{m}$  spectral band [Ref. 7: p. 10.1]. Developed by *AGEMA INFRARED SYSTEMS* in 1965, it is designed for both real-time imaging directly from the scanner or on playback from a video tape recorder (VTR). The recently developed CATS E software package is designed to use the high processing speed and storage capacity of an AT computer which allows the acquisition and storage of 1500 CATS images on the hard disk. Spotmeters, profiles, areas of special interest, statistics, and histograms can be activated for real time measurement as well as for the evaluation of frozen images.

#### **B. DESCRIPTION OF THE SYSTEM**

The basic system consists of a black and white monitor chassis for each of the short and long wavelengths, the AGEMA system cards (TIC-8000), and a dual optical scanner unit. In addition to this off the shelf system, the Naval Postgraduate School has added a Sony RGB color monitor, a Cannon color printer, and an IMB AT microcomputer configured with the latest AGEMA CATS E operating program (Version 2.1), Figure 3.1.

##### **1. Electro-Optical Scanning Mechanism**

The electromagnetic energy emitted from a target is focused by infrared lenses into a vertical prism rotating at 180 rpm, and its optical output is passed

through a horizontal prism which rotates at 18,000 rpm. The rotation of both prisms is controlled by slotted discs which are electronically connected to horizontal and vertical triggering circuits to provide triggering pulses to the monitor. The motors are synchronized so that four fields of 100 horizontal scanning lines each produce one interlaced frame. There are 70 active lines per field and the scanning rate is 25 fields per second. The output from this prism passes through a selectable filter, the aperture unit and finally onto the single point detector unit located on the wall of the nitrogen cooled Dewar chamber (cooled to  $-196^{\circ}\text{C}$  for approximately 2 hours per filling of liquid nitrogen). An Indium-Antimonide (InSb) detector is used in the  $3\text{--}5.6\text{ }\mu\text{m}$  band and a Mercury-Cadmium-Telluride (HgCdTe) detector in the  $8\text{--}14\text{ }\mu\text{m}$  band. The resulting electronic output signal from the detector is proportional to the radiation incident upon it. This electronic signal is amplified within the scanner and sent to one of the black and white monitor chassis [Ref. 7: p. 10.2].

## **2. Optics**

Optics for the AGEMA 780 system consist of a silicon lens for operation in the  $2\text{--}5.6\text{ }\mu\text{m}$  range and a germanium lens for the  $8\text{--}12\text{ }\mu\text{m}$  band. The standard 33 mm lens focuses from .5 m to infinity with an instantaneous field of view (pixel size) of 3.4 m radians and a scan coverage of  $20 \times 20$  degrees. The aperture stop can be adjusted between  $f/1.8$  and  $f/20$ . Data was collected using lenses with 3.5 and 7 degree fields of view,  $f/1.8$  aperture stop and no filters.

## **3. Black and White Monitor Chassis and Color Monitor**

The video signal from the scanner unit is amplified and processed within the monitor chassis and applied to the display screen. This black and white screen is covered by a mask with vertical and horizontal scales which are illuminated by the display raster [Figure 3.2]. A standard 19 inch television screen has been coupled to the system to enlarge the display screen of the black and white monitor chassis.

The AGA's numerical measure of the received and detected radiation is known as the thermal value, measured in isotherm units (IU), which is a practical arbitrary unit of measurement. The relationship between thermal value and received photon radiation is linear, while the relationship between thermal value and object temperature is non-linear. Three calibration constants are required to calculate the correct temperature at each aperture setting of the camera. The AGEMA camera used in this experiment was calibrated one week before the measurements were taken and the constants are shown in Table 3.1. The Thermovision camera measures the scene radiance and the results are expressed in isotherm units (IU) which is an arbitrary unit of measurement. A thermal range scale with settings from 2-1000 in 9 increments is located on the front panel. Next to this is the thermal control which sets the thermal level of the image. The ability of the CATS 2.1 program to store the thermal range and thermal level is a great improvement over the DISCO interface previously used in all Naval Postgraduate School data taking. The Sony color monitor and Cannon color printer allow the user to analyze the data in a much more quantitative way. The color display consists of a number of "sliced levels" of the total energy being displayed. The temperature range of each color is displayed in the picture by a color-temperature scale. The same color indicates different temperature ranges for different settings of thermal range and thermal level controls. Thus, the same color appearing in different places in the display represents the same power impinging on the detector [Ref. 7: p. 10.9].

#### **4. Computer and Software Package**

The AGEMA camera is connected to an IBM AT microcomputer with a 20 mb hard disk and a 12 Mhz clock cycle. The system is configured with the AGEMA system cards (TIC-8000) and a software package called CATS 2.10 (version E) [Ref. 8]. The infrared images generated by the CATS program are stored

on the IBM AT hard disk or diskette in the form of normal PC-DOS files. These files are characterized by the extension .IMG and are stored under the directory /CATS/IMAGES. A computer program called AGACATS (Appendix D) was written in FORTRAN and compiled with microsoft FORTRAN V. It can be used to analyze images read from the image files created by the CATS program. The image comparison between the two program is very good [Figure 3.3]. The advantage of the AGACATS program is that it makes the data from the AGEMA camera compatible and accessible to any microcomputer. One image file comprises 20,446 bytes of which the first 846 contain heading, calibration, and other miscellaneous information. The image is contained in the last 19,600 bytes which correspond to the digital thermal values of each pixel. The following algorithms generated by the AGEMA Corporation are used in the reading from the CATS files and processing the data:

- A.  $T_0 = B/I_N(R/I_0 + F) - 273.15$  (degrees C)
- B.  $I_0 = I'_0/(\epsilon * \tau) - (1 - \epsilon)/\epsilon * I_{AMB} - (1 - \tau)/(\epsilon - \tau) * I_{ATM}$  (IU)
- C.  $I_{AMB} = R/(\exp(B/T_{AMB}) - F)$  (IU)
- D.  $I_{ATM} = R/(\exp(B/T_{ATM}) - F)$  (IU)
- E.  $I'_0 = L + OC + R(d - 128/254)$  (IU)

where:

- $L$  = Thermal level (IU)
- $OC$  = Offset correction (normally zero, IU)
- $R$  = Thermal range (IU)
- $d$  = Digital sample value for the measured point ( $1 < d < 255$ )
- $\epsilon$  = Emissivity factor



$\tau$  = Transmission factor for the atmosphere

$R, B, F$  = Calibration constants

## C. THERMAL MEASUREMENT TECHNIQUES

There are two basic methods of measuring the temperature of an object using the AGA Thermovision camera: relative and direct.

### 1. Relative Measurement

Relative measurement uses an external reference with known temperature and emissivity factor. Both objects are placed next to each other and the thermal range and level are set at the lowest levels consistent with displaying both reference and object in the same isotherm [Figure 3.4].

### 2. Direct Measurement

This method utilizes the instrument's built-in temperature compensation system that permits temperature measurement without the use of an external temperature reference. Under these simplified conditions, assuming  $\epsilon_0 = 1$ , the calibration curves can be used directly for translating the measured thermal value to temperature [Figure 3.5].

All measurements in this experiment were made using the direct measurement technique. The following step by step measurement procedure is taken from Reference 7.

- Adjust the THERMAL RANGE and THERMAL LEVEL (L) controls to obtain a satisfactory thermal picture (Note setting of L).
- Adjust the ISOTHERM LEVEL (i) control to brighten up the point of interest on the object in view.

- Add the values of "L" and "i" from (a) and (b). The result will be the measured thermal value  $I'_0$  (IU).

Under these conditions, the calibration curves can now be used for translating the measured thermal value,  $I'_0$  to temperature [Figure 3.5].

In the normal color image, the isotherm levels are arranged in a linear fashion such that each color represents an equal number of isotherm units. These units are then converted to temperature using calibration curves provided by the AGEMA Corporation. As can be seen by the curves, temperature is a function of isotherm units and is non-linear. Each color represents a different range of temperatures depending on where they fall on the calibration curve. The Microsoft FORTRAN program shown in Appendix D converts the linear color scale (with its non-linear temperature relationship) to a non-linear color scale with the linear temperature relationship. The benefit of having each color represent an equal number of degrees is that it eliminates the necessity to use the calibration curves [Figure 3.6].

In choosing the colors for the presentation, a zero or non-level is indicated by the color black and the top color level is white, with ten different colors in between. The program is unable to distinguish any variability in temperature within the black or white color region. The operator is warned of temperature values above or below the selected range by the cue "overfill" or "underfill."

## **IV. VALIDATION OF THE SCHWARTZ-HON MODEL**

### **A. SCHWARTZ-HON MODEL**

The Schwartz-Hon algorithm involves a study done at the Naval Research Laboratory in Washington, D.C. to model radiance of the sea surface as a function of viewing angle. This model is complicated by the fact that the ocean is a rough surface that changes with varying wind speed. The infrared radiance of the sea is described by two components: Self emission and sky reflectance. Assuming that the entire ocean is emitting at some fixed temperature, emissivity is purely a function of surface roughness. Specifically, for a given flat horizontal element of surface area, the water has an emissivity that is only a function of viewing angle with respect to the surface normal [Ref. 1: p. 2]. The ocean can be thought of as an ensemble of small facets each of which emits and reflects infrared radiation. It is easy to see that the distribution of facet orientations can have a large effect on the infrared radiation emanating from the sea surface. If the wind was calm and the sea was smooth, all the facets would be horizontally oriented. When an ocean surface roughened by high winds is viewed near grazing, most of the facets seen by the sensor are tipped away from the horizontal toward the sensor. This phenomenon impacts upon both the amount of radiation emitted from the sea and the amount of radiation reflected from the sky [Ref. 9: p. 838]. The radiance of the surface depends on the slope distribution and orientation of the fluid surface which, in turn, is dependent on the wind speed [Ref. 1: p. 7]. Figure 4.1 shows only the incoming sky radiance at the proper angle reflecting off the facet orientations toward the sensor. The Schwartz-Hon probabilistic model of the apparent radiance of a rough sea surface requires:

- The development of an accurate sea surface model that incorporates wind velocity as a parameter.
- Computation of the surface emissivity from the model.
- Subsequent inference of surface temperature.

### **1. Computer Program-EMISS (Schwartz-Hon)**

EMISS is a computer program developed by Mr. John Cook of the Naval Oceanographic & Atmospheric Research Laboratory (NOARL) that utilized the newly developed Schwartz-Hon model to compute infrared (IR) emissivity of the sea surface and the effective specular reflection angle for incoming sky radiance. The program requires inputs of view angle and wind speed and yields a calculated sea surface emissivity over the selected ocean area or footprint and an effective specular angle.

The sea surface is not smooth; therefore roughness must be accounted for since it affects the modeling of emissivity. To simplify the computer model, Schwartz and Hon assumed that the sea surface temperature was constant and emissivity was only a function of the surface roughness. In addition it was assumed that the sea surface was composed of many flat, reflecting surfaces and the emissivity of each surface was dependent on its slope and the viewing angle of the detector. A large number of these flat surfaces were spatially averaged over a footprint. An azimuth angle was chosen in the direction along the footprint from which elevation and slope values were taken. Rays were taken from each element of the footprint to the view point. The emissivity of the footprint was then calculated as the spatial average of the emissivity over all elements of the footprint [Ref. 1: p. 3] [Figure 4.1].

In addition to the output of average emissivity over a given ocean area, the EMISS program also outputs a zenith angle for incoming radiance from the sky associated with the mean apparent wave slope of the footprint. This is calculated

by assuming that the average emissivity over the footprint is due to a single sloping surface of smooth water [Ref. 1: p. 2]. The model extrapolates from the mean emissivity to one for zero wind speed. After calculating the slope angle ( $\alpha$ ) of the sloping surface, the model outputs an effective sky radiance ( $L_{SKY}$ ) or reflection angle ( $\theta_R$ ) using the relationship:

$$\theta_R = \theta_i - 2\alpha$$

As the viewing angle increases toward the normal to the mean apparent wave slope of the footprint ( $N_F$ ), emissivity approaches a maximum. As viewing angle increases past  $N_F$  and approaches grazing (90 degrees), sea surface emissivity as a function of angle approaches zero. Figure 4.2 depicts the graph of emissivity vs. nadir angle for several different wind speeds [Ref. 1: p. 25].

## 2. Shapiro Algorithm in EMISS

An algorithm developed by Mr. Ralph Shapiro of ST Systems Corporation was also designed to calculate the emissivity and reflection angle for incoming sky radiance at view angles from 0°–90° [Ref. 10: p. 24]. It was found that for very large view angles (above 85°) substantial errors in infrared reflectivity were found. These errors were originally thought to be a result of the shadowing effect on the back sides of the wave fronts. For  $\theta_V$  equal to zero, the front and back sides of the waves each occupy one-half of the view of the water surface, regardless of the slope of the wave. As  $\theta_V$  increases, a larger proportion of the water surface appears as a wave front [Ref. 10: Appendix A]. As in the Schwartz-Hon algorithm, the effect of wind on the sea surface causes the emissivity of the surface to increase. The Shapiro model of reflectivity vs. view angle for various wind speeds as seen in Figure 4.3 shows that for view angles between 0°–65° the reflectivity of the sea surface is constant and, as  $\theta_V$  approaches 90°, the reflectivity decreases with wind speed.

The majority of infrared (IR) sensors in use by the Navy today operate at very low altitudes thus making the larger view angle portion of the graph very important. The EMISS program utilizes the latest water surface emissivity model developed by Sidran [Ref. 11: p. 3176-3183] which is the basis for all models in use by the Navy today. The Sidran model along with the Shapiro algorithm have only been validated to view angles ( $\theta_V$ ) less than or equal to  $85^\circ$ . The EMISS computer program will be applied to validation of the Shapiro algorithm in the range of  $\theta_V$  between  $85^\circ$  and  $90^\circ$ .

### 3. PC-TRAN and LOWTRAN 6

An atmospheric propagation code was needed to predict the net emission of radiation in the atmospheric path. The model most suited for this experiment was the low resolution FORTRAN computer code called LOWTRAN 6. LOWTRAN calculates atmospheric radiance and transmission for a specified path through the atmosphere with a wavelength range from .25 to  $28.5 \mu\text{m}$  and a resolution of  $20 \text{ cm}^{-1}$ . The output transmittance is the product of all the transmittances due to water vapor line absorption, water vapor continuum absorption, mixed gases, nitrogen, and aerosol absorption, and aerosol and molecular scattering. The code includes effects caused by atmospheric refraction and the curvature of the earth. The atmosphere is treated as a stack of up to 33 atmospheric layers, from 0 to 100 km altitude. As the path passes through each layer in the model, the atmospheric components of interest are computed and summed over the path and wavelength band.

For portability and ease of use, PC-TRAN by the Ontar Corporation [Ref. 12], was used in place of LOWTRAN 6 for all calculations. This software package allows the user to perform all LOWTRAN 6 calculations, display the calculation on the computer screen, and generate hard copy plots. PC-TRAN inputs are shown in Table 4.1.

## **B. EXPERIMENTAL VALIDATION OF THE SCHWARTZ-HON SEA RADIANCE MODEL**

### **1. Introduction**

An experiment was carried out to validate the Schwartz and Hon algorithm at low grazing angles. A validation of the Schwartz-Hon computer model for the emissivity of the sea surface was accomplished by comparison of measured sea surface radiances taken with the AGEMA Thermovision 780 series camera to those calculated by the PC-TRAN computer code. All the factors which effect the radiance measurements were taken into account and the degree to which they effect the data was estimated. This work is a continuation of research done by LT Ridgeway [Ref. 3], and Major Psihogios [Ref. 4]. Many of their recommendations and data-taking techniques were used in this experiment.

### **2. Meteorological Conditions**

Clear sky conditions and a variety of wind speeds would be the best conditions to validate the Schwartz-Hon algorithm. The weather on the day of the experiment was initially overcast and cloudy with a large fog bank over the bay. Initial temperature was 13.4°C, relative humidity was 91%, and windspeed was relatively constant throughout the experiment. The fog began to dissipate and a horizon was clearly visible after approximately half the images were taken.

## **C. EXPERIMENTAL PROCEDURE**

On May 2, 1990, 93 images of the R/V *Point Sur* and the sea/sky interface were taken in the Monterey Bay with the AGEMA Thermovision camera. The camera was set up at the Marine Oceanographic Beach Laboratory of the Naval Postgraduate School by Professor A. W. Cooper and his staff [Figure 4.4]. As noted by LT Ridgeway [Ref. 3] and Major Psihogios [Ref. 4], correlating the physical

horizon of the observer with the estimated horizon of the thermal image taken with the AGEMA camera was a significant problem. To calculate the height of the camera above the surface of the water, the original building plans for the Oceanography Department Beach Lab were used to calculate the observation height above mean sea level. Tide level was obtained via modem from the Monterey Bay Aquarium buoy and a total height above the mean sea level for the camera was obtained.

### **1. Correlation of the Physical Horizon with the Computer Display**

PC-TRAN was then used to correlate the viewed horizon with the AGEMA camera display screen. View angles were entered into PC-TRAN to determine the last incidence angle before a ray launched toward the horizon continued on into space. This was accomplished by noting the path length calculated by the PC-TRAN program. For the view angle ray-path that continued on to space, the computed path length would be large compared to the previous view angle. This view angle was used to correlate the viewed horizon with the AGEMA screen [Ref. 3: p. 33].

By knowing the number of pixels on the AGEMA screen and using the mouse cursor function in the newly-developed AGACAT computer code to read temperatures along a vertical line, the thermal discontinuity or horizon can be seen both in the color display and in the spot temperature difference of the image. The lowest temperature in this region represents the ocean and the upper temperature represents the sky. The lens used in the experiment had a field-of-view of  $3.5^\circ$  and the AGACAT program uses a picture area of  $140 \times 140$  pixels for VGA monitors. Using the VGA monitor as an example, the field of view is divided by the number of horizontal pixel units to yield  $.0250^\circ$  per cursor movement. Elevation angles above and below the horizon can now be measured to an accuracy of  $.0250^\circ$ .



## 2. Measurements

The procedure for the validation of the Schwartz-Hon model includes the following terms:

- $\theta_V$  = Zenith angle or view angle (degrees).
- $\theta_i = 180^\circ - \theta_V$  or  $\theta_i$  = Reflection angle (degrees).
- $\theta_R$  = Incidence angle or effective sky radiance angle (Schwartz-Hon model, degrees).
- $\epsilon_{SS}$  = Sea surface emissivity (Schwartz-Hon computer model).
- $\rho_{SS}$  = Sea surface reflectivity ( $\rho_{SS} = 1 - \epsilon_{SS}$ ).
- Range = AGA sea surface distance (from LOWTRAN 6) (km).
- $L_T$  = In-band radiance of the R/V *Point Sur* ( $\text{W}/\text{cm}^2 - \text{sr}$ ).
- $L_{SKY}$  = In-band radiance from the sky at  $\theta_R$  (measured by the AGEMA camera) ( $\text{W}/\text{cm}^2 - \text{sr}$ ).
- $L_{SST}$  = In-band sea surface radiance due to the sea surface temperature  $L_{SST}$  ( $\text{W}/\text{cm}^2 - \text{sr}$ ).
- $L_{SSE}$  = Total in-band radiance from the sea surface ( $\text{W}/\text{cm}^2 - \text{sr}$ ) ( $\epsilon_{SS} * L_{SST}$ ) + ( $\rho_{ss} * L_{SKY}$ ) (measured with the AGA camera).
- $L_{SSC}$  = Calculated sea surface radiance at  $\theta_V$  ( $\text{W}/\text{cm}^2 - \text{sr}$ ).
- $L_{SSM}$  = Measured sea surface radiance (measured with the AGA camera) ( $\text{W}/\text{cm}^2 - \text{sr}$ ).
- $T_{BR} = L_{SSE} - L_{SST} / \left[ 1/\pi * \frac{\partial W}{\partial T} \Big|_{T = T_{SST}} \right] + T_{SST}$  (blackbody temperature at sea surface, °C).
- $T_{SSE}$  = Sea surface temperature corresponding to  $L_{SSE}$  (°C).
- $T_{SST}$  = Sea surface temperature (°C).
- $T_{SSC}$  = Corresponding in-band blackbody temperature ( $L_{SSC}$ ) (°C).
- $T_{SSM}$  = Corresponding in-band blackbody temperature ( $L_{SSM}$ ) (°C).
- $T_{BB}$  = In-band blackbody temperature ( $T_{BB} = \sqrt[4]{W(T)/\Delta q * \sigma}$ ) (radiance value to in-band blackbody temperature conversion) (°C) where:

- $W(T)$  = Radiant emittance.
- $\Delta q$  = % of radiant emittance in wavelength of interest.
- $\sigma = 5.6697 \times 10^{-12}$  [Watts/cm<sup>2</sup> K<sup>4</sup>].
- Inputs required by the computer program PC-TRAN are listed in Table 4.1.
- Inputs required for angle measurements are shown on Figure 4.5.

## D. DATA COLLECTION

The above equations are used to compare the sea surface temperature and radiance values that were calculated using the Schwartz-Hon algorithm and LOW-TRAN 6 ( $L_{SSE}$  and  $T_{SSE}$ ) to temperature and radiance measured with the AGEMA Thermovision camera ( $L_{SSM}$  and  $T_{SSM}$ ). The required meteorological readings and a brief description of the variables used in the calculations follows:

### 1. Meteorological Data

Meteorological data taken at the time of the experiment was collected from four different sources:

- A) Shipboard measurements of air temperature, sea surface temperature, dew point, relative humidity, wind speed and direction were taken by computer at five minute intervals (Table 4.2).
- B) Meteorological readings were collected from the Monterey Bay Aquarium buoy located at 36–48.5°N, 122–24.4°W. A modem was connected to a Macintosh SE/30 computer to collect the real time data (Table 4.3).
- C) Radiosondes were launched from the R/V *Point Sur* every four hours for the duration of the cruise. A special launch was made immediately following the data-taking portion of the experiment with the results listed in Table 4.4.
- D) Data was also taken on site using a Solomat measuring device connected to a COMPAQ 3 portable computer. This instrument is capable of measuring temperature, pressure, humidity, and windspeed and the results are listed in Table 4.5.

### 2. $\theta_V$ : View Angle Measurement

As shown in Figure 4.5,  $\theta_V$  is the viewing angle from the camera lens to the ship. This angle was determined by finding the relative height of the camera

( $H_C$ ) above the surface of the water. The height of the ground above mean sea level (MSL) where the camera was positioned was obtained from the original geographical site plans used to construct the Oceanographic Beach Lab and is labeled  $H_D$ . Tide heights were obtained from the Monterey Bay Aquarium buoy [Table 4.3] and the height of the camera above sea level is determined by adding  $H_C + H_D$  and subtracting the difference in tide height from mean sea level (MSL).

### 3. $\theta_i$ and $\theta_R$ Measurement

As shown on Figure 4.5,  $\theta_i$  is the angle from the normal line tangent to the earth's surface to the view direction. This angle is calculated by entering the view angle ( $\theta_V$ ) into PC-TRAN and reading out the corresponding  $\theta_i$ .  $\theta_R$  or the incidence angle was determined using the computer program developed by Schwartz and Hon called EMISS [Ref. 1: p. 9]. The required inputs into the program are zenith angle at the reflection point of the reflected ray ( $\theta_i$ ) and a corresponding wind speed measured at the time of the experiment. The program outputs the zenith angle at the reflection point of the incident ray ( $\theta_R$ ) along with a value of the emissivity ( $\epsilon_{SS}$ ).

### 4. $L_{SKY}$ and $L_{SST}$ Measurement

In-band sky radiance reflected from the sea surface at  $\theta_R$  ( $L_{SKY}$ ) is measured directly from the AGEMA camera and also computed using PC-TRAN. An IBM-PC computer program called "The Blackbody Calculator," created by Integrated Sensors Incorporated, was used to calculate the radiance at the sea surface temperature ( $L_{SST}$ ) [Fig. 4.6] [Ref. 13]. Inputs to the program include temperature (Kelvin), bandpass of the AGA scanner (8–14  $\mu\text{m}$ ), emissivity, and the total radiance band of the black body curve. The program computes the in-band radiance by integration of Planck's radiation law for the input source temperature, emissiv-

ity and bandpass. The total in-band radiance, assuming a Lambertian surface, is determined by dividing the bandpass flux by a factor of  $\pi$ .

### 5. $L_{SSE}$ and $T_{BR}$ Measurement

Total in-band radiance from the sea surface ( $L_{SSE}$ ) consists of the in-band radiance due to the surface temperature ( $L_{SST}$ ) multiplied by the sky radiance incident on the surface ( $L_{SKY}$ ) which will be reflected into the sensor with a reflectivity ( $\rho_{SS}$ ), Equation (2.13). Other factors such as transmittance and radiance effects between the AGA camera and the sea surface must be taken into account in the calculation of  $L_{SSE}$ . First a radiance temperature ( $T_{BR}$ ) corresponding to the total sea surface radiance ( $L_{SSE}$ ) was calculated:

$$T_{BR} = [L_{SSE} - L_{SST}] / \left[ 1/\pi * \frac{\partial W}{\partial T} \right]_{T=T_{SST}} + T_{SST} \quad (4.1)$$

where:

$$T_{BR} - T_{SST} = \Delta T$$

$T_{BR}$  is a blackbody temperature which gives the same in-band radiance as the target of interest.  $T_{BR}$  was used in PC-TRAN in the radiance mode to calculate a radiance value at the AGEMA camera.

### 6. In-band Blackbody Temperature ( $T_{BB}$ )

Radiant emittance values are converted to in-band blackbody temperatures by inversion of the Stefan-Boltzmann Law:

$$T_{BB} = \sqrt[4]{W(T)/\Delta q * \sigma} \quad (4.2)$$

where:

$T_{BB}$  = In - band blackbody temperature

$W(T)$  = Radiant emittance

$$\sigma = 5.6697 * 10^{-12} [\text{watts/cm}^2 \text{K}^4]$$

$$\Delta q = \% \text{ of radiant emittance in wavelength of interest}$$

The proportional radiation or percentage of radiant emittance in the wavelength of interest ( $\Delta q$ ) is read from Table 4.6. If the longer wavelength (14  $\mu\text{m}$ ) is selected for  $\lambda_1$  and the shorter wavelength (8  $\mu\text{m}$ ) selected for  $\lambda_2$ , then the difference between the radiation values  $q_1$  and  $q_2$  gives the desired proportional radiation  $\Delta q = q_1 - q_2$  [Ref. 14: pp. 54-55].

## 7. $L_{SSC}$ and $L_{SSM}$ Measurement

Calculated sea surface radiance ( $L_{SSC}$ ) is compared to radiance measured directly using the AGEMA camera ( $L_{SSM}$ ) at selected viewing angles. For the calculation of Equation (2.14),

$$L_{SSE} = (\epsilon_{SS} * L_{SST}) + (\rho_{SS} * L_{SKY}) \quad (2.14)$$

$L_{SSE}$  is evaluated with Sky Radiance ( $L_{SKY}$ ) computed using PC-TRAN in radiance mode at the calculated Schwartz-Hon effective incidence angle obtained using the EMISS program.  $\epsilon_{SS}$  and  $\rho_{SS}$  are also obtained from the EMISS program. The sea surface radiance ( $L_{SST}$ ) is computed using the following equation:

$$L_{SST} = \frac{W_{SS}(T_{SS})(1 - \rho_{SS})}{\pi} \quad (4.3)$$

where:

$$W_{SS} = \sigma T^4 = \text{blackbody radiant exitance of the sea surface}$$

This calculated radiance value is compared to the radiance value measured using the AGEMA camera ( $L_{SSM}$ ) at the selected viewing angle.  $L_{SSM}$  is calculated by taking the apparent sea surface temperature measured with the AGEMA camera ( $L_{SST}$ ) at the effective viewing angle ( $\theta_R$ ) and converting it to a corresponding radiance value.

## 8. $T_{SSC}$ and $T_{SSM}$ Measurement

Radiance values  $L_{SSC}$  and  $L_{SSM}$  were converted to equivalent blackbody temperature values  $T_{SSC}$  and  $T_{SSM}$  using Equation (4.2).

## **V. DATA ANALYSIS, RECOMMENDATIONS AND CONCLUSIONS**

### **A. INTRODUCTION**

In this chapter, radiance values obtained with the AGEMA Thermovision camera will be compared to values given by the PC-TRAN computer program. Effects such as wind speed, sky conditions, and vertical profile data will be discussed and compared to previous experiments.

#### **1. PC-TRAN Inputs**

The inputs to the PC-TRAN program are shown in Table 4.1. The radiosonde data that was entered consisted of 34 (software limited) atmospheric levels approximately 140 m apart beginning at an altitude of 6 meters. Radiosonde launch time was approximately 12 min after the AGEMA thermal radiance values were obtained.

#### **2. Validation of the Schwartz-Hon Model**

The method used in the validation of the Schwartz-Hon algorithm is as follows:

1. The reflection angle ( $\theta_i$ ) of the sky radiance was obtained by subtracting the viewing angle ( $\theta_v$ ) from  $180^\circ$ .
2. Effective incidence angle ( $\theta_R$ ) and emissivity ( $\epsilon_{SS}$ ) were obtained from the computer program EMISS using the Schwartz-Hon computer model and the wind speed at the experiment site.
3. Sky radiance ( $L_{SKY}$ ) was computed for the reflection angle ( $\theta_R$ ) by measuring spot temperatures with the AGEMA camera and applying Equation (2.1), Planck's Law. A value of sky radiance is also computed using PC-TRAN and Equation (2.14).

4. The radiance emitted by the sea surface ( $L_{SST}$ ) was computed using the sea surface temperature, emissivity from the EMISS program, and Equation (2.1), Planck's Law.
5. Total radiance emitted by the sea surface ( $L_{SSE}$ ) was computed using Equation (2.14), where  $L_{SKY}$  is measured using the AGA,  $L_{SST}$  is calculated using the measured sea surface temperature and the emissivity value coming from the EMISS program.
6.  $T_{BR}$ , Equation (4.1), was used as a target for PC-TRAN executed in the radiance mode.
7. Computed reflected sky radiance ( $L_{SSC}$ ) was found using Equation (2.14) with PC-TRAN computed sky radiance ( $L_{SKY}$ ).
8. The radiance measured with the AGEMA camera ( $L_{SSM}$ ) was compared to the radiance calculated using the Schwartz-Hon model ( $L_{SSC}$ ).
9. The radiance measured with the AGEMA camera ( $L_{SSM}$ ) was compared to the radiance calculated using the Shapiro algorithm ( $L_{SSC}$ ).

## B. DATA ANALYSIS AND RESULTS

The analysis of the experiment presented in Chapter IV yields some useful results:

The first set of data (Tables 5.1–5.6) show the temperature and radiance values of the AGEMA thermal images taken on May 2, 1990, from 1030 to 1230 local time. The radiosonde release of 1010 local was used to apply to PC-TRAN. The table shows spot temperatures and equivalent radiances measured with vertical movement of the cursor on a picture file obtained at zero baseline elevation, with the horizon estimated (as previously described) at 90.025 degrees from zenith. Table 5.1 shows a zero elevation angle with subsequent tables increasing the elevation angle in increments of 2.8°. The zenith angle of the apparent horizon is greater than 90° due to the refractive index of the atmosphere explained in Chapter II. The data sets were collected between 1030 and 1230 hours local under clear sky conditions. The AGEMA camera was calibrated 6 days before the experiment and the constants are listed in Table 3.1.



## 1. Sky Radiance Comparison

The sky radiance computed using PC-TRAN is compared with that measured using the AGEMA camera, and the results are shown in Tables 5.7 and 5.8 along with Figures 5.1 and 5.2. The thermal radiance values show a decrease in temperature with elevation angle which corresponds to the altitude variation of temperature in the radiosonde profile. The maximum value of the radiance was  $4.5837 \text{ mW/cm}^2 - \text{sr}$  at a view angle of  $89.075^\circ$  and a minimum was  $2.8775 \text{ mW/cm}^2 - \text{sr}$  at  $7.4375^\circ$ . The mean error between AGEMA and PC-TRAN for zenith angles between  $85^\circ$  and  $90^\circ$  is 5.01% and 13.58% for angles between  $75^\circ$  and  $85^\circ$ . This compares favorably with experiments performed under clear sky conditions in November of 1987 and July of 1988. In November, the mean error for zenith angles between  $85^\circ$  and  $90^\circ$  was 5.11% and for angles between  $75^\circ$  and  $85^\circ$ , 27.75%. In July the errors were 9.13% and 7.52%, respectively. Both measured and computed sky radiance values show a monotonic and closely parallel increase with elevation angle from  $74^\circ$  to  $89^\circ$ , with about a 10% under estimation in the calculation. Above  $89^\circ$ , the measured value shows a significant drop (4%).

Better radiance values were expected in the May experiment because of the recent calibration of the AGEMA camera and the fact that the radiosondes were launched minutes after the images were taken rather than hours as in previous years.

## 2. Schwartz-Hon Validation

Table 5.9 lists the figures used in the final calculations of  $L_{SSC}$  using PC-TRAN and  $L_{SSM}$  using the Schwartz-Hon algorithm. Figure 5.3 summarizes the results using the Statgraphics program on the Macintosh SE/30 computer. Figure 5.4 shows the radiance values that were converted to in-band blackbody temperatures using Equation (4.2). There are no distinguishable patterns in Figures

5.3 and 5.4 that would prove that the Schwartz-Hon algorithm is degraded at low grazing angles. The average deviation of the sea surface radiance predicted in the Schwartz-Hon model with LOWTRAN was 7.94%. This compares favorably with the 14 and 15 July 1988 experiments which had average deviations of 4.65% and 3.24%, also on clear sky days.

Table 5.11 and Figure 5.7 show a synopsis of all the experiments conducted in the last three years on the Schwartz-Hon validation. With similar sky conditions, the curves are nearly identical in shape with varying distance between them. As noted by Ridgeway [Ref. 3] and Psihogios [Ref. 4], a probable cause of the error between the algorithm and the measured values of radiance may be the wind speed and errors due to observation techniques and measurements. Since emissivity is purely a function of surface roughness and view angle and sea surface radiance depends on the emissivity, varying wind speed can be expected to change the radiance values. Figure 5.8 shows a graph of percentage error between  $L_{SSC}$  and  $L_{SSM}$  as a function of wind speed. Regression lines calculated from the data in Table 5.12 show no clear dependence on wind speed on percentage error between  $L_{SSC}$  and  $L_{SSM}$  so it may be concluded that the Schwartz-Hon model has adequately accounted for wind speed. Figure 5.7 gives radiance values versus low grazing angles at various wind speeds.

### 3. Shapiro Algorithm

The program "EMISS" provides an alternative algorithm for sea radiance computation developed by Shapiro. This has been applied to our data with the results shown in Table 5.10 and Figures 5.5 and 5.6. In comparing these results to those obtained with the Schwartz-Hon algorithm, it can be seen that the shape of the graphs are very similar but the difference in radiance values are much greater. The

mean percentage error between calculated and measured radiance values is 7.94% for Schwartz-Hon and 15.31% for the Shapiro algorithm.

#### **4. Recommendations and Conclusions**

The Schwartz-Hon algorithm for computation of emissivity and equivalent specular reflection angle for a rough sea surface has been evaluated for use in modelling of Tactical Decision Aid (TDA) ship target/background contrast. The results obtained over a restricted range of environmental conditions (significantly, wind speed, cloud cover, sea surface, and sky temperature) show prediction of radiance contrast generally in the range of 2 to 13% deviation from radiometric measurement. This is considered sufficiently accurate to recommend further use of the algorithm in development of predictive models for environment sensitive target input for TDA use. However, due to limited data base with the wide potential variations of the uncontrolled environmental parameters, reservations must be retained pending expansion of the data base to many more observations with a wider range of parameters, notably wind speed and atmospheric profile.

Further evaluation is also required of factors such as errors in measured wind speed due to sensing at a location remote from the target. Direct comparison of LOWTRAN 6 sky radiance with AGA measurement showed agreement sufficiently close ( $\leq 15\%$ ) for use in TDA development, although again more comparisons in the "grazing incidence" region are required. Direct comparison of the Shapiro and Schwartz-Hon emissivity algorithms indicate errors for Shapiro about twice that of Schwartz and Hon within the limited data base. A continuation of the measurement series at Monterey is recommended with attention paid to a complete specification of environmental parameters.

# APPENDIX A

## FIGURES

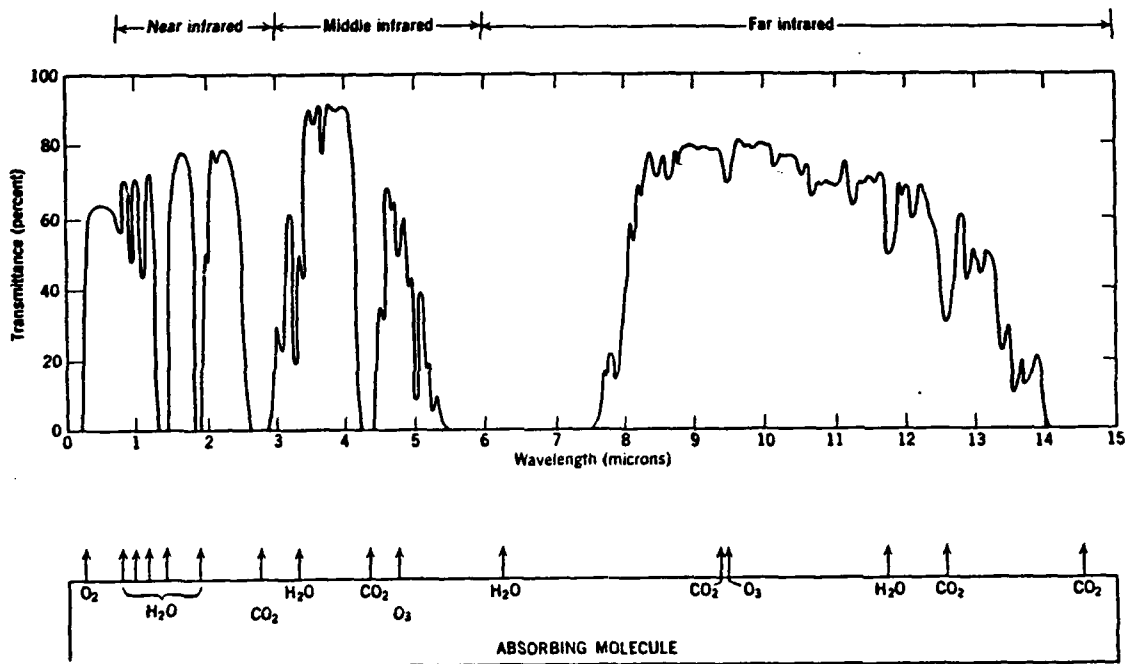


**Figure 2.1: Transmittance through the atmosphere for a 6000 ft horizontal path at sea level [Ref. 5: p. 115].**

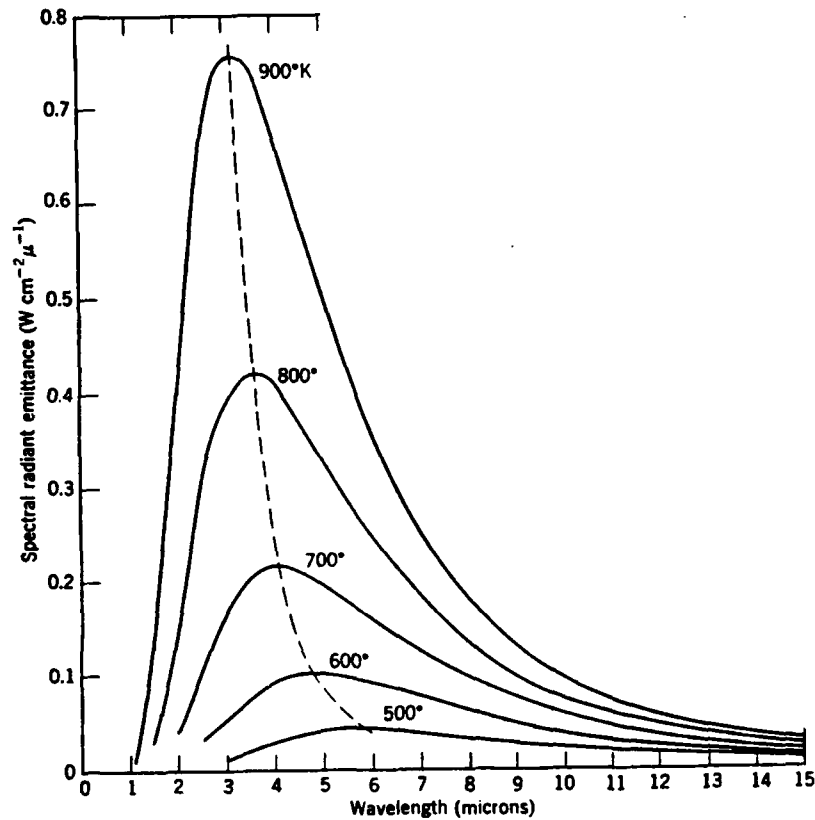


Figure 2.2: Spectral radiant emittance of a blackbody at temperatures ranging from 500–900 °K [Ref. 5: p. 36].

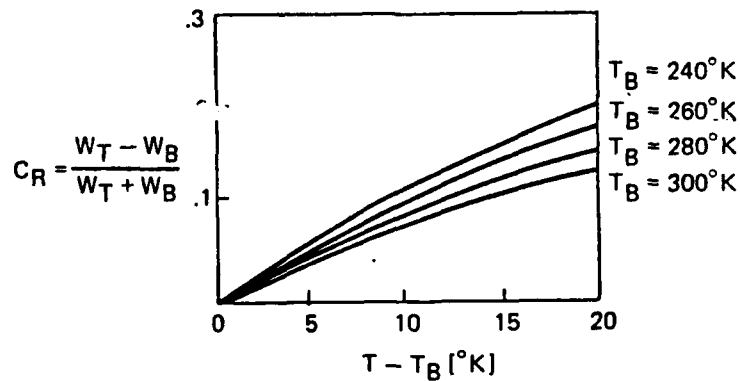


Figure 2.3: Radiation contrast for the 8–14  $\mu\text{m}$  band as a function of target to background temperature difference [Ref. 6: p. 29].

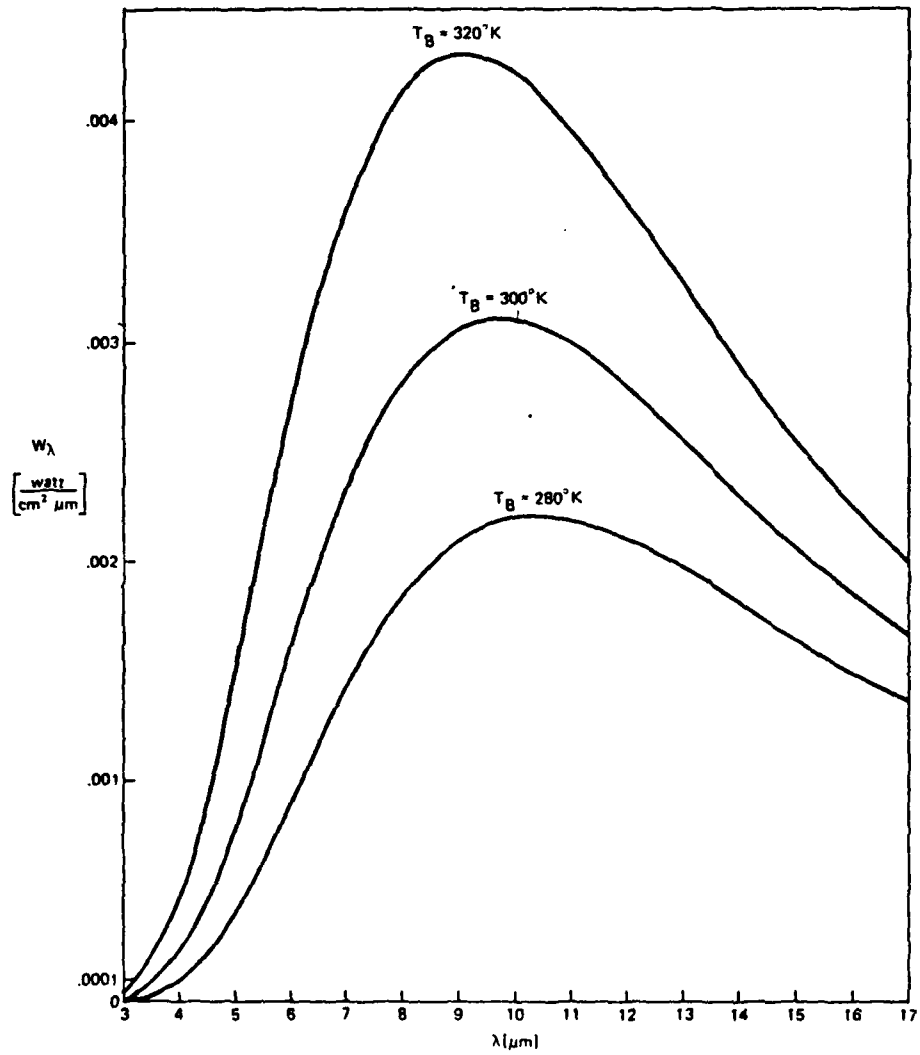
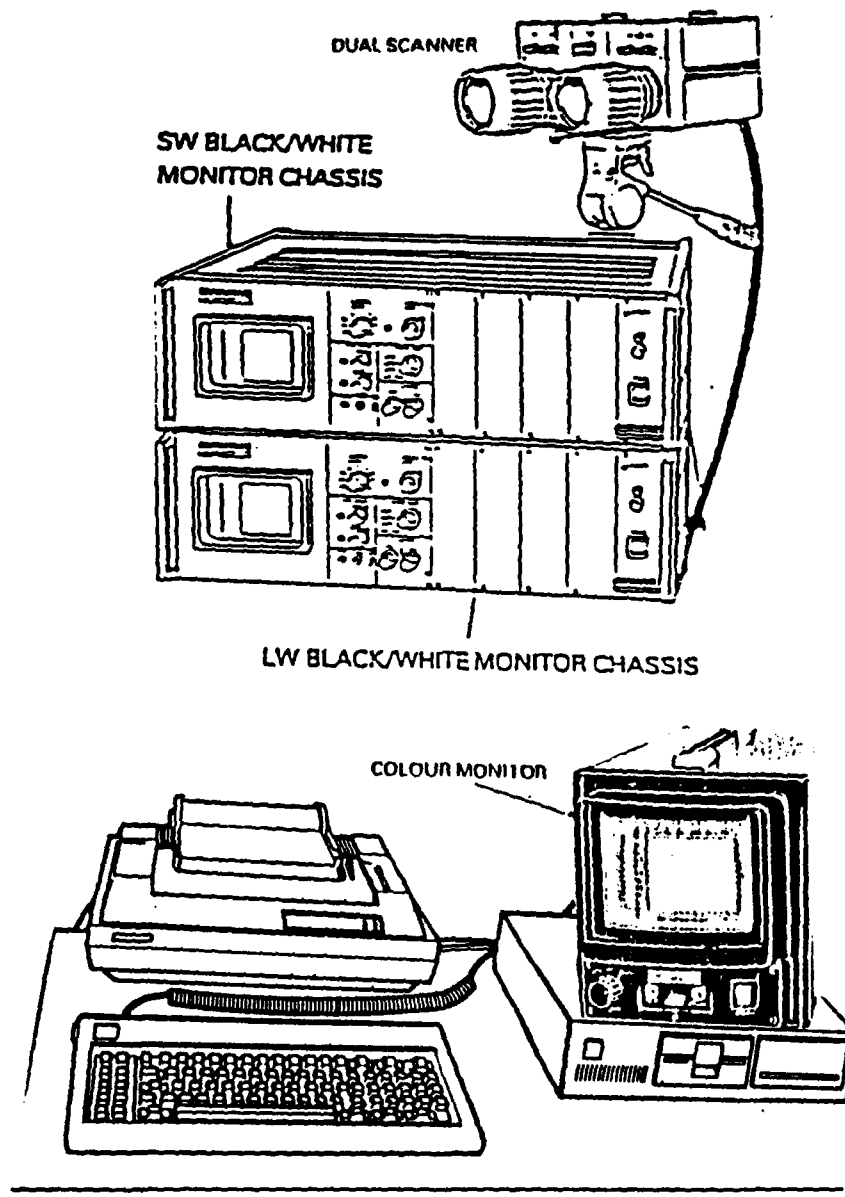
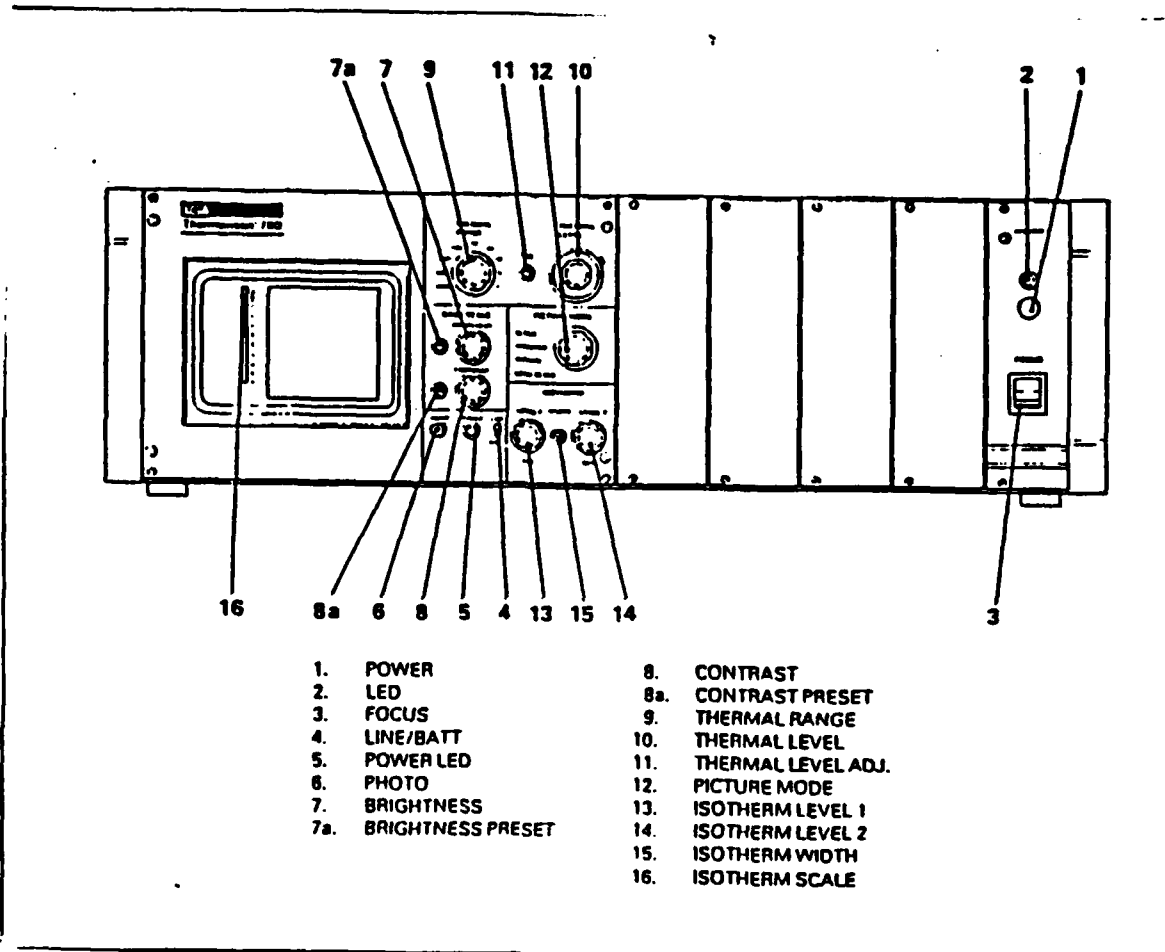


Figure 2.4: Planck's law for spectral radiant emittance at three back-ground temperatures [Ref 6: p. 23].



**Figure 3.1: Thermovision 789 Series with TIC 8000 and CATS E software package.**



Item	Description	Function
1	POWER	This push ON/OFF button controls the ac supply to the THV 780 system.
9	THERMAL RANGE	This nine position switch selects the thermal span of interest. The switch is calibrated between 2 and 100 IU.
10	THERMAL LEVEL	This control sets the thermal level of the thermal image.
11	THERMAL L. ADJ	This control provides fine adjustment for calibration of the thermal level

Figure 3.2: Black and white monitor chassis showing location of power, thermal range, and thermal level.



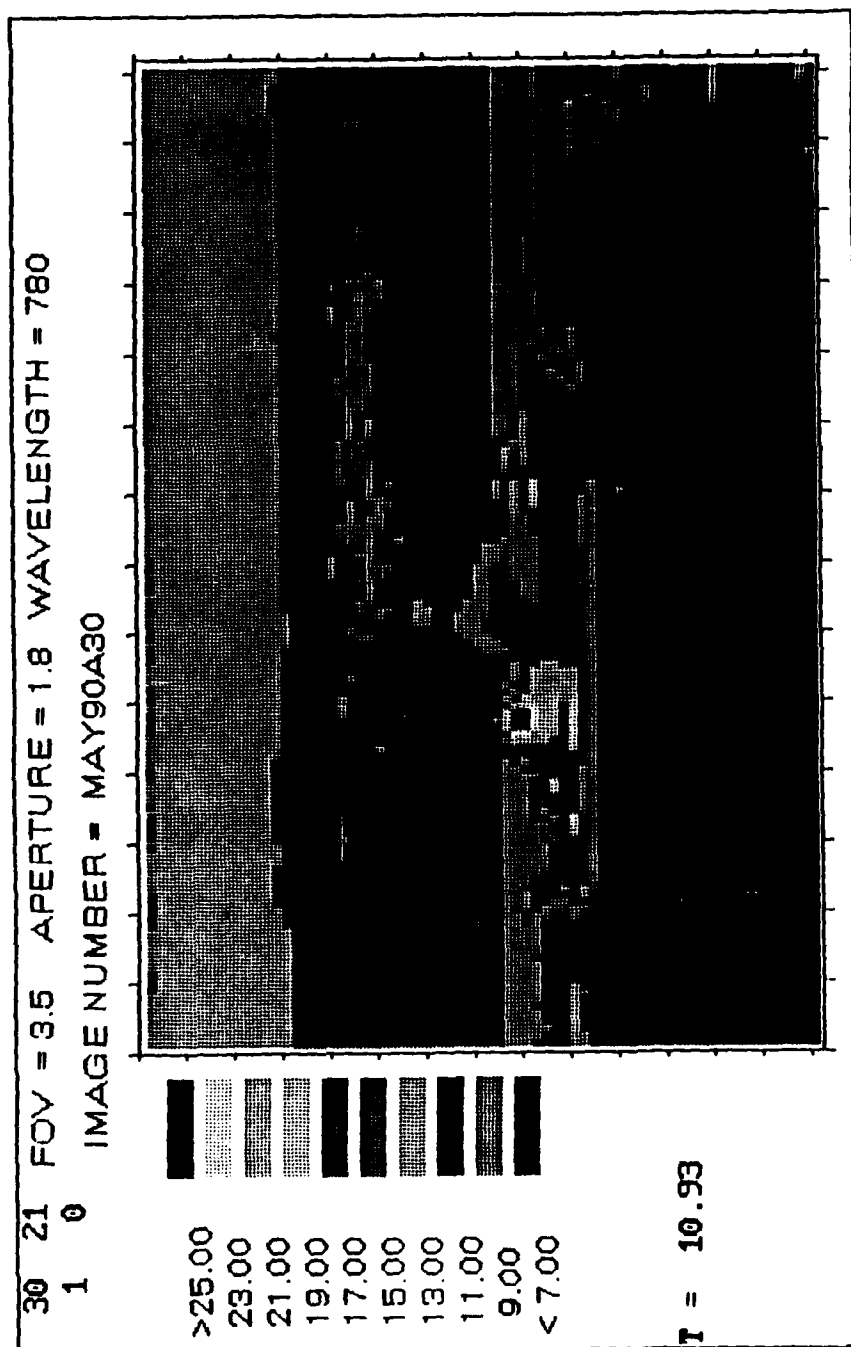
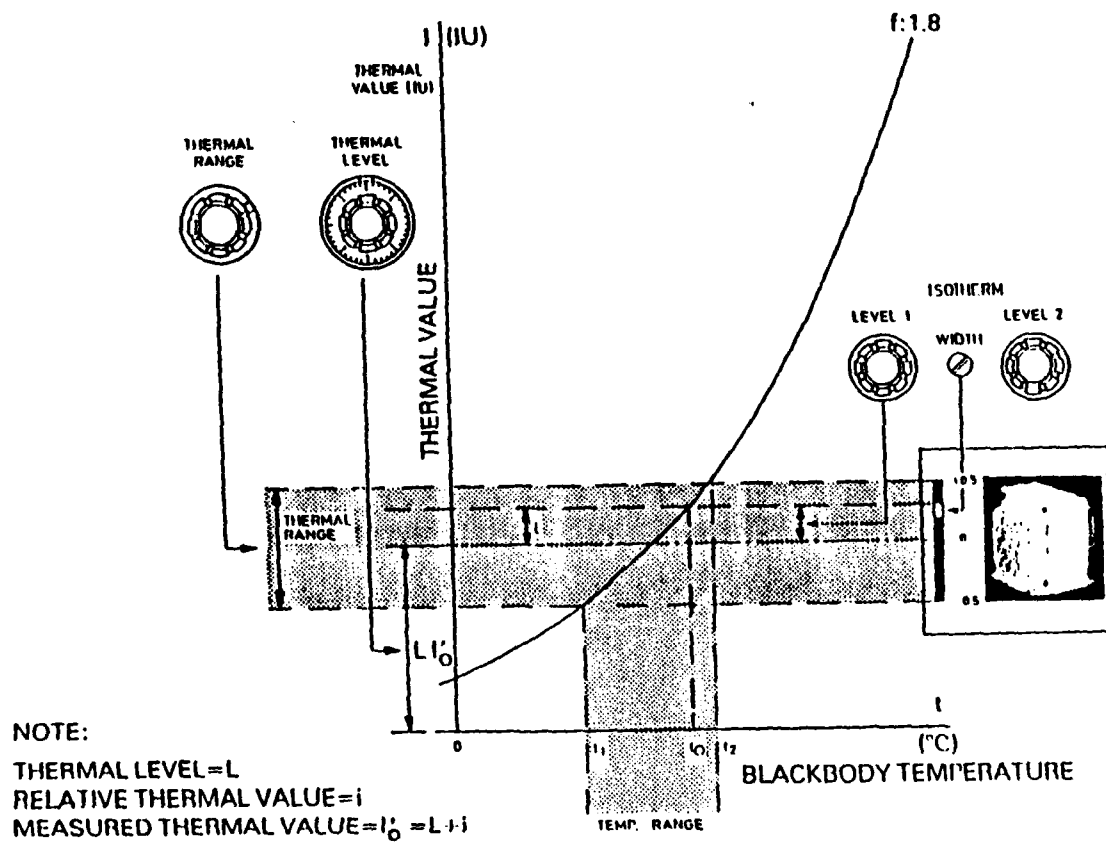


Figure 3.3: AGACATS image transferred from the TIC 8000 configured with the CATS E program.



**Figure 3.4: Measurements utilizing the thermal level and thermal range settings.**

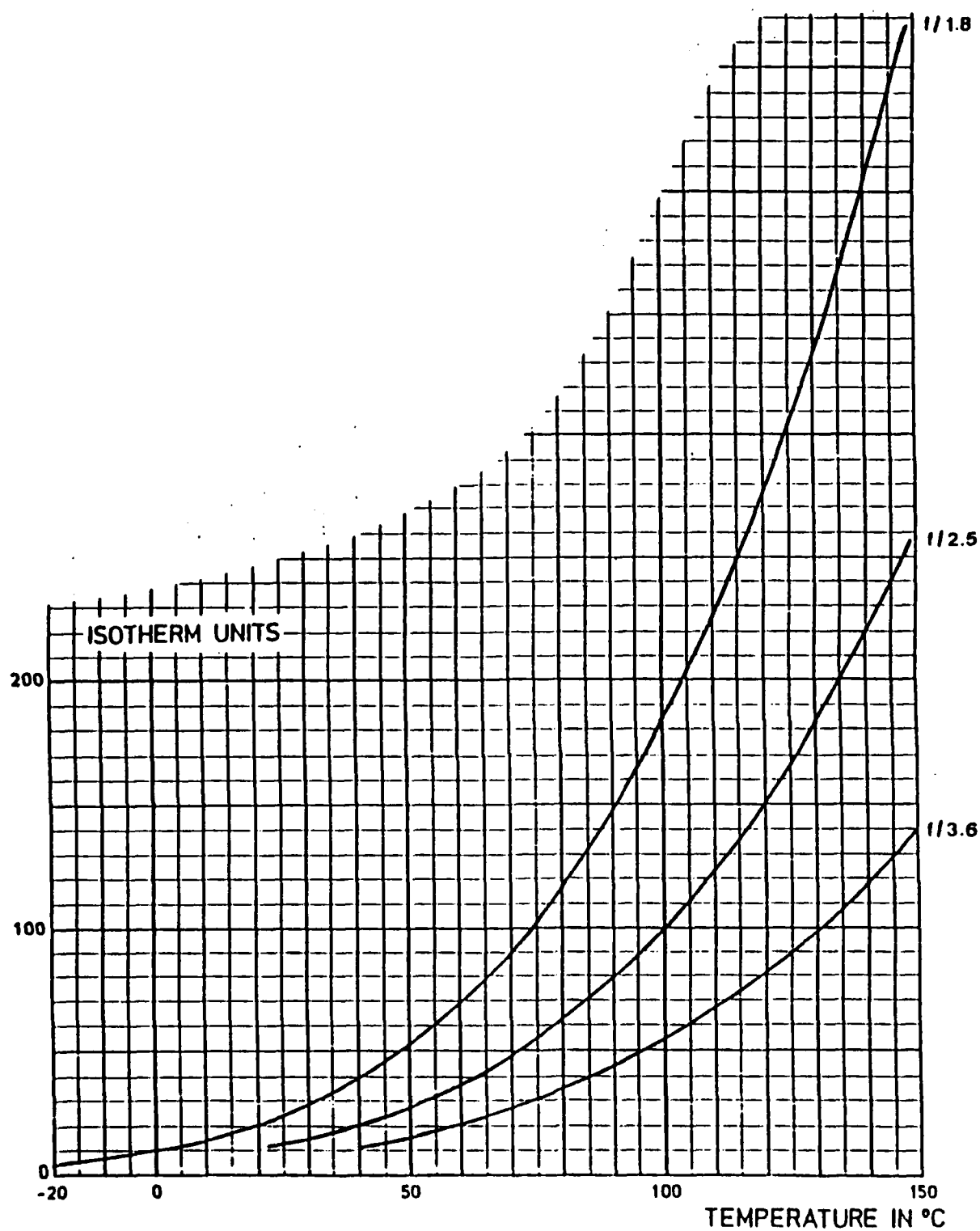
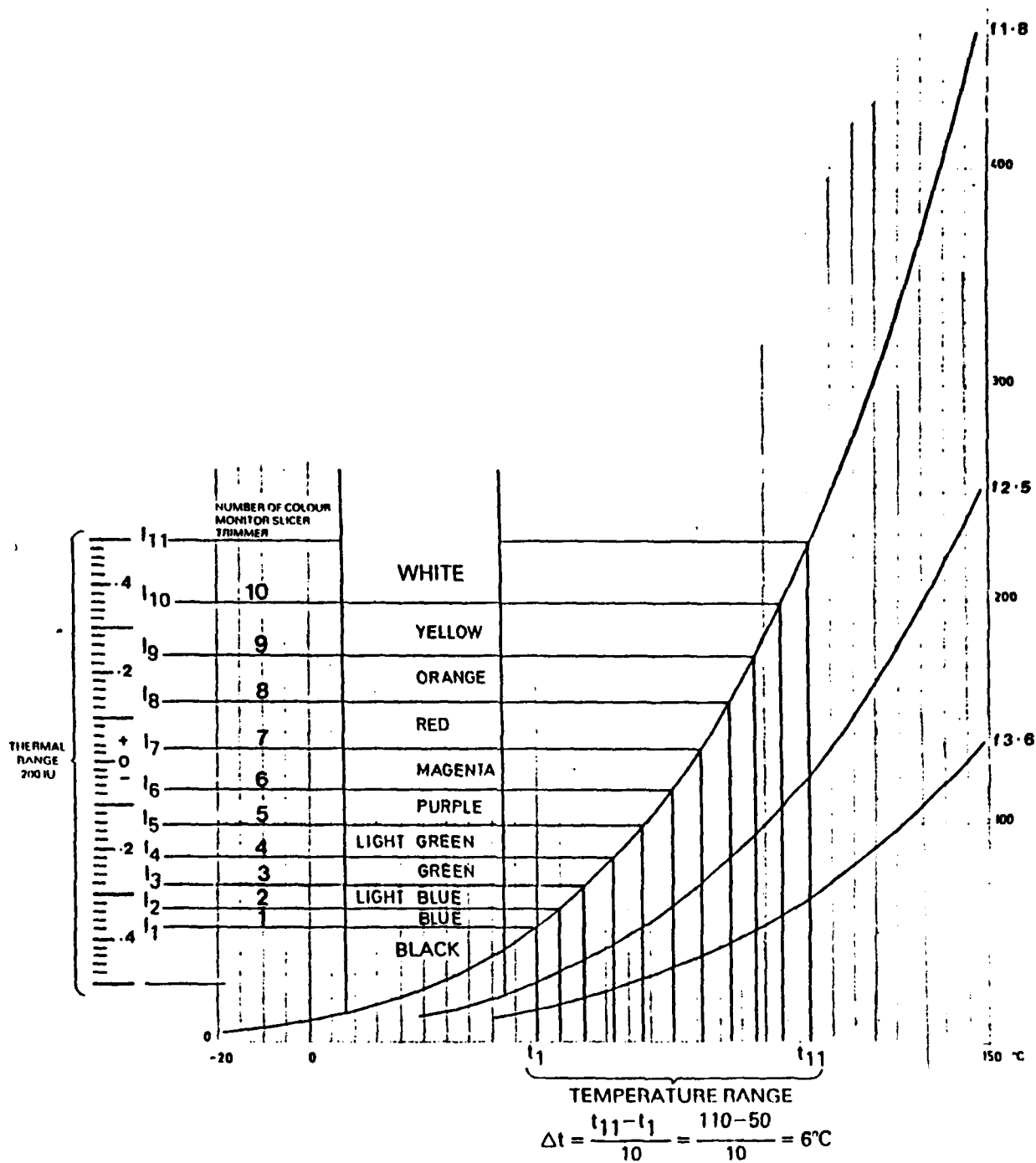


Figure 3.5: Calibration curves used for translating the measured thermal value  $I'_0$  to temperature.



**Figure 3.6: Conversion of the linear color scale with corresponding non-linear temperature to a non-linear color scale with a linear temperature relationship.**

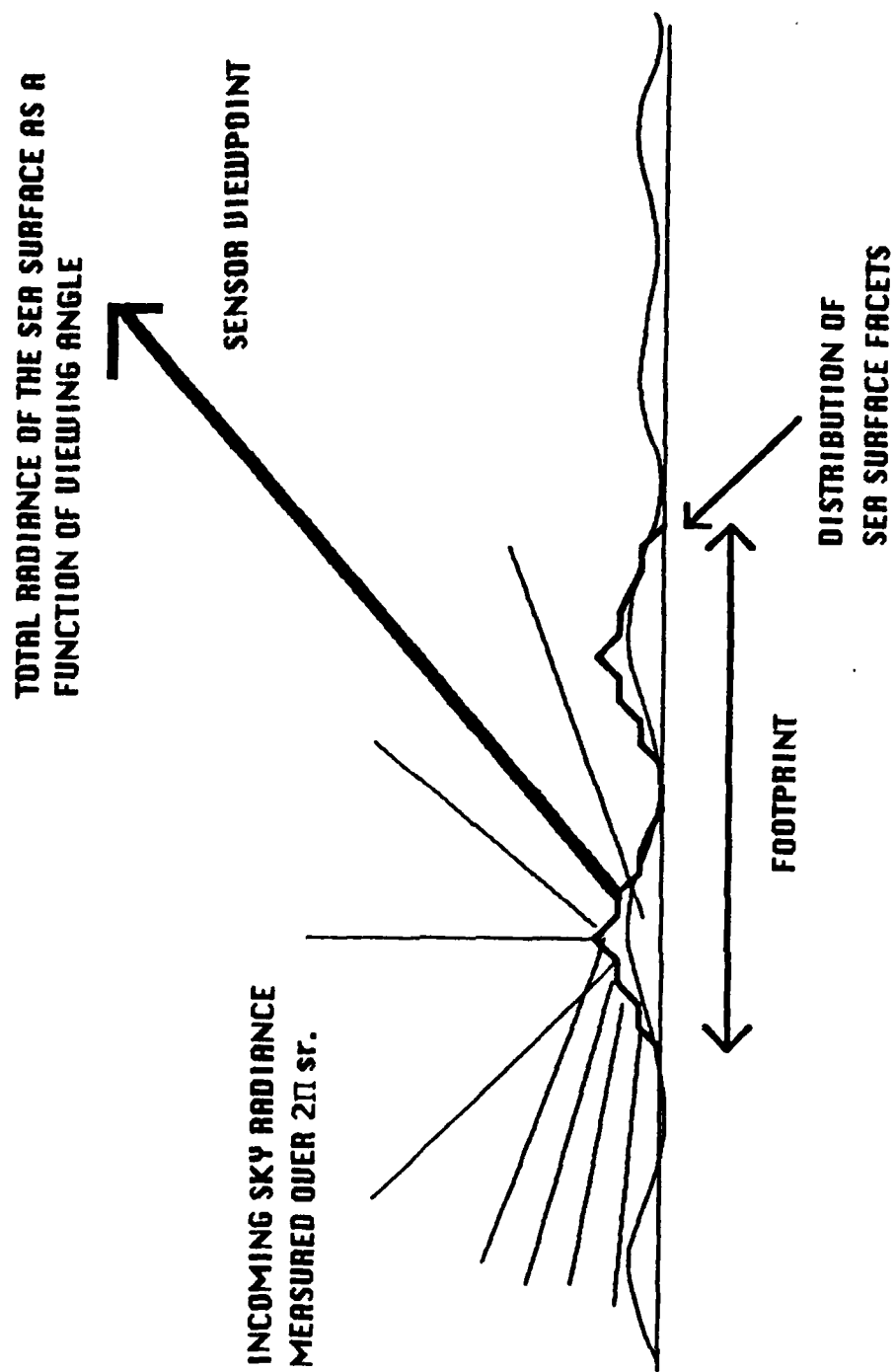


Figure 4.1: A probabilistic model of the radiance of a rough sea surface.

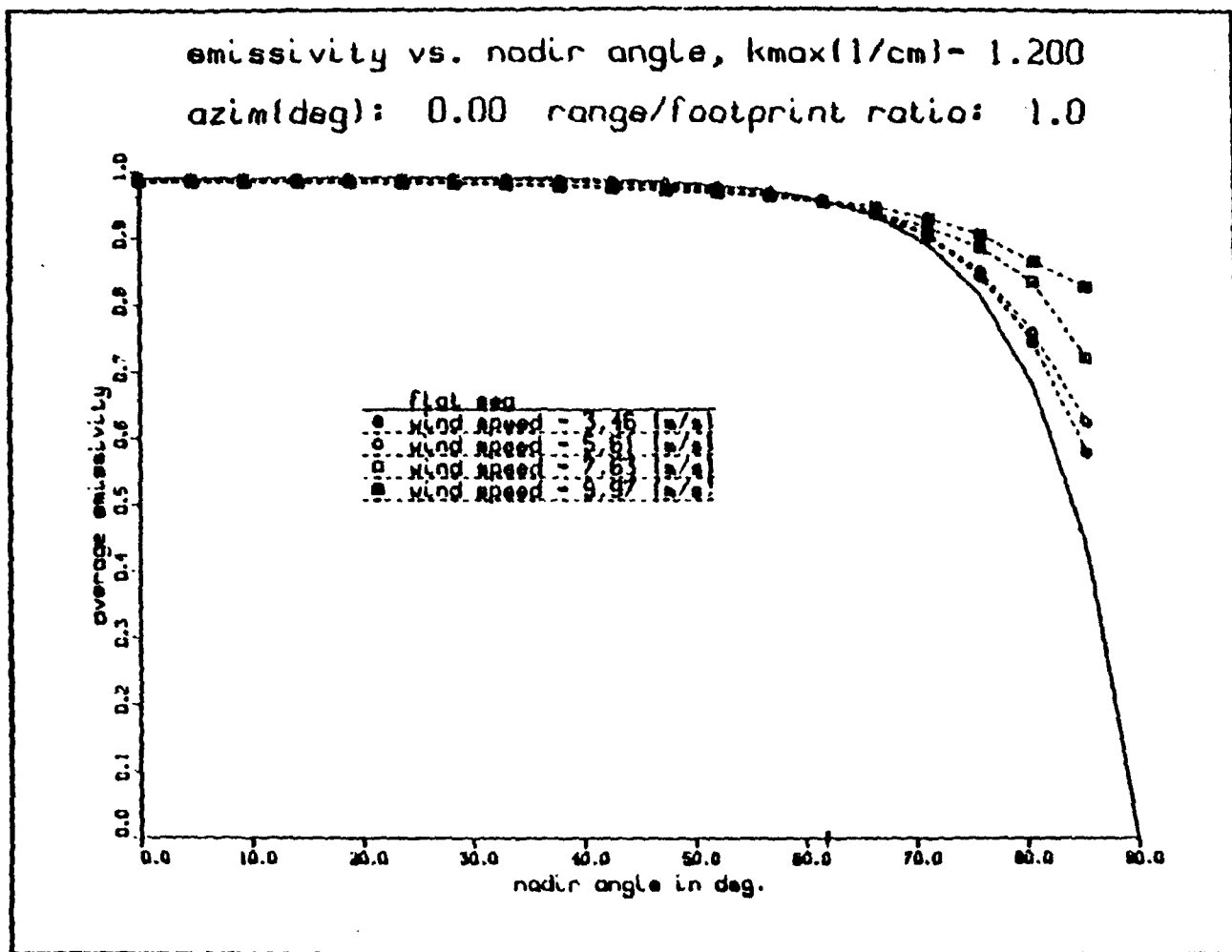


Figure 4.2: Emissivity vs. nadir angle [Ref. 1: p. 25].

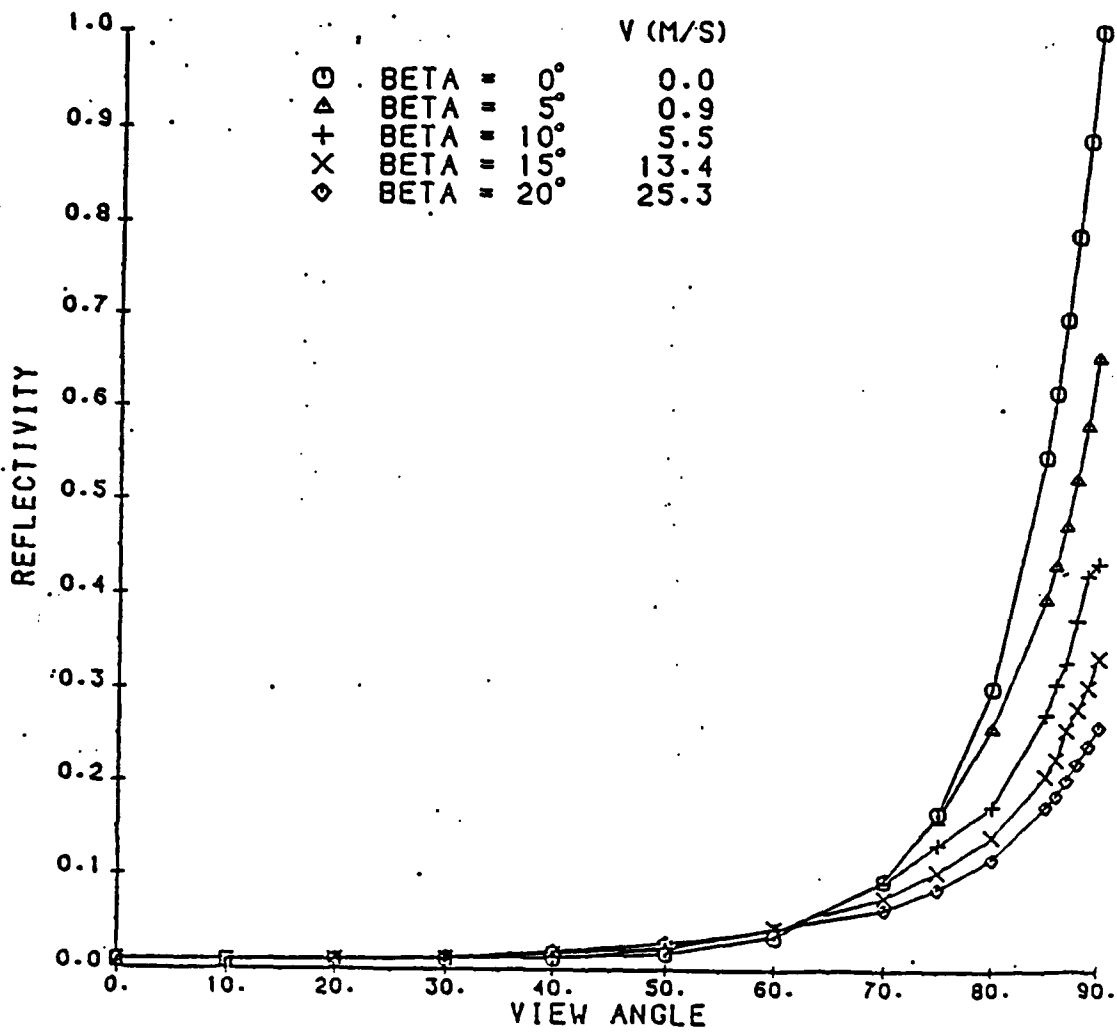


Figure 4.3: Average infrared reflectivity of the ocean surface 8-14  $\mu\text{m}$  as a function of view angle ( $\theta_V$ ) and wave slope angle ( $B$ ) caused by changes in wind velocity.

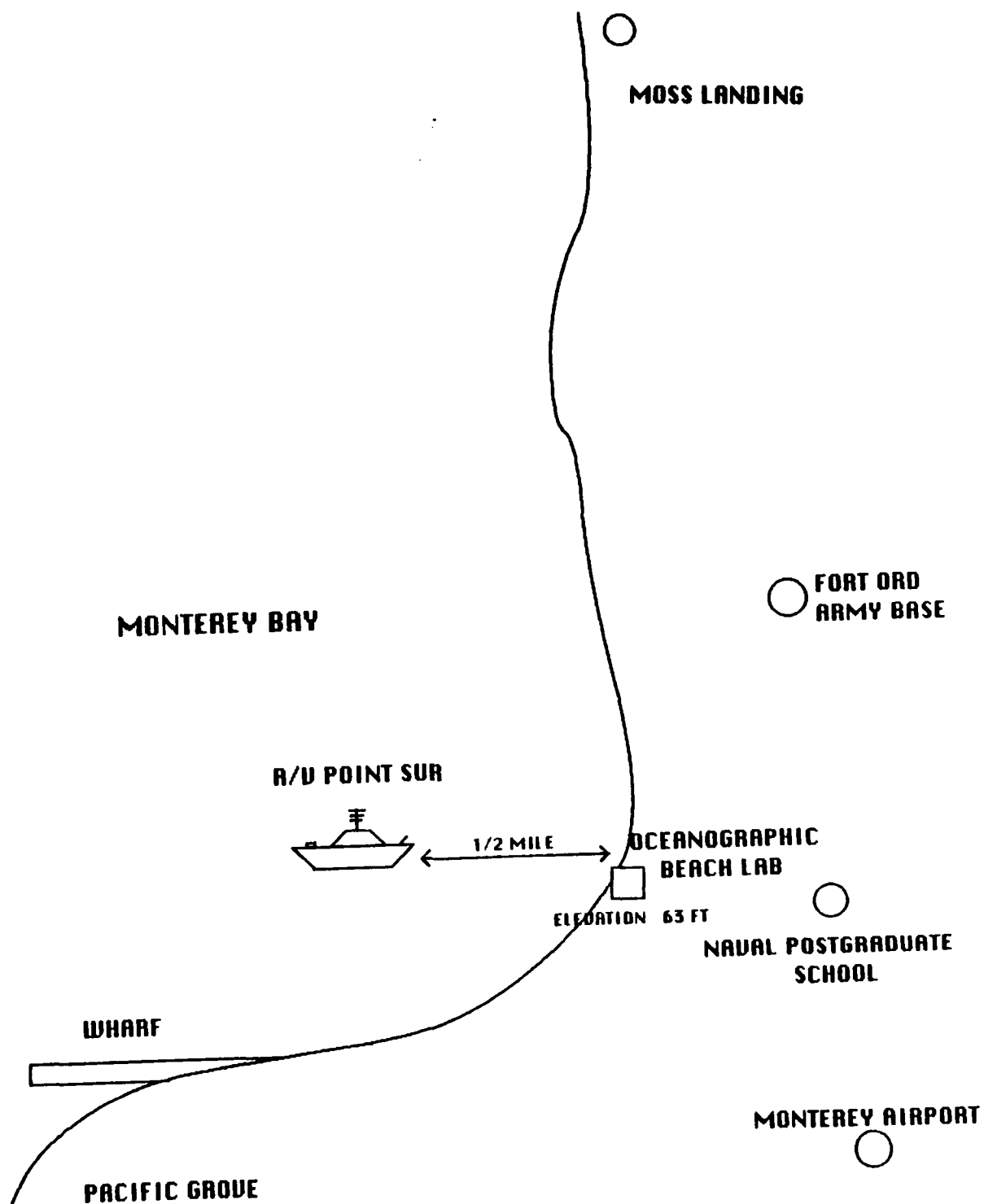
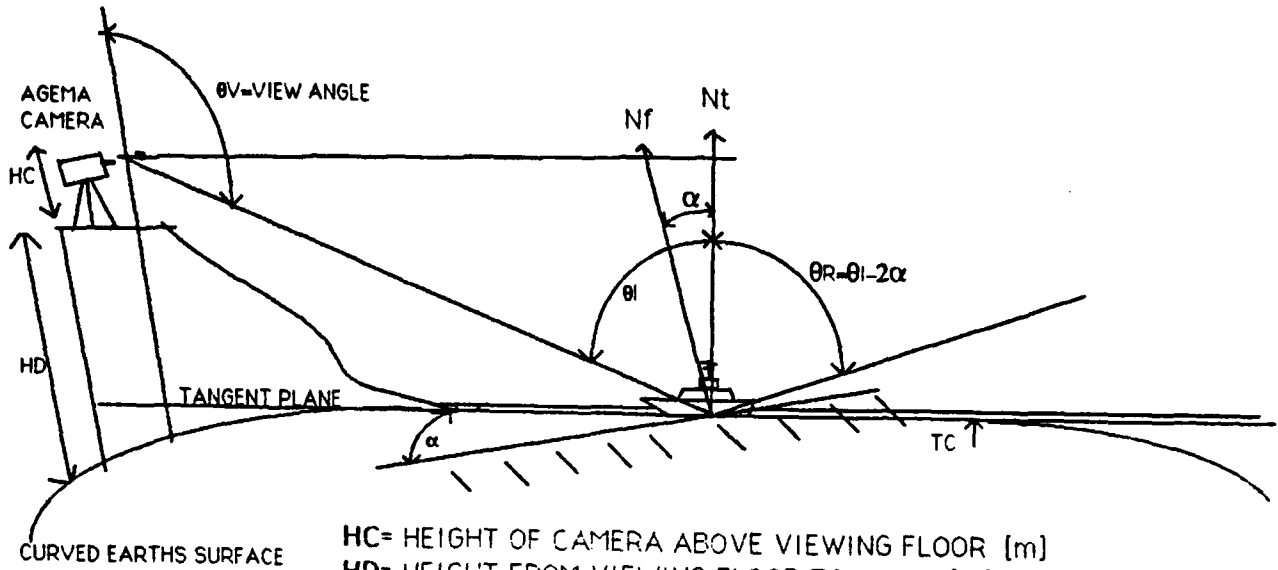


Figure 4.4: Experiment site.





$HC$  = HEIGHT OF CAMERA ABOVE VIEWING FLOOR [m]  
 $HD$  = HEIGHT FROM VIEWING FLOOR TO MLLW [m]  
 $TC$  = CURRENT WAVE HEIGHT [m]  
 $H$  = HEIGHT OF CAMERA =  $HC + HD + TC$  [m]  
 $\theta_V$  = VIEW ANGLE AT OBSERVER HEIGHT  $H$  (DEG)  
 $\theta_I$  = ZENITH ANGLE AT REFLECTION POINT OF REFLECTED RAY (DEG)  
 $\theta_R$  = ZENITH ANGLE AT REFLECTION POINT OF INCIDENT RAY (DEG) (SKY RADIANCE OUTPUT FROM SCHWARTZ AND HON)  
 $\alpha$  = WAVE TILT (DEG)  
 $N_f$  = NORMAL TO TILTED SMOOTH WATER SURFACE  
 $N_t$  = NORMAL TO TANGENT PLANE OF EARTH'S SURFACE = 0 DEGREE ELEVATION ANGLE

**Figure 4.5: AGA set up picture inputs to the Schwartz-Hon algorithm.**

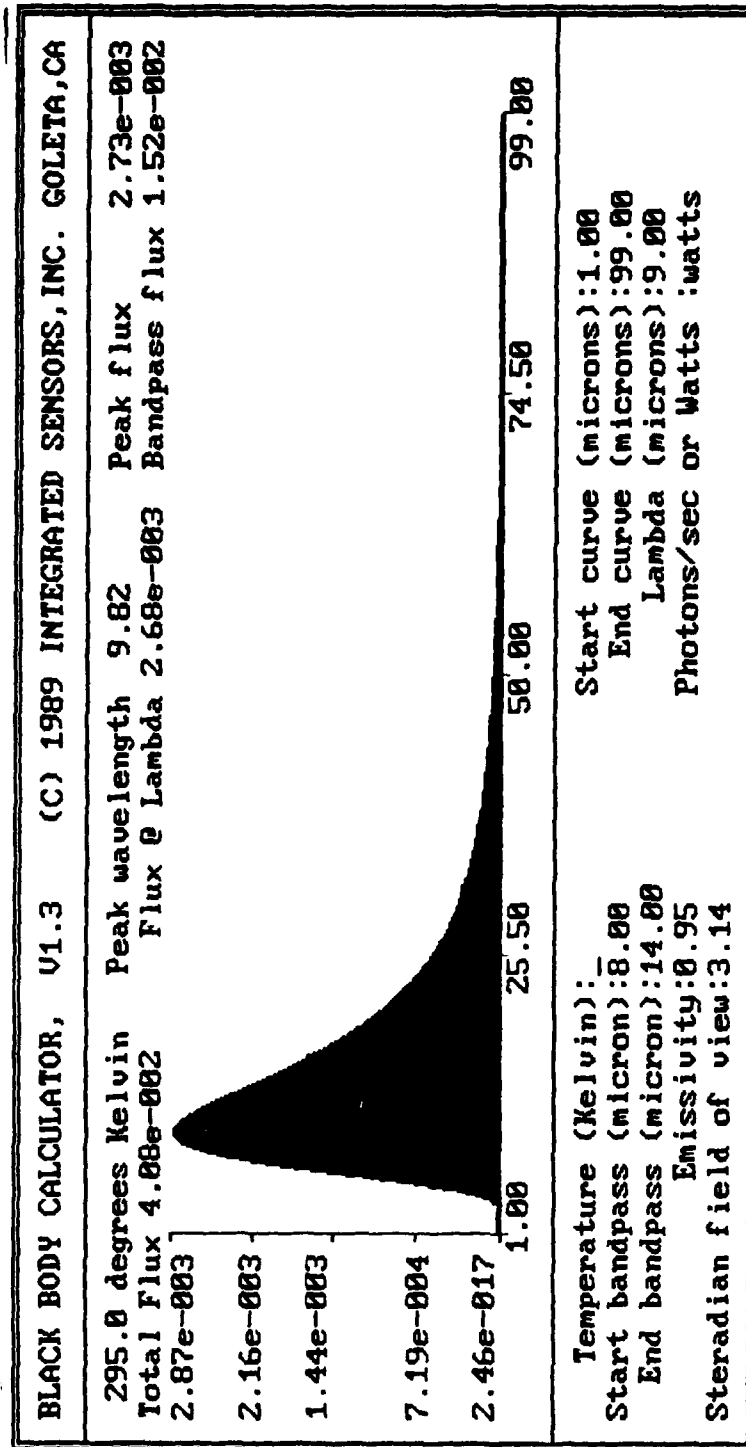
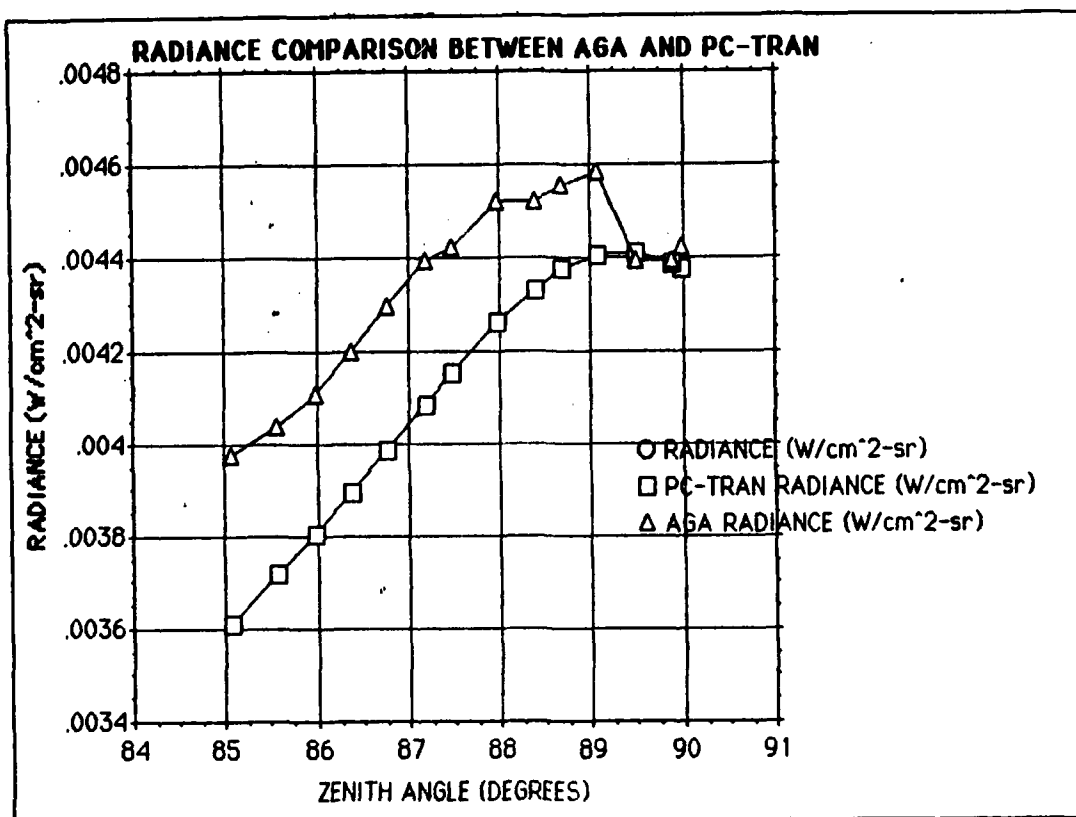


Figure 4.6: Blackbody calculator.



**Figure 5.1: Sky radiance comparison between AGA and PC-TRAN measured radiance for zenith angles between 85–90 degrees (May 2, 1990).**

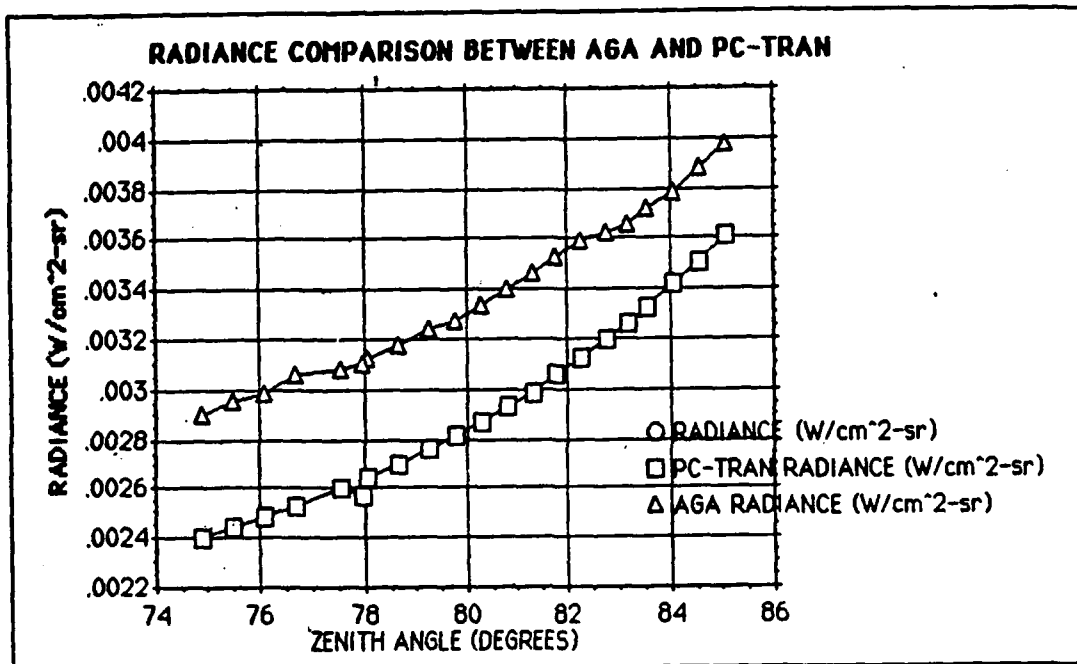


Figure 5.2: Sky radiance comparison between AGA and PC-TRAN measured radiance for zenith angles between 75–85 degrees (May 2, 1990).

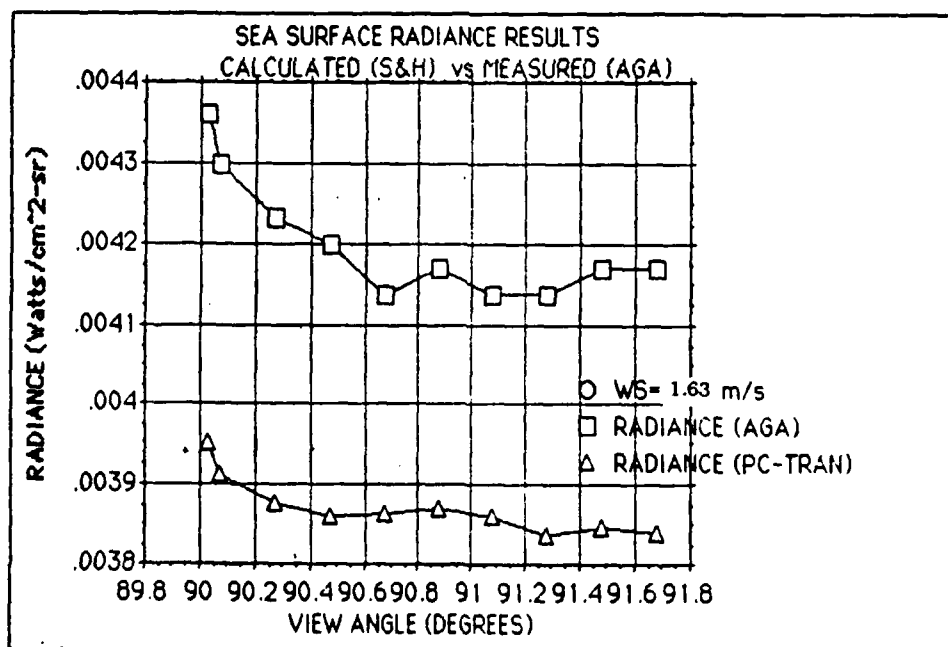


Figure 5.3: Calculated vs. measured radiance using the Schwartz-Hon algorithm at low grazing angles (May 2, 1990).

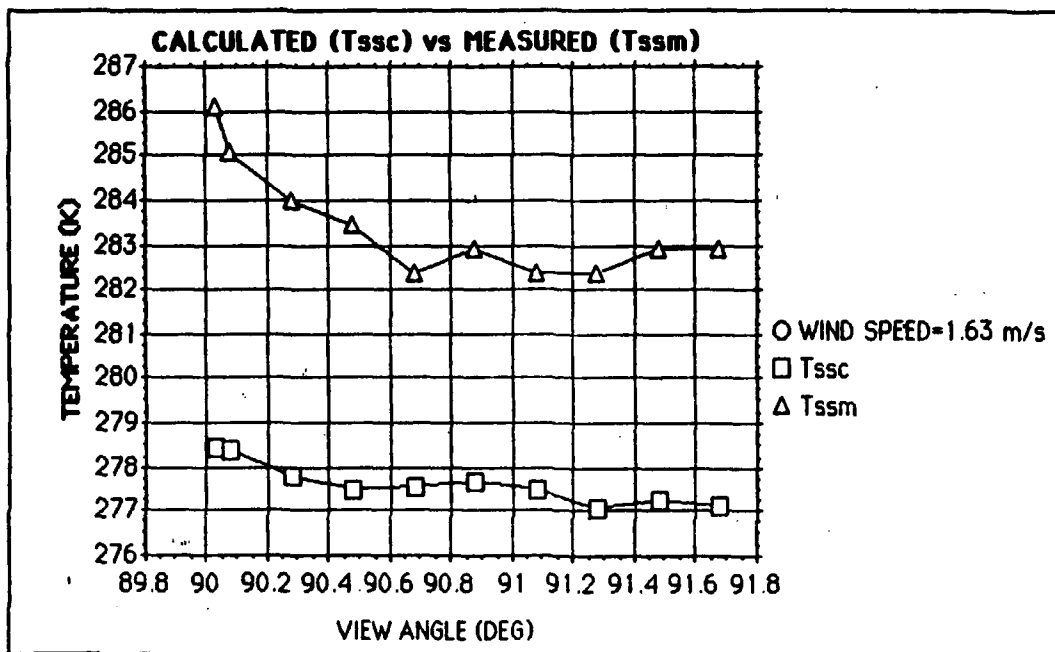


Figure 5.4: Calculated vs. measured effective in-band blackbody sea surface temperature at low grazing angles using the Schwartz-Hon algorithm (May 2, 1990).

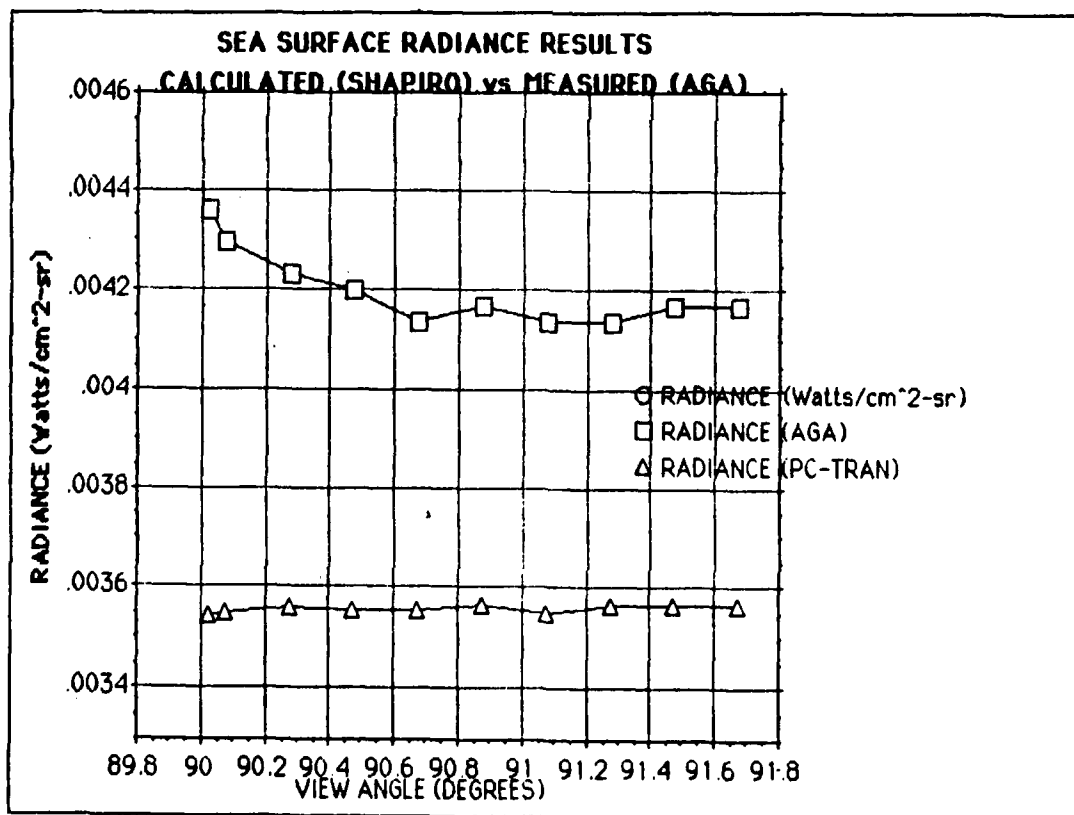


Figure 5.5: Calculated vs. measured radiance using the Shapiro algorithm and PC-TRAN at low grazing angles (May 2, 1990).

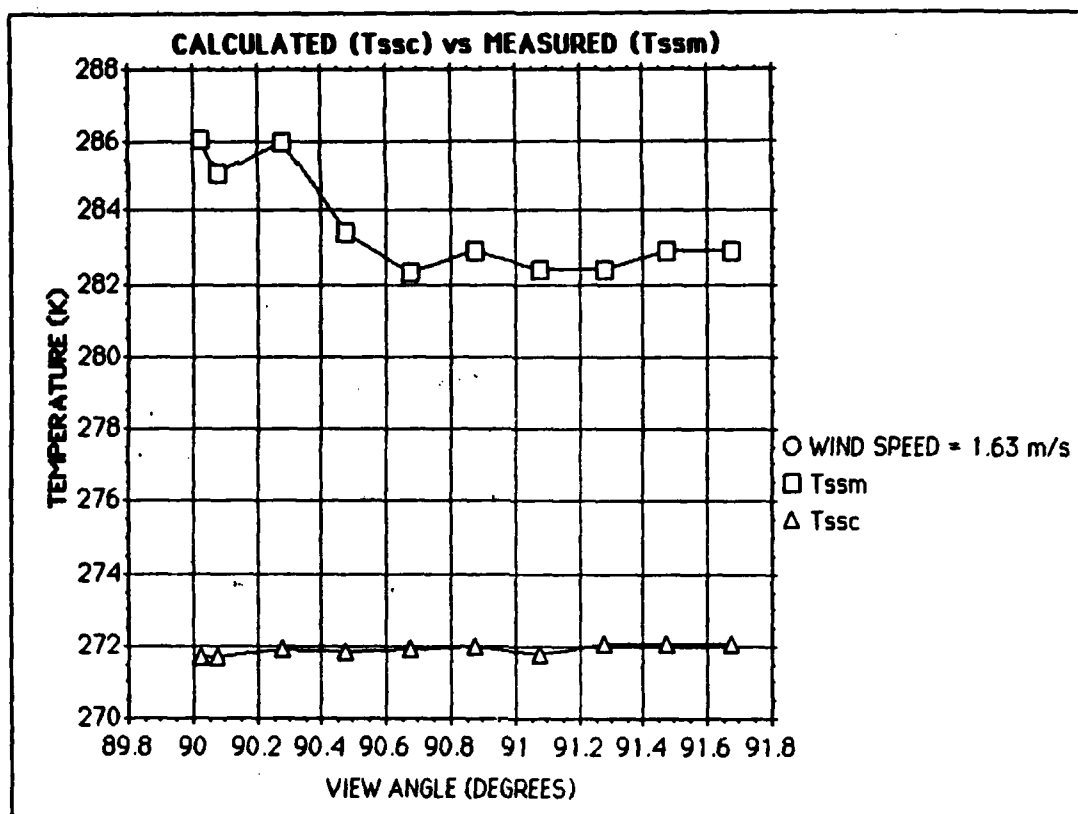
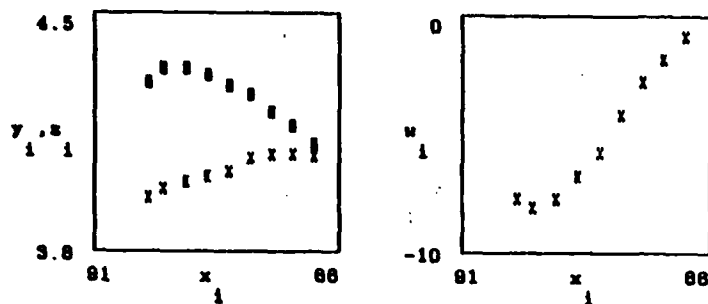
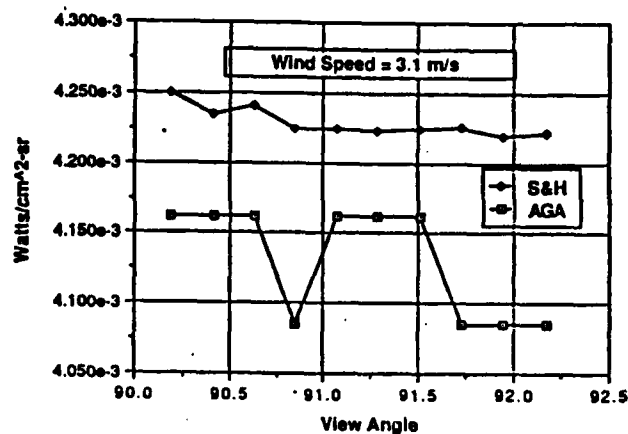


Figure 5.6: Calculated vs. measured effective in-band blackbody sea surface temperature at low grazing angles using the Shapiro algorithm (May 2, 1990).



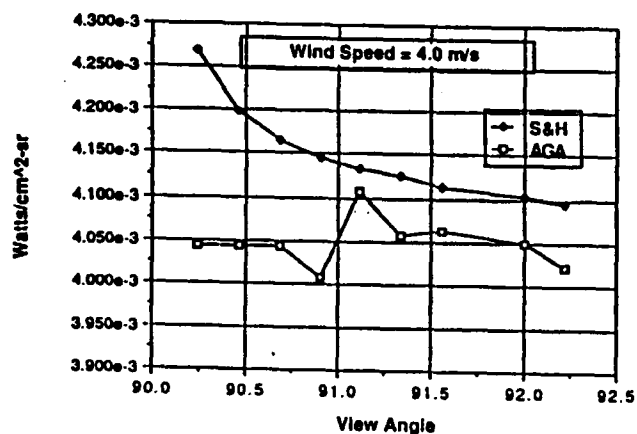
wind speed = 2.057 m/sec

Fair sky radiance vs zenith angle (4NOV 87)  
 $x_1$  = zenith angle (°)  
 $y_1$  = AGA radiance ( $\text{mW}/\text{cm}^2\text{-sr}$ ) (rectangle points)  
 $z_1$  = LOWTRAN 6 radiance ( $\text{mW}/\text{cm}^2\text{-sr}$ ) (x points)  
 $w_1$  = error =  $(z_1/y_1 - 1) \%$



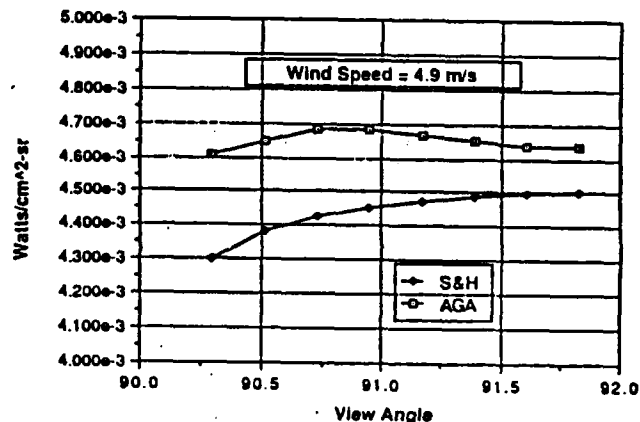
(UNCLASSIFIED)

Calculated (S&H) vs. Measured (AGA)  
 Sea Surface Radiance Results for View Angles Near the  
 Horizon (14 Jul 88 Experiment)



(UNCLASSIFIED)

Calculated (S&H) vs. Measured (AGA)  
 Sea Surface Radiance Results for View Angles Near the  
 Horizon (15 Jul 88 Experiment)



(UNCLASSIFIED)

Calculated (S&H) vs. Measured (AGA)  
 Sea Surface Radiance Results for View Angles Near the  
 Horizon (25 Jul 88 Experiment)

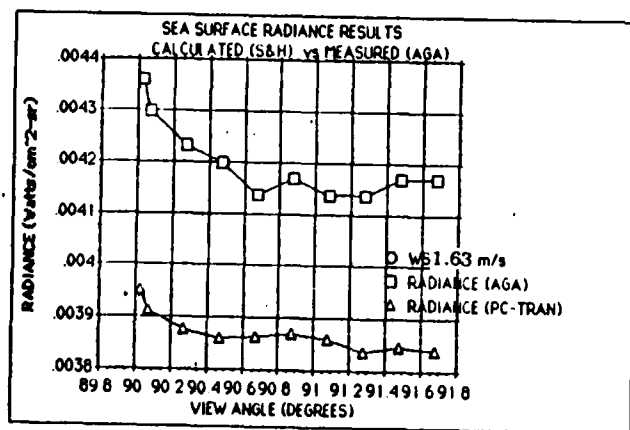


Figure 5.7: Synopsis of Schwartz-Hon validation experiments at low grazing angles performed from 1987 to 1990.

PERCENTAGE ERROR BETWEEN CALCULATED AND  
MEASURED SEA SURFACE RADIANCE VS WIND SPEED

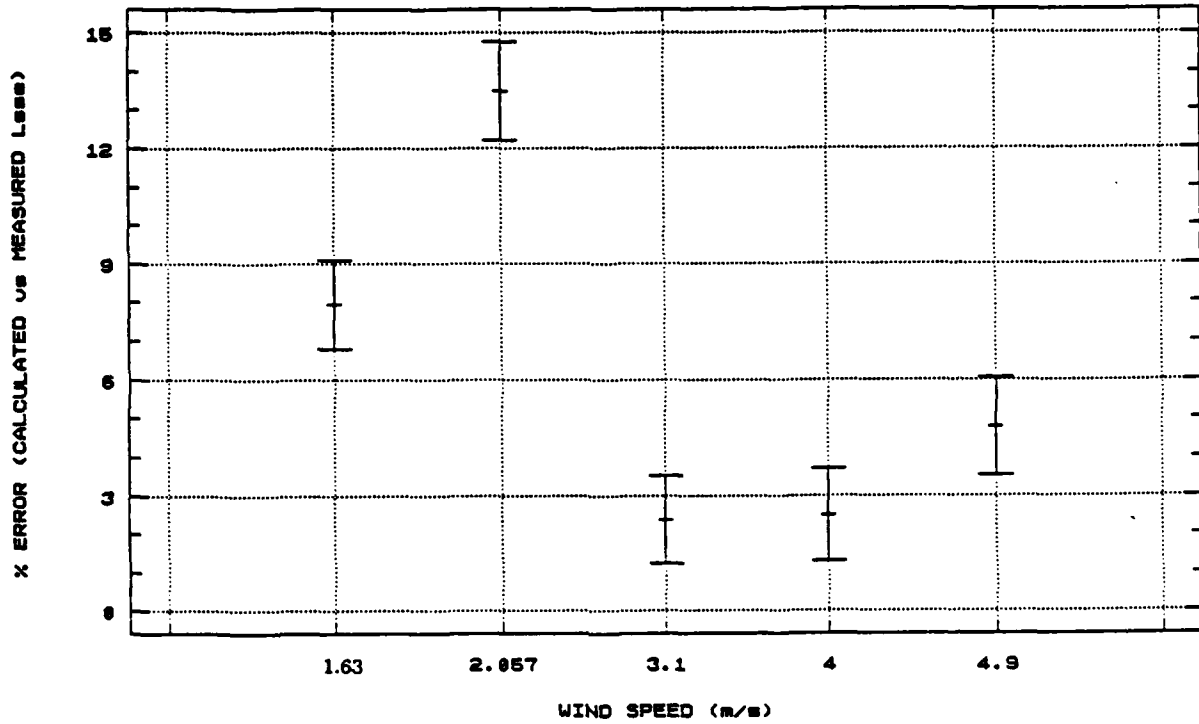


Figure 5.8: Percentage error between  $L_{SSC}$  and  $L_{SSM}$  at one standard deviation as a function of wind speed.



## APPENDIX B

### TABLES

Table 2.1

**Values of the Spectral Integral of the Thermal Derivative of  
Planck's Law for Wavelengths Ranging from 3–14  $\mu\text{m}$   
[Ref. 6: p. 28]**

		$\frac{\partial W}{\partial T} = \int_{\lambda_1}^{\lambda_2} \frac{\partial W_{\lambda}(T_B)}{\partial T} d\lambda \left[ \frac{w}{\text{cm}^2 \cdot ^\circ\text{K}} \right] \text{ for}$			
$\lambda_1 [\mu\text{m}]$	$\lambda_2 [\mu\text{m}]$	$T_B = 280^\circ\text{K}$	$T_B = 290^\circ\text{K}$	$T_B = 300^\circ\text{K}$	$T_B = 310^\circ\text{K}$
3	5	$1.1 \times 10^{-5}$	$1.54 \times 10^{-5}$	$2.1 \times 10^{-5}$	$2.81 \times 10^{-5}$
3	5.5	$2.01 \times 10^{-5}$	$2.73 \times 10^{-5}$	$3.62 \times 10^{-5}$	$4.72 \times 10^{-5}$
3.5	5	$1.06 \times 10^{-5}$	$1.47 \times 10^{-5}$	$2 \times 10^{-5}$	$2.65 \times 10^{-5}$
3.5	5.5	$1.97 \times 10^{-5}$	$2.66 \times 10^{-5}$	$3.52 \times 10^{-5}$	$4.57 \times 10^{-5}$
4	5	$9.18 \times 10^{-6}$	$1.26 \times 10^{-5}$	$1.69 \times 10^{-5}$	$2.23 \times 10^{-5}$
4	5.5	$1.83 \times 10^{-5}$	$2.45 \times 10^{-5}$	$3.22 \times 10^{-5}$	$4.14 \times 10^{-5}$
8	10	$8.47 \times 10^{-5}$	$9.65 \times 10^{-5}$	$1.09 \times 10^{-4}$	$1.21 \times 10^{-4}$
8	12	$1.58 \times 10^{-4}$	$1.77 \times 10^{-4}$	$1.97 \times 10^{-4}$	$2.17 \times 10^{-4}$
8	14	$2.15 \times 10^{-4}$	$2.38 \times 10^{-4}$	$2.62 \times 10^{-4}$	$2.86 \times 10^{-4}$
10	12	$7.34 \times 10^{-5}$	$8.08 \times 10^{-5}$	$8.81 \times 10^{-5}$	$9.55 \times 10^{-5}$
10	14	$1.3 \times 10^{-4}$	$1.42 \times 10^{-4}$	$1.53 \times 10^{-4}$	$1.65 \times 10^{-4}$
12	14	$5.67 \times 10^{-5}$	$6.10 \times 10^{-5}$	$6.52 \times 10^{-5}$	$6.92 \times 10^{-5}$

**Table 3.1**  
**Individual Calibration of the 780 Dual Scanner**



**INDIVIDUAL CALIBRATION OF: 780 LWB**

**SERIAL NUMBERS**

Scanner : 4011  
 Detector : LWB  
 Filter : NOF  
 Lens : 3.5, s/n 8121

**CALIBRATION CONDITIONS**

Ambient Temperature : 22°C  
 Relative Humidity : 50%  
 Objective Distance : 2m  
 Calibration Date : 4/26/90  
 Operator : Al Fudali

**CALIBRATION CURVE CONSTANTS**

Aperture	A	B	C
1.8	-2514	1654	-0.2
2.5	-2260	1705	-0.3
3.6	-1304	1876	-0.2
5.1	-1193	1933	-0.3
7.2	-1973	1940	-1.0
10	900	1802	1.0
14	-3847	2122	-4.3
20	- 207	2546	-0.2

**Table 4.1**

**PC-TRAN Inputs**

\* Indicates input used in Schwartz-Hon Model analysis.

1. **ATMOSPHERIC MODEL**
  - A. Specify meteorological data
  - B. Tropical model atmosphere
  - C. Midlatitude summer
  - D. Midlatitude winter
  - E. Subarctic summer
  - F. Subarctic winter
  - G. 1962 U.S. standard
  - \*H. Radiosonde data
2. **TYPES OF ATMOSPHERIC PATH**
  - A. Horizontal
  - \*B. Vertical or slant path between two altitudes
  - C. Vertical or slant path to space
3. **MODES OF EXECUTION**
  - A. Transmittance mode
  - \*B. Radiance mode
4. **SPECIFY TEMPERATURE/PRESSURE ALTITUDE PROFILES TO BE USED**
  - \*A. Normal
5. **SPECIFY WATER VAPOR ALTITUDE PROFILE USED**
  - \*A. Normal
6. **OZONE PROFILE**
  - \*A. Normal
  - B. Tropical
  - C. Midlatitude summer
  - D. Midlatitude winter
  - E. Subarctic summer
  - F. Subarctic winter
  - G. 1962 U.S. standard atmosphere
7. **SPECIFY NORMAL OPERATIONS OR RADIOSONDE DATA WILL BE USED EITHER INITIALLY OR ON SUBSEQUENT RUNS**
  - A. Normal
  - \*B. Radiosonde
8. **SPECIFY NORMAL OPERATIONS OR SUPPRESS PRINTING**
  - \*A. Normal
  - B. Suppress printing
9. **TEMPERATURE OF THE EARTH AT THE LOCATION AT WHICH CALCULATION IS TO BE PERFORMED**

- \*A.(from data)
- 10. SPECIFY THE SURFACE ALBEDO OF THE EARTH
  - \*A.Assume blackbody default
- 11. EXTINCTION TYPE
  - A.No aerosol attenuation
  - B.Rural extinction, 23 km VIS
  - C.Rural extinction, 5 km VIS
  - \*D.Navy maritime
  - E.Maritime, 23 km VIS
  - F.Urban, 5 km VIS
  - G.Troposphere, 50 km VIS
  - H.User defined
  - I. Fog 1, 0.2 km VIS
  - J. Fog 2, 0.5 km VIS
- 12. SEASONAL DEPENDENCE OF PROFILES
  - \*A.Default to season of model
  - B.Spring/summer
  - C.Fall/winter
- 13. PROFILE AND EXTINCTION FOR STRATOSPHERIC AEROSOLS
  - \*A.Default to stratospheric background
  - B.Stratospheric background
  - C.Aged volcanic type/moderate volcanic profile
  - D.Fresh volcanic type/high volcanic profile
  - E.Aged volcanic type/high volcanic profile
- 14. SPECIFY AIR MASS CHARACTER
  - A.Open ocean
  - \*B.3
  - .
  - .
  - .
  - .
  - J. Strong continental influence
- 15. DETERMINE THE INCLUSION OF CIRRUS ATTENUATION
  - \*A.No cirrus
  - B.Use cirrus profile
- 16. U.S. ARMY VERTICAL STRUCTURE ALGORITHM (not used)
- 17. SPECIFY METEOROLOGICAL RANGE (km) (default)
- 18. CURRENT WIND SPEED (from data)
- 19. 24 HOUR AVERAGE WIND SPEED (from data)
- 20. PRECIPITATION RATE (0 from data)
- 21. ATMOSPHERIC LEVELS

- \*A.Initial altitude (0 at target)
- \*B.Final altitude (0 at target)
- \*C.Initial zenith angle as measured from the initial altitude ( $\theta_R$  from Schwartz-Hon)
- D.Path length
- E.Earth center angle subtended by the initial and final altitudes

## 22. RADIUS OF THE EARTH

- A.Specify radius
- \*B.Default (6371.23 km)

## 23. PROGRAM OPERATION

- \*A.Normal program operation
- B.Select downward type two long path

## 24. SPECTRAL RANGE (corresponds to 8–12 $\mu\text{m}$ band)

- \*A.Initial frequency ( $833.0 \text{ cm}^{-1}$ )
- \*B.Final frequency ( $1250 \text{ cm}^{-1}$ )
- \*C.Frequency increment ( $5 \text{ cm}^{-1}$ )

**Table 4.2**  
**Shipboard Meteorological Readings**  
**R/V POINT SUR**  
**May 2, 1990**

Lat (N)	Long (W)	Month	Day	Time (Z)	Wind Dir (°)	Wind Spd (m/s)	SS Temp (°C)	DP Temp (°C)	Rel Hum	Air Temp (°C)
36-36.6	121-152.8	5	2	1807	090	1.49	10.37	10.02	9.56	13.89
36-36.6	121-152.8	5	2	1812	097	1.46	10.34	9.53	9.48	13.71
36-36.6	121-152.8	5	2	1817	157	1.60	10.45	9.70	9.51	13.70
36-36.9	121-152.8	5	2	1822	131	1.79	10.82	9.69	9.27	14.16
36-37.0	121-152.8	5	2	1827	023	3.05	11.85	9.61	8.62	14.20
36-37.0	121-152.8	5	2	1832	031	3.05	12.45	9.30	8.12	13.94
36-37.0	121-152.8	5	2	1837	136	2.99	12.86	9.03	7.76	13.83
36-37.4	121-153.3	5	2	1842	131	2.66	13.23	9.02	7.57	14.15
36-37.8	121-154.1	5	2	1847	131	2.59	13.95	9.27	7.34	13.83
36-38.2	121-155.0	5	2	1852	131	2.27	13.14	8.90	7.55	13.26
36-38.7	121-155.8	5	2	1857	131	2.10	11.39	8.52	8.25	12.74
36-39.0	121-156.6	5	2	1902	131	1.93	10.52	8.37	8.66	12.53
36-38.6	121-157.3	5	2	1907	131	1.86	11.73	8.33	7.97	12.06
36-37.8	121-157.8	5	2	1912	131	1.76	11.56	8.39	8.10	12.12
36-37.1	121-158.2	5	2	1917	131	1.66	10.90	8.47	8.50	11.70
36-36.4	121-158.7	5	2	1922	132	1.64	10.23	8.49	8.90	11.73
36-35.7	121-159.2	5	2	1927	131	1.63	10.06	8.45	8.97	11.07
36-35.0	121-159.6	5	2	1932	136	1.60	9.90	8.46	9.07	10.44
36-34.3	121-159.9	5	2	1937	137	1.59	10.41	8.56	8.83	10.12
36-33.6	121-159.8	5	2	1942	135	1.59	11.01	8.58	8.50	10.03
36-32.8	121-159.5	5	2	1947	133	1.61	11.11	8.53	8.41	10.11
36-32.1	121-159.3	5	2	1952	131	1.59	11.13	8.49	8.38	10.27
36-31.4	121-159.0	5	2	1957	131	1.57	11.28	8.42	8.26	10.36
36-30.6	121-158.7	5	2	2002	131	1.56	11.38	8.36	8.17	10.52
36-29.9	121-158.4	5	2	2007	131	1.53	11.56	8.30	8.04	10.71
36-29.1	121-158.3	5	2	2012	131	1.51	11.52	8.28	8.05	10.89
36-28.3	121-158.2	5	2	2017	131	1.49	11.55	8.28	8.04	10.97
36-27.5	121-158.1	5	2	2022	131	1.43	11.46	8.32	8.11	10.91
36-26.7	121-157.8	5	2	2027	131	1.42	11.49	8.24	8.05	10.70
36-26.0	121-157.6	5	2	2032	131	1.42	11.45	8.25	8.07	10.23
36-25.2	121-157.4	5	2	2037	131	1.36	11.16	8.28	8.25	10.31
36-24.3	121-157.1	5	2	2042	131	1.49	11.29	8.14	8.10	10.25
36-23.6	121-156.8	5	2	2047	131	1.49	11.11	8.08	8.16	10.24
36-23.0	121-156.4	5	2	2052	131	1.42	11.12	8.07	8.15	10.24
36-22.3	121-156.0	5	2	2057	131	1.49	11.30	8.04	8.04	10.16
36-21.5	121-155.7	5	2	2102	131	1.44	11.46	8.09	7.98	10.19
36-20.8	121-155.3	5	2	2107	131	1.39	11.64	8.00	7.84	10.18
36-20.4	121-155.0	5	2	2112	131	1.46	10.71	7.95	8.32	10.06
36-20.4	121-155.0	5	2	2117	131	1.58	9.87	7.95	8.78	10.13
36-20.3	121-155.0	5	2	2122	131	1.60	9.69	7.97	8.90	10.31
36-20.3	121-155.1	5	2	2127	131	1.63	9.66	8.02	8.96	10.38
36-20.3	121-155.1	5	2	2132	131	1.67	9.66	8.11	9.00	10.44
36-20.3	121-155.7	5	2	2137	131	1.51	9.75	8.11	8.96	10.44
36-20.4	121-156.7	5	2	2142	131	1.44	9.77	8.25	9.03	10.45
36-20.4	121-157.7	5	2	2147	131	1.39	9.77	8.27	9.04	10.62
36-20.4	121-158.6	5	2	2152	131	1.41	9.82	8.33	9.04	10.60
36-20.5	121-159.6	5	2	2157	131	1.40	9.89	8.37	9.03	10.55
36-20.5	121-100.6	5	2	2202	131	1.38	9.96	8.41	9.01	10.51
36-20.4	122-101.4	5	2	2207	131	1.33	9.99	8.38	8.98	10.49
36-20.1	122-101.8	5	2	2212	131	1.27	9.99	8.47	9.02	10.44
36-20.0	122-101.7	5	2	2217	131	1.36	9.98	8.54	9.08	10.46
36-20.0	122-101.6	5	2	2222	439	1.36	9.97	8.33	8.77	10.49

**Table 4.3**  
**Monterey Bay Aquarium Weather and**  
**Oceanographic Data Acquisition System**  
**May 2, 1990**

TM: Time of day (hh:mm PST) on May 2, 1990  
WS: Wind speed (m/sec)  
WD: Wind direction (deg T)  
AT: Air temperature (deg C)  
HU: % relative humidity  
BA: Barometric pressure (mbars)  
TH: Tidal height from NOAA tide gauge (m)

TM	WS	WD	AT	HU	BA	TH
10:10	3.42	324	14.16	84	1008.5	0.14
10:15	3.56	321	14.38	84	1008.4	0.13
10:20	2.34	295	14.58	83	1008.4	0.15
10:25	1.02	290	14.79	82	1008.5	0.12
10:30	0.60	269	14.87	81	1008.5	0.11
10:35	1.08	327	15.16	80	1008.4	0.08
10:40	1.05	349	15.27	79	1008.4	0.10
10:45	2.63	356	15.56	78	1008.3	0.09
10:50	2.43	356	15.70	77	1008.3	0.09
10:55	0.92	1	15.85	76	1008.3	0.08
11:00	0.75	358	16.10	75	1008.2	0.07
11:05	0.17	44	16.55	73	1008.1	0.07
11:10	0.05	85	16.85	72	1008.1	0.07
11:15	0.61	325	17.16	70	1008.1	0.06
11:20	3.75	325	17.36	69	1008.1	0.06
11:25	3.90	329	17.57	67	1008.1	0.06
11:30	2.11	308	17.88	66	1008.1	0.06
11:35	0.29	316	18.29	65	1008.1	0.07
11:40	1.29	133	18.61	65	1008.1	0.06
11:45	1.66	131	18.72	65	1008.1	0.08
11:50	1.04	120	18.94	65	1008.1	0.08
11:55	2.19	135	18.83	64	1008.1	0.09
12:00	2.35	129	18.82	64	1008.0	0.10
12:05	1.99	117	18.99	63	1008.1	0.12
12:10	2.85	133	18.92	63	1008.0	0.11
12:15	2.96	136	18.30	65	1008.0	0.13
12:20	3.41	138	17.80	66	1008.0	0.14
12:25	3.32	138	17.48	67	1007.9	0.14
12:30	2.25	137	17.15	69	1008.0	0.15
12:35	1.35	126	16.99	70	1008.0	0.19
12:40	0.60	123	17.25	70	1007.9	0.21
12:45	1.93	86	17.44	70	1007.9	0.20
12:50	1.29	118	17.56	70	1007.9	0.23
12:55	1.10	109	18.01	69	1007.9	0.26
13:00	1.70	88	18.47	68	1007.8	0.28

**Table 4.4**  
**Radiosonde Data – R/V Point Sur**  
**May 2, 1990**

Launch time: 90 05 02 at 1947 GMT

<b>Time</b>	<b>Hght</b>	<b>Press</b>	<b>Temp</b>	<b>Hum</b>	<b>Td</b>
0 0	10	1013.0	10.4	93	9.3
0 40	237	985.9	12.1	65	5.6
1 20	379	969.4	17.4	30	-0.3
2 0	498	956.0	18.7	25	-1.7
2 40	617	942.8	18.7	23	-2.8
3 20	753	928.0	18.3	23	-3.1
4 10	943	907.6	17.5	26	-2.2
5 0	1154	885.3	16.1	28	-2.4
5 50	1297	870.5	16.7	21	-5.7
6 30	1430	857.0	15.9	22	-5.8
7 10	1550	844.9	15.1	23	-5.9
7 50	1670	833.1	14.5	18	-9.5
8 30	1789	821.3	13.4	18	-10.4
8 50	1848	815.5	13.0	17	-11.5
9 40	2003	800.6	11.7	17	-12.5
10 20	2128	788.7	10.9	19	-11.8
11 0	2272	775.2	9.6	22	-11.1
11 30	2377	765.4	8.7	23	-11.3
12 0	2469	756.8	7.9	24	-11.4
12 30	2560	748.6	7.2	24	-12.0
13 10	2678	737.9	6.3	25	-12.3
13 30	2742	732.1	5.8	25	-12.7
14 10	2867	720.9	4.9	26	-13.0
15 0	3033	706.5	5.6	5	-31.2
16 0	3242	688.6	4.3	24	-14.5
16 50	3410	674.5	2.9	28	-13.8
17 30	3532	664.3	2.0	28	-14.6
18 10	3654	654.4	1.0	29	-15.1
19 0	3799	642.6	-0.3	30	-15.8
19 50	3941	631.3	-1.6	32	-16.2
20 50	4108	618.2	-2.9	38	-15.2
21 30	4218	609.6	-3.4	34	-17.0
22 20	4360	598.7	-3.9	32	-18.2
23 50	4649	577.2	-5.1	23	-23.1



**Table 4.5**  
**Meteorological Data**  
**Solomat Portable Measuring Unit**

- Time – 1533 (Greenwich mean time)
- Air temperature – 13.4°C
- Barometer – 759.4 torr
- Wind direction – 340°T
- Wind speed – 3.58 m/sec
- Relative humidity – 85%
- Sea description – calm, sea state 1
- Sky conditions – fog, cloud layer 0–500 ft
- comments – 1113Z – horizon visible  
1152Z – fog lifted, clear blue sky

Table 4.6

Proportional Radiation Equals the Percentage of  
Radiant Emittance in the Wavelength of Interest

$$q = f(\lambda T) \text{ [Ref 14: pp. 54-55]}$$

$\frac{\lambda \cdot T}{\text{cm} \cdot \text{K}}$	q	$\frac{\lambda \cdot T}{\text{cm} \cdot \text{K}}$	q	$\frac{\lambda \cdot T}{\text{cm} \cdot \text{K}}$	q
0.050	$1.3652 \cdot 10^{-9}$	0.140	$7.9053 \cdot 10^{-3}$	0.460	$5.8057 \cdot 10^{-1}$
0.052	$3.6788 \cdot 10^{-9}$	0.150	$1.3023 \cdot 10^{-2}$	0.480	$6.0880 \cdot 10^{-1}$
0.054	$9.1749 \cdot 10^{-9}$	0.160	$1.9962 \cdot 10^{-2}$	0.500	$6.3494 \cdot 10^{-1}$
0.056	$2.1358 \cdot 10^{-8}$	0.170	$2.8858 \cdot 10^{-2}$	0.520	$6.5912 \cdot 10^{-1}$
0.058	$4.6745 \cdot 10^{-8}$	0.180	$3.9754 \cdot 10^{-2}$	0.540	$6.8146 \cdot 10^{-1}$
0.060	$9.6798 \cdot 10^{-8}$	0.190	$5.2613 \cdot 10^{-2}$	0.560	$7.0209 \cdot 10^{-1}$
0.062	$1.9069 \cdot 10^{-7}$	0.200	$6.7331 \cdot 10^{-2}$	0.580	$7.2116 \cdot 10^{-1}$
0.064	$3.5907 \cdot 10^{-7}$	0.210	$8.3750 \cdot 10^{-2}$	0.600	$7.3877 \cdot 10^{-1}$
0.066	$6.4902 \cdot 10^{-7}$	0.220	$1.0168 \cdot 10^{-1}$	0.620	$7.5505 \cdot 10^{-1}$
0.068	$1.1302 \cdot 10^{-6}$	0.230	$1.2091 \cdot 10^{-1}$	0.660	$7.8402 \cdot 10^{-1}$
0.070	$1.9025 \cdot 10^{-6}$	0.240	$1.4122 \cdot 10^{-1}$	0.700	$8.0885 \cdot 10^{-1}$
0.072	$3.1045 \cdot 10^{-6}$	0.250	$1.6239 \cdot 10^{-1}$	0.740	$8.3020 \cdot 10^{-1}$
0.074	$4.9236 \cdot 10^{-6}$	0.260	$1.8423 \cdot 10^{-1}$	0.780	$8.4861 \cdot 10^{-1}$
0.076	$7.6070 \cdot 10^{-6}$	0.270	$2.0653 \cdot 10^{-1}$	0.820	$8.6455 \cdot 10^{-1}$
0.078	$1.1473 \cdot 10^{-5}$	0.280	$2.2911 \cdot 10^{-1}$	0.860	$8.7840 \cdot 10^{-1}$
0.080	$1.6923 \cdot 10^{-5}$	0.290	$2.5183 \cdot 10^{-1}$	0.900	$8.9048 \cdot 10^{-1}$
0.082	$2.4453 \cdot 10^{-5}$	0.300	$2.7454 \cdot 10^{-1}$	0.940	$9.0105 \cdot 10^{-1}$
0.084	$3.4668 \cdot 10^{-5}$	0.310	$2.9712 \cdot 10^{-1}$	0.980	$9.1033 \cdot 10^{-1}$
0.086	$4.8287 \cdot 10^{-5}$	0.320	$3.1947 \cdot 10^{-1}$	1.00	$9.1455 \cdot 10^{-1}$
0.088	$6.6159 \cdot 10^{-5}$	0.330	$3.4150 \cdot 10^{-1}$	1.10	$9.3217 \cdot 10^{-1}$
0.090	$8.9269 \cdot 10^{-5}$	0.340	$3.6314 \cdot 10^{-1}$	1.20	$9.4532 \cdot 10^{-1}$
0.092	$1.1874 \cdot 10^{-4}$	0.350	$3.8432 \cdot 10^{-1}$	1.30	$9.5331 \cdot 10^{-1}$
0.094	$1.5586 \cdot 10^{-4}$	0.360	$4.0502 \cdot 10^{-1}$	1.40	$9.6304 \cdot 10^{-1}$
0.096	$2.0204 \cdot 10^{-4}$	0.370	$4.2518 \cdot 10^{-1}$	1.50	$9.6909 \cdot 10^{-1}$
0.098	$2.5885 \cdot 10^{-4}$	0.380	$4.4479 \cdot 10^{-1}$	1.60	$9.7390 \cdot 10^{-1}$
0.100	$3.2804 \cdot 10^{-4}$	0.390	$4.6382 \cdot 10^{-1}$	1.70	$9.7777 \cdot 10^{-1}$
0.110	$9.2957 \cdot 10^{-4}$	0.400	$4.8227 \cdot 10^{-1}$	1.80	$9.8091 \cdot 10^{-1}$
0.120	$2.1727 \cdot 10^{-3}$	0.420	$5.1738 \cdot 10^{-1}$	1.90	$9.8349 \cdot 10^{-1}$
0.130	$4.3866 \cdot 10^{-3}$	0.440	$5.5012 \cdot 10^{-1}$	2.00	$9.8563 \cdot 10^{-1}$

**Table 5.1**  
**Temperature and Radiance of Thermal Image**

---

Date: May 2, 1990	Image Number: 48	Time: 1128L	Elevation Angle: 0
Bandwidth: 8-14 $\mu\text{m}$	Horizon: pixel line #67	Lens: 3.5° FOV	

---

R/V Point Sur	Meteorological Data	
	Monterey Bay Buoy	AGEMA Camera
Time: 1127L	Time: 1130L	Time: 1128L
Range: .5 miles	Range: 1 mile	Scanner: 780
Air Temp: 11.07°C	Air Temp: 17.88	Serial No: 4011
SS Temp: 10.06°C	Wind Speed: 2.11 m/sec	FOV: 3.5°
Wind Speed: 1.63 m/s	Wind Dir: 308°	Filter: NOF
Wind Dir: 131°	Rel Humid: 66%	Aperture: 1.8
Dew Point: 8.45°C	Pressure: 1008.1 MB	Thermal Range: 10
Rel Humid: 89.7		Thermal Level: 37.1
Sky: Clear		Emissivity: .97
		Transmittance: .84

Image Line Number	Zenith Angle (degrees)	Spot Temperature (degrees C)	Radiance W/cm <sup>2</sup> -sr)
3	88.375	16.6	4.5200E-3
7	88.475	16.7	4.5200E-3
11	88.575	16.9	4.5518E-3
15	88.675	17.0	4.5518E-3
19	88.775	17.3	4.5830E-3
23	88.875	17.3	4.5830E-3
27	88.975	17.4	4.5837E-3
31	89.075	17.4	4.5847E-3
35	89.175	17.3	4.5830E-3
39	89.275	16.6	4.5200E-3
43	89.375	14.8	4.3926E-3
47	89.475	14.6	4.3926E-3
51	89.575	14.5	4.3608E-3
55	89.675	14.4	4.3608E-3
59	89.775	14.7	4.3926E-3
63	89.875	14.8	4.3926E-3
65	89.925	14.8	4.3926E-3
66	89.950	15.1	4.4245E-3

Table 5.1 (continued)

Image Line Number	Zenith Angle (degrees)	Spot Temperature (degrees C)	Radiance W/cm <sup>2</sup> -sr
67	89.975	15.1	4.4245E-3
68	90.000	14.8	4.3926E-3
69	90.025	14.5	4.3608E-3
70	90.050	13.9	4.3290E-3
71	90.075	13.5	4.2971E-3
75	90.175	13.2	4.2653E-3
79	90.275	12.8	4.2335E-3
83	90.375	12.2	4.2001E-3
87	90.475	12.1	4.2016E-3
91	90.575	11.8	4.1698E-3
95	90.675	11.4	4.1380E-3
99	90.775	11.4	4.1380E-3
103	90.875	11.5	4.1698E-3
107	90.975	11.4	4.1698E-3
111	91.075	11.6	4.1380E-3
115	91.175	11.3	4.1698E-3
119	91.275	11.5	4.1380E-3
123	91.375	11.6	4.1698E-3
127	91.475	11.8	4.1698E-3
131	91.575	11.6	4.1698E-3
135	91.675	11.4	4.1698E-3
139	91.775	11.9	4.1380E-3

**Table 5.2**  
**Temperature and Radiance of Thermal Image**

---

Date: May 2, 1990   Image Number: 52   Time: 1132L   Elevation Angle: 2.8°

---

Image Line Number	Zenith Angle (degrees)	Spot Temperature (degrees C)	Radiance (W/cm <sup>2</sup> -sr)
3	85.575	10.0	4.0425E-3
7	85.675	10.2	4.0744E-3
11	85.775	10.4	4.0744E-3
15	85.875	10.7	4.1062E-3
19	85.975	11.0	4.1062E-3
23	86.075	11.3	4.1380E-3
27	86.175	11.6	4.1699E-3
31	86.275	12.0	4.2017E-3
35	86.375	12.3	4.2017E-3
39	86.475	12.6	4.2335E-3
43	86.575	12.8	4.2335E-3
47	86.675	13.1	4.2654E-3
51	86.775	13.4	4.2972E-3
55	86.875	13.7	4.2972E-3
59	86.975	13.9	4.3290E-3
63	87.075	14.3	4.3608E-3
67	87.175	14.6	4.3927E-3
71	87.275	14.8	4.3927E-3
75	87.375	14.9	4.3927E-3
79	87.475	15.0	4.4245E-3
83	87.575	15.3	4.4563E-3
87	87.675	15.6	4.4563E-3
91	87.775	15.9	4.4882E-3
95	87.875	16.1	4.4882E-3
99	87.975	16.1	4.5200E-3
103	88.075	16.5	4.5200E-3
107	88.175	16.6	4.5200E-3
111	88.275	16.7	4.5518E-3
115	88.375	16.6	4.5518E-3
119	88.475	16.7	4.5518E-3
123	88.575	16.9	4.5837E-3
127	88.675	17.0	4.5837E-3
131	88.775	17.3	4.5837E-3
135	88.875	17.3	4.5837E-3
139	88.975	17.4	4.5837E-3

**Table 5.3**  
**Temperature and Radiance of Thermal Image**

---

Date: May 2, 1990   Image Number: 53   Time: 1133L   Elevation Angle: 5.6

---

Meteorological Data		
R/V Point Sur	Monterey Bay Buoy	AGEMA Camera
Time: 1132	Time: 1135	Time: 1133
Range: .5 miles	Range: 1 mile	Scanner: 780
Air Temp: 11.07	Air Temp: 18.29°C	Serial No: 4011
SS Temp: 9.90°C	Wind Speed: .29 m/sec	FOV: 3.5°
Wind Speed: 1.59 m/sec	Wind Dir: 316°	Filter: NOF
Wind Dir: 135°	Rel Humid: 65%	Aperture: 1.8
Dew Point: 8.56		Thermal Range: 10
Rel Humid: 88.3%		Thermal Level: 31.3
		Transmittance: .84

Image Line Number	Zenith Angle (degrees)	Spot Temperature (degrees C)	Radiance (W/cm <sup>2</sup> -sr)
3	82.775	3.4	3.6287E-3
7	82.875	3.7	3.6287E-3
11	82.975	3.8	3.6287E-3
15	83.075	4.0	3.6606E-3
19	83.175	4.2	3.6606E-3
23	83.275	4.3	3.6606E-3
27	83.375	4.6	3.6924E-3
31	83.475	4.7	3.6924E-3
35	83.575	5.0	3.7242E-3
39	83.675	5.0	3.7242E-3
43	83.775	5.4	3.7561E-3
47	83.875	5.7	3.7561E-3
51	83.975	5.9	3.7879E-3
55	84.075	6.1	3.7879E-3
59	84.175	6.3	3.7879E-3
63	84.275	6.7	3.8197E-3
67	84.375	6.8	3.8515E-3
71	84.475	7.1	3.8515E-3
75	84.575	7.4	3.8834E-3
79	84.675	7.6	3.8834E-3

**Table 5.3 (continued)**

<b>Image Line Number</b>	<b>Zenith Angle (degrees)</b>	<b>Spot Temperature (degrees C)</b>	<b>Radiance W/cm<sup>2</sup>-sr</b>
83	84.775	8.0	3.9152E-3
87	84.875	8.2	3.9152E-3
91	84.975	8.6	3.9470E-3
95	85.075	9.1	3.9789E-3
99	85.175	9.4	3.9789E-3
103	85.275	9.8	4.0107E-3
107	85.375	10.3	4.0107E-3
111	85.475	10.5	4.0425E-3
115	85.575	10.8	4.0744E-3
119	85.675	11.0	4.0744E-3
123	85.775	11.4	4.1062E-3
127	85.875	11.6	4.1062E-3
131	85.975	12.0	4.1380E-3
135	86.075	11.4	4.1699E-3
139	86.175	11.6	4.2017E-3

**Table 5.4**  
**Temperature and Radiance of Thermal Image**

---

Date: May 2, 1990   Image Number: 54   Time: 1134   Elevation Angle: 8.4

---

R/V Point Sur	Meteorological Data Monterey Bay Buoy	AGEMA Camera
Time: 1132	Time: 1135	Time: 1134
Range: .5 miles	Range: 1 mile	Scanner: 780
Air Temp: 11.07°C	Air Temp: 18.29	Serial No: 4011
SS Temp: 9.90°C	Wind Speed: .29 m/sec	FOV: 3.5°
Wind Speed: 1.60 m/sec	Wind Dir: 316°	Filter: NOF
Wind Dir: 136°	Rel Humid: 65%	Aperture: 1.8
Dew Point: 8.45°C	Pressure: 1008.1 mb	Thermal Range: 10
Rel Humid: 89.7%		Thermal Level: 26.9
		Emissivity: .97

Image Line Number	Zenith Angle (degrees)	Spot Temperature (degrees C)	Radiance (W/cm <sup>2</sup> -sr)
3	79.975	-1.6	3.3104E-3
7	80.075	-1.3	3.3104E-3
11	80.175	-1.1	3.3423E-3
15	80.275	-1.1	3.3423E-3
19	80.375	-1.0	3.3423E-3
23	80.475	-.9	3.3741E-3
27	80.575	-.6	3.3741E-3
31	80.675	-.3	3.3741E-3
35	80.775	-.2	3.4059E-3
39	80.875	0	3.4059E-3
43	80.975	.2	3.4377E-3
47	81.075	.4	3.4377E-3
51	81.175	.5	3.4377E-3
55	81.275	.7	3.4696E-3
59	81.375	.9	3.4696E-3
63	81.475	1.2	3.4696E-3
67	81.575	1.2	3.5014E-3
71	81.675	1.4	3.5014E-3
75	81.775	1.7	3.5332E-3
79	81.875	1.9	3.5332E-3
83	81.975	2.0	3.5332E-3



**Table 5.4 (continued)**

<b>Image Line Number</b>	<b>Zenith Angle (degrees)</b>	<b>Spot Temperature (degrees C)</b>	<b>Radiance W/cm<sup>2</sup>-sr)</b>
87	82.075	2.2	3.5651E-3
91	82.175	2.5	3.5651E-3
95	82.275	2.8	3.5969E-3
99	82.375	3.0	3.5969E-3
103	82.475	3.1	3.6287E-3
107	82.575	3.4	3.6287E-3
111	82.675	3.6	3.6287E-3
115	82.775	3.8	3.6606E-3
119	82.875	4.1	3.6606E-3
123	82.975	4.3	3.6606E-3
127	83.075	4.5	3.6606E-3
131	83.175	4.9	3.7242E-3
135	83.275	5.0	3.7242E-3
139	83.375	5.3	3.7242E-3

**Table 5.5**

**Temperature and Radiance of Thermal Image**

Date: May 2, 1990 Image Number: 55 Time: 1135 Elevation Angle: 11.2

R/V Point Sur	Meteorological Data	
	Monterey Bay Buoy	AGEMA Camera
Time: 1137	Time: 1135	Time: 1135
Range: .5 miles	Range: 1 mile	Scanner: 780
Air Temp: 10.44°C	Air Temp: 18.29	Serial No: 4011
SS Temp: 9.90°C	Wind Speed: .29 m/sec	FOV: 3.5°
Wind Speed: 1.60 m/sec	Wind Dir: 316°	Filter: NOF
Wind Dir: 136°	Dew Point: 65%	Aperture: 1.8
Dew Point: 8.45°C	Pressure: 1008.1 mb	Thermal Range: 10
Rel Humid: 89.7%		Thermal Level: 22.7
		Emissivity: .97
		Transmittance: .84

Image Line Number	Zenith Angle (degrees)	Spot Temperature (degrees C)	Radiance (W/cm <sup>2</sup> -sr)
3	77.175	-5.9	3.0494E-3
7	77.275	-5.7	3.0590E-3
11	77.375	-5.6	3.0653E-3
15	77.475	-5.4	3.0781E-3
19	77.575	-5.3	3.0812E-3
23	77.675	-5.1	3.0940E-3
27	77.775	-4.9	3.0940E-3
31	77.875	-4.9	3.1067E-3
35	77.975	-4.6	3.1067E-3
39	78.075	-4.5	3.1226E-3
43	78.175	-4.3	3.1290E-3
47	78.275	-4.1	3.1417E-3
51	78.375	-3.9	3.1513E-3
55	78.475	-3.9	3.1640E-3
59	78.575	-3.7	3.1640E-3
63	78.675	-3.5	3.1767E-3
67	78.775	-3.3	3.1831E-3
71	78.875	-3.2	3.2149E-3
75	78.975	-2.9	3.2149E-3

Table 5.5 (continued)

Image Line Number	Zenith Angle (degrees)	Spot Temperature (degrees C)	Radiance W/cm <sup>2</sup> -sr
79	79.075	-2.9	3.2149E-3
83	79.175	-2.6	3.2149E-3
87	79.275	-2.4	3.2468E-3
91	79.375	-2.3	3.2468E-3
95	79.475	-2.1	3.2468E-3
99	79.575	-2.0	3.2786E-3
103	79.675	-1.9	3.2786E-3
107	79.775	-1.6	3.2786E-3
111	79.875	-1.4	3.3104E-3
115	79.975	-1.2	3.3104E-3
119	80.075	-1.1	3.3423E-3
123	80.175	-1.1	3.3423E-3
127	80.275	-.7	3.3423E-3
131	80.375	-.7	3.3423E-3
135	80.475	-.4	3.3741E-3
139	80.575	-.3	3.3741E-3

**Table 5.6**  
**Temperature and Radiance of Thermal Image**

---

Date: May 2, 1990   Image Number: 56   Time: 1135   Elevation Angle: 14.0

---

R/V Point Sur	Meteorological Data Monterey Bay Buoy	AGEMA Camera
Time: 1137	Time: 1135	Time: 1135
Range: .5 miles	Range: 1 mile	Scanner: 780
Air Temp: 10.44°C	Air Temp: 18.29	Serial No: 4011
SS Temp: 9.90°C	Wind Speed: .29 m/sec	FOV: 3.5°
Wind Speed: 1.60 m/sec	Wind Dir: 316°	Filter: NOF
Wind Dir: 136°	Dew Point: 65%	Aperture: 1.8
Dew Point: 8.45°C	Pressure: 1008.1 mb	Thermal Range: 10
Rel Humid: 89.7%		Thermal Level: 21.0
		Emissivity: .97
		Transmittance: .84

Image Line Number	Zenith Angle (degrees)	Spot Temperature (degrees C)	Radiance (W/cm <sup>2</sup> -sr)
3	74.375	-8.9	2.8775E-3
7	74.475	-8.8	2.8839E-3
11	74.575	-8.8	2.8839E-3
15	74.675	-8.5	2.8998E-3
19	74.775	-8.5	2.8998E-3
23	74.875	-8.4	2.9062E-3
27	74.975	-8.3	2.9125E-3
31	75.075	-8.1	2.9221E-3
35	75.175	-8.0	2.9285E-3
39	75.275	-7.8	2.9285E-3
43	75.375	-8.0	2.9411E-3
47	75.475	-7.6	2.9507E-3
51	75.575	-7.5	2.9571E-3
55	75.675	-7.4	2.9635E-3
59	75.775	-7.4	2.9635E-3
63	75.875	-7.2	2.9730E-3
67	75.975	-7.0	2.9857E-3
71	76.075	-6.9	2.9921E-3
75	76.175	-6.7	3.0017E-3

Table 5.6 (continued)

Image Line Number	Zenith Angle (degrees)	Spot Temperature (degrees C)	Radiance W/cm <sup>2</sup> -sr
79	76.275	-6.5	3.0144E-3
83	76.375	-6.4	3.0176E-3
87	76.475	-6.2	3.0303E-3
91	76.575	-6.2	3.0303E-3
95	76.675	-5.9	3.0494E-3
99	76.775	-5.7	3.0590E-3
103	76.875	-5.5	3.0717E-3
107	76.975	-5.5	3.0717E-3
111	77.075	-5.3	3.0812E-3
115	77.175	-5.1	3.0940E-3
119	77.275	-4.9	3.1067E-3
123	77.375	-4.8	3.1131E-3
127	77.475	-4.6	3.1226E-3
131	77.575	-4.5	3.1290E-3
135	77.675	-4.3	3.1417E-3

**Table 5.7**  
**Radiance Comparison Between**  
**The AGEMA Camera and PC-TRAN**  
**May 2, 1990**

---

Angles from 75°–85°    FOV: 3.5°    24 Hours Average Wind Speed: 1.63 m/sec

---

Zenith Angle (°)	Boundary Temp (°K)	AGA Radiance (W/cm <sup>2</sup> -sr)	PC-TRAN Radiance (W/cm <sup>2</sup> -sr)	% Error AGA/PC-TRAN
85.075	282.1	3.9789E-3	3.612E-3	9.22
84.575	280.4	3.8834E-3	3.513E-3	9.53
84.075	279.1	3.7879E-3	3.419E-3	9.73
83.575	278.0	3.7242E-3	3.332E-3	10.53
83.175	277.2	3.6606E-3	3.265E-3	10.80
82.775	276.8	3.6287E-3	3.202E-3	11.75
82.275	275.8	3.5969E-3	3.128E-3	13.04
81.775	274.7	3.5332E-3	3.059E-3	13.42
81.275	273.7	3.4696E-3	2.992E-3	13.77
80.775	272.8	3.4059E-3	2.931E-3	13.94
80.275	272.3	3.3423E-3	2.872E-3	14.07
79.775	271.4	3.2786E-3	2.817E-3	14.07
79.275	270.6	3.2468E-3	2.764E-3	14.87
78.675	269.3	3.1767E-3	2.705E-3	13.37
78.075	268.5	3.1226E-3	2.649E-3	14.73
77.975	267.7	3.1067E-3	2.572E-3	16.52
77.575	267.9	3.0812E-3	2.605E-3	14.84
76.675	267.1	3.0590E-3	2.531E-3	15.41
76.075	266.1	2.9921E-3	2.485E-3	16.95
75.475	265.4	2.9507E-3	2.442E-3	17.24
74.875	264.6	2.9024E-3	2.400E-3	17.32

**Table 5.8**  
**Radiance Comparison Between**  
**The AGE MA Camera and PC-TRAN**  
**May 2, 1990**

---

Angles from 85°-90°    FOV: 3.5°    24 Hours Average Wind Speed: 1.63 m/sec

---

Zenith Angle (°)	Boundary Temp (°K)	AGA Radiance (W/cm <sup>2</sup> -sr)	PC-TRAN Radiance (W/cm <sup>2</sup> -sr)	% Error AGA/PC-TRAN
89.975	288.1	4.4245E-3	4.376E-3	1.10
89.875	287.8	4.3926E-3	4.387E-3	.13
89.475	287.6	4.3926E-3	4.410E-3	.39
89.075	290.4	4.5836E-3	4.408E-3	3.83
88.675	290.0	4.5518E-3	4.376E-3	3.86
88.375	289.6	4.5200E-3	4.334E-3	4.12
87.975	289.1	4.5200E-3	4.260E-3	5.75
87.475	288.0	4.4245E-3	4.152E-3	6.16
87.175	287.6	4.3927E-3	4.083E-3	7.05
86.775	286.4	4.2972E-3	3.990E-3	7.15
86.375	285.3	4.2017E-3	3.896E-3	7.28
85.975	284.0	4.1062E-3	3.806E-3	7.31
85.575	283.8	4.0425E-3	3.718E-3	8.03
85.075	282.1	3.9789E-3	3.612E-3	9.22

**Table 5.9**  
**Validation of the Schwartz-Hon Algorithm**  
**May 2, 1990**

Sky: Clear    24 Hour Average Windspeed: 1.63 m/s    Sea Surface Temperature: 284.7°K     $\Delta q$ : 3.6064E-1

View Angle $\theta_V$	Incidence Angle $\theta_I$	Reflection Angle $\theta_R$ (Schwartz-Hon)	Emissivity Sea Surface $\epsilon_{SS}$ (Schwartz-Hon)	Sky Radiance At Reflection Angle (AGA) ( $L_{SKY}$ )	Sky Radiance At Reflection Angle (PC-TRAN) ( $L_{SKY}$ )	Total Radiance Sea Surface ( $L_{SSE}$ )
90.025	89.925	86.072	.183	4.1380E-3	3.827E-3	4.1671E-3
90.075	89.925	86.046	.187	4.1380E-3	3.821E-3	4.1671E-3
90.275	89.275	85.715	.232	4.0744E-3	3.748E-3	4.1260E-3
90.475	89.525	85.683	.215	4.0744E-3	3.741E-3	4.1223E-3
90.675	89.325	75.651	.229	4.0744E-3	3.733E-3	4.1254E-3
90.875	89.125	85.639	.243	4.0425E-3	3.731E-3	4.1043E-3
91.075	88.925	85.537	.257	4.0425E-3	3.709E-3	4.1079E-3
91.275	88.725	85.435	.271	4.0425E-3	3.687E-3	4.1115E-3
91.475	88.525	85.333	.285	4.0107E-3	3.666E-3	4.0923E-3
91.675	88.325	85.232	.299	4.0107E-3	3.645E-3	4.0963E-3

Sea Surface Radiance At SST ( $L_{SST}$ )	Blackbody Temp of Sea Surface ( $L_{BR}$ )	Sea Surface Radiance At $\theta_V$ (AGA) ( $L_{SSM}$ )	Sea Surface Radiance At $\theta_V$ (PC-TRAN) ( $L_{SSC}$ )	% Error	Temp Conversion ( $T_{SSM}$ ) °K	Temp Conversion ( $T_{SSC}$ ) °K
4.2972E-3	285.08	4.3608E-3	3.9130E-3	10.26	286.10	278.45
4.2972E-3	285.09	4.2971E-3	3.9100E-3	9.00	285.05	278.40
4.2972E-3	281.75	4.2335E-3	3.8754E-3	8.46	283.99	277.78
4.2972E-3	281.75	4.2016E-3	3.8605E-3	8.12	283.45	277.51
4.2972E-3	281.75	4.1380E-3	3.8622E-3	6.67	282.37	277.54
4.2972E-3	281.33	4.1698E-3	3.8685E-3	7.23	282.91	277.66
4.2972E-3	281.33	4.1480E-3	3.8601E-3	6.72	282.37	277.51
4.2972E-3	281.33	4.1380E-3	3.8370E-3	7.27	282.37	277.09
4.2972E-3	280.91	4.1698E-3	3.8458E-3	7.77	282.91	277.25
4.2972E-3	280.91	4.1698E-3	3.8400E-3	7.91	282.91	277.14



Table 5.10

**Validation of the Shapiro Algorithm**  
**May 2, 1990**

Sky: Clear    24 Hour Average Windspeed: 1.63 m/s    Sea Surface Temperature: 284.7°K     $\Delta q$ : 3.6064E-1

View Angle $\theta_V$	Incidence Angle $\theta_I$	Reflection Angle $\theta_R$ (Shapiro)	Emissivity Sea Surface $\epsilon_{SS}$ (Shapiro)	Sky Radiance At Reflection Angle (AGA) ( $L_{SKY}$ )	Sky Radiance At Reflection Angle (PC-TRAN) ( $L_{SKY}$ )	Total Radiance Sea Surface ( $L_{SSE}$ )
90.025	89.975	81.832	.390	3.5332E-3	3.066E-3	3.8311E-3
90.075	89.925	81.794	.393	3.5332E-3	3.061E-3	3.8334E-3
90.275	89.275	81.291	.433	3.4696E-3	2.994E-3	3.8279E-3
90.475	89.525	81.484	.418	3.4696E-3	3.019E-3	3.8155E-3
90.675	89.325	81.329	.430	3.4696E-3	2.999E-3	3.8254E-3
90.875	89.125	81.175	.443	3.4377E-3	2.980E-3	3.8184E-3
91.075	89.925	81.015	.454	3.4377E-3	2.960E-3	3.8279E-3
91.275	88.725	80.760	.466	3.4059E-3	2.928E-3	3.8212E-3
91.475	88.525	80.504	.477	3.3741E-3	2.898E-3	3.8144E-3
91.675	88.325	80.248	.488	3.3423E-3	2.868E-3	3.8082E-3

Sea Surface Radiance At SST ( $L_{SST}$ )	Blackbody Temp of Sea Surface ( $L_{BB}$ )	Sea Surface Radiance At $\theta_V$ (AGA) ( $L_{SSM}$ )	Sea Surface Radiance At $\theta_V$ (PC-TRAN) ( $L_{SSC}$ )	% Error	Temp Conversion ( $T_{SSM}$ ) °K	Temp Conversion ( $T_{SSC}$ ) °K
4.2972E-3	278.54	4.3608E-3	3.5461E-3	18.68	286.10	271.68
4.2972E-3	278.57	4.2971E-3	3.5468E-3	17.46	285.05	271.69
4.2972E-3	278.51	4.2335E-3	3.5582E-3	15.95	285.99	271.92
4.2972E-3	278.34	4.2016E-3	3.5532E-3	15.43	283.45	271.82
4.2972E-3	278.47	4.1380E-3	3.5572E-3	14.04	282.37	271.89
4.2972E-3	278.38	4.1698E-3	3.5635E-3	14.54	282.91	272.02
4.2972E-3	278.51	4.1380E-3	3.5496E-3	14.22	282.38	271.75
4.2972E-3	278.42	4.1380E-3	3.5660E-3	13.82	282.38	272.07
4.2972E-3	278.33	4.1698E-3	3.5654E-3	14.49	282.91	272.05
4.2972E-3	278.25	4.1698E-3	3.5654E-3	14.49	282.91	272.05

**Table 5.11**  
**Validation of the Schwartz-Hon Model (1987-1990)**

<b>Date</b>	<b>Sky Conditions</b>	<b>Wind Speed (m/s)</b>	<b>Sea Surface Temperature (degrees C)</b>	<b>Mean % Error (<math>L_{SSC}/L_{SSM}</math>)</b>
4 Nov 87	Overcast	2.057	14.1	13.49
14 Jul 88	Clear sky	3.110	12.8	4.65
15 Jul 88	Clear sky	4.510	11.7	3.24
25 Jul 88	Overcast	4.900	15.4	4.785
2 May 90	Clear sky	1.630	11.7	7.94

**Table 5.12**

**Synopsis of Schwartz-Hon Validation Experiments at Low Grazing Angles  
Performed from 1987 to 1990**

**14 July 1988**  
**Clear Sky**  
**Wind Speed of 3.1 m/s**  
**Mean Error 2.374%**

<b>View Angle</b>	<b>Emissivity</b>	<b><math>L_{SSC}/L_{SSM}</math> % Error</b>
90.19	.323	2.1
90.41	.335	1.750
90.63	.346	1.898
90.85	.358	3.427
91.07	.370	1.513
91.29	.382	1.465
91.51	.393	1.489
91.73	.405	3.451
91.95	.417	3.280
92.17	.429	3.353

**15 July 1988**  
**Clear Sky**  
**Wind Speed of 4.0 m/s**  
**Mean Error 2.49%**

<b>View Angle</b>	<b>Emissivity</b>	<b><math>L_{SSC}/L_{SSM}</math> % Error</b>
90.24	.391	5.560
90.46	.401	3.858
90.68	.411	2.992
90.90	.421	3.393
91.12	.431	0.633
91.34	.440	1.676
91.56	.450	1.206
92.00	.460	1.284
92.22	.470	1.815

**2 May 1990**  
**Clear Sky**  
**Wind Speed of 1.63 m/s**  
**Mean Error 7.94%**

<b>View Angle</b>	<b>Emissivity</b>	<b><math>L_{SSC}/L_{SSM}</math> % Error</b>
90.025	.183	10.26
90.075	.187	9.00
90.275	.232	8.46
90.475	.215	8.12
90.675	.229	6.67
90.875	.243	7.23
91.075	.257	6.72
91.275	.271	7.27
91.475	.285	7.77
91.675	.299	7.91

**4 Nov 1987**  
**Overcast Sky**  
**Wind Speed of 2.057 m/s**  
**Mean Error 13.49%**

<b>View Angle</b>	<b>Emissivity</b>	<b><math>L_{SSC}/L_{SSM}</math> % Error</b>
90.109	.215	20.49
90.328	.229	15.15
90.547	.244	12.15
90.766	.259	13.43
90.984	.273	13.10
91.203	.288	12.33
91.422	.302	11.64
91.641	.317	9.66

**25 July 1988**  
**Overcast**  
**Wind Speed of 4.9 m/s**  
**Mean Error 4.79%**

<b>View Angle</b>	<b>Emissivity</b>	<b><math>L_{SSC}/L_{SSM}</math> % Error</b>
90.29	.443	7.137
90.51	.452	6.001
90.73	.460	5.762
90.95	.469	5.211
91.17	.477	4.406
91.39	.485	3.676
91.61	.494	3.112
91.83	.502	2.975

## APPENDIX C

### A. ATTEMPTED COMPARISON OF OPERATIONAL FLIR RANGE WITH TDA PREDICTIONS

The original area of this thesis research effort was to be the experimental validation of Forward Looking Infrared Radar (FLIR) tactical decision aids for use by VP patrol aircraft. This was to be a continuation of work being done by the Naval Academic Center for Infrared Technology (NACIT) group at the Naval Postgraduate School in conjunction with the Naval Oceanographic and Atmospheric Research Laboratory. The hardware used to carry out this experiment consisted of the recently calibrated AGEMA 780 Thermovision Camera, the research vessel R/V *Point Sur*, and P3-C aircraft from NAS Moffett Field, California.

On May 2, 1990, the R/V *Point Sur*, based out of the Moss Landing Marine Laboratory, was positioned approximately .5 miles from the shore of the Naval Postgraduate School Oceanographic Beach Laboratory. The ship contained a full suite of meteorological instruments and radiosondes and was specially rigged with 16 calibrated thermistor temperature sensors. These sensors were attached to the hull of the ship with a clear epoxy cement and covered with a latex compound to avoid direct solar heating. They recorded the hull, blockhouse and stack temperatures every 20 seconds for the duration of the experiment.

The AGEMA Thermovision Camera was set up on a ridge outside the beach laboratory with a clear view of the entire Monterey Bay. Approximately 100 images of the ship, sky and ocean were taken at various viewing angles and wind speeds. At the same time the ship was in the bay and the AGEMA pictures were being taken, P3-C aircraft from Moffett Field, California, equipped with the AN/AAS-36 Infra-Red Detecting Set (IRDS), were to make repeated passes at pre-planned altitudes over the R/V *Point Sur*. Actual FLIR ranges for detection, classification

and identification were to be recorded by various fleet operators under actual maritime patrol conditions. Both day and night sorties would be flown and passes on all aspects of the ship recorded. All Forward Looking Infrared Displays would be recorded on standard video tap with an accompanying voicetrack. The targets were to be detected in the wide field of view and classified and identified in the narrow field of view. All meteorological conditions would be recorded in the aircraft and later compared to actual shipboard recordings and radiosonde data.

## **B. PROBLEMS ENCOUNTERED**

Problems that were encountered during this phase of the experiment included:

1. On the day of the experiment, the entire Monterey Bay was covered in thick fog from the surface to 600 feet. The P3-C aircraft was unable to visually sight the R/V *Point Sur* or take any FLIR readings.
2. The thermistor readings that were being recorded by computer onboard the ship were accidentally overwritten and all data for that portion of the cruise was lost.
3. Of the four P3-C flights scheduled, only one was able to record any useful data. Two flights aborted for weather and two aborted for equipment failure.

## **C. RECOMMENDATIONS FOR FUTURE EXPERIMENTS**

1. The R/V *Point Sur* cruises are in May and November with May being the worst month for fog and low clouds in the Monterey Peninsula. More than one opportunity to get the ship, aircraft, and camera in the same place at the same time is needed. The R/V *Point Sur* should be able to stop in the Monterey Bay on the return as well as outward leg of the cruise.
2. Dedicated P3-C flights from Moffett Field should be made to collect data on FLIR ranges for detection, classification, and recognition. Flight crews were not well briefed or prepared for this mission because it was added on to the end of 10-12 hour anti-submarine missions or long reconnaissance flights.
3. A computer program for the thermistor data should be written that cannot be overwritten by unfamiliar operators.

4. The prospective importance of such operational data for validation and improvement of Tactical Decision Aid FLIR performance prediction justifies more dedicated effort for ensuring data.

#### **D. POINTS OF CONTACT FOR FOLLOW-ON EXPERIMENTS**

P3-C aircraft	COMPATWING 10 NAS Moffett Field, California 94035 (415-966-4942) (Attention: Special Projects Officer)
AGEMA Camera	AGEMA Infrared 108 Arena Street El Segundo, California 90245 (213-322-6257) (Attention: Mr. Al Fudali)
R/V Point Sur	Marine Superintendents Office Moss Landing Marine Lab 893 Blanco Circle Moss Landing, California (408-633-3057)
Metro Data	Monterey Bay Aquarium (24 hour) (408-647-8382) 1200 Baud Modem NOCD Moffett Field, California (415-966-5197) Naval Postgraduate School Meteorology Department (Cruise data maintained on the mainframe computer) (Attention: Mr. Paul Jesson) (408-646-3269)

## **APPENDIX D**

### **FORTRAN PROGRAM**

#### **A. USING THE AGACAT PROGRAM**

The following computer program AGACAT was written to allow a user access to thermal imaging data taken with the AGEMA Corporation 780 Thermovision camera. The use of this program requires an IBM or compatible computer with either an EGA or VGA monitor and a Microsoft mouse.

The Naval Academic Center for Infrared Technology (NACIT), located at the Naval Postgraduate School in Monterey, California maintains a current library of AGEMA Thermovision files. This data includes ship, sea/sky interface, and blackbody images. A copy of this program and image listings can be obtained by writing or calling Professor E. Milne or Professor A. W. Cooper at the Naval Postgraduate School, Monterey, California, 93940-5100, (480-646-2452) (408-646-2886).

The operation of the AGACAT program requires a font file HELVB.FON. Any mouse and mouse driver must be loaded before loading AGACAT.

After installing the AGACAT program on the hard disc, execute the program. The program will query "Enter filename and path of data file." The filenames vary but must end with the extension ".img." The program will then give the user the choice of printing out the constants used in the thermal image calculation. The choices are "1" for printing the constants and "0" for not printing the constants.

The next question asked concerns the list of variables that may be changed by the user. These variables include LEVEL OFFSET, EMISSIVITY, AREA EMISSIVITY, OBJECT DISTANCE, ESTIMATED TRANSMISSION, ATMOSPHERIC TRANSMISSION, and AMBIENT TEMPERATURE. The user must type "&LIST1"

followed by the equal sign (=), followed by the desired value. After the last desired value, type / to end the entries.

The program will then accept the new values, reprint them and compute the maximum and minimum temperatures contained in the thermal image. The user is given the choice of accepting the variables and viewing the thermal image by selecting <ENTER>. Other choices include entering a new temperature threshold level, typing 1000 to stop, 2000 to read in a new file, or 3000 to change variables. The threshold level changes the lowest false color to the desired temperature value. The subsequent question asks the user for the temperature difference between false colors. This value breaks the ten colors of the thermal image into the desired levels. Again, the thermal image can now be viewed by selecting <ENTER>.

When viewing the actual thermal image, information included on the screen includes image number, date/time group, field of view, aperture, wavelength, waveband, and filters. The bottom left hand corner of the screen shows the spot temperature of the mouse cursor labeled "T." An average temperature of a selected area can be bounded using an included "box" function. By momentarily (on the order of one second) holding down the left hand button and moving the mouse, the upper left corner of the box can be positioned anywhere above the lower right corner of the image. Similarly, holding the right hand mouse button moves the bottom right corner of the box. The value "TA" is the computed average temperature of the area contained inside the box. The numerical values below the "T" and "TA" show the corresponding pixel values of the mouse cursor and the corners of the box.



```

C      PROGRAM AGACATFD AUG 31 1990
C
C      (CONVERT AGEWA CORPORATION CATS PROGRAM IN MICROSOFT FORTRAN)
C
C      WRITTEN BY LT GREGORY M. LAWLER (USN) AND PROFESSOR E. MILNE
C      NAVAL POSTGRADUATE SCHOOL PHYSICS DEPARTMENT
C      MONTEREY, CALIFORNIA, 93943-5000
C
C      This program will read in files generated by the Agema Corporation
C      CATS program and produce a false color display of the image generated
C      by the aga thermovision. One can then find the temperature at any
C      given point in the display and also the average temperature inside an
C      rectangle of any size. The constants in the files may be printed out.
C
      include 'D:\INCLUDE\fgraph.fi'      ! graphics interface file
      include 'D:\INCLUDE\fgraph.fd'      ! defines and names constants
C
C      VARIABLE DECLARATIONS
C
      character*20 filn$,head$*846,picture$*19600,fil$*16,text$*11
      character*20 fonl$/'t'helv'hi5w8t /,FOV$*5,APER$*4,FILTER$*4
      character*6 pgmver$,imagEdr$*2,notused$*1,missing$*36,comment$*401
      * ,imageid$*13,UNUSED$*1,TITLE$*46,SCANNER$*13,NU$*1,NU2$*1
      * ,NU3$*64,NU4$*64,ANS$*6,LINE$*7,LINE8$*8,BLK$*8/'      '/'
      INTEGER*1 IPIX(19600)
      INTEGER*2 IMAGE(140,140),L,min,max,maxx,maxy,m1,m2,m3,m4,JP,IP,LC
      INTEGER*2 I,J,I1,J1,I2,J2,L1,L2,L3,L4,L6,L7,L8,L9,K,JPIX(140,140)
      integer*2 imgver,jorigin,kprep,isigamp,IH,IDATE(3),ITIME(4),K1
      INTEGER*2 IC(10) /1,9,2,10,5,4,13,6,14,15/,I3,J3,I1,L0,KK,LL
      INTEGER*2 DUMMY
      INTEGER*4 IER,ISUM,JSUM
      RECORD /VIDEOCONFIG/SCREEN
      RECORD /XYCOORD/S
      real*8factor,R,B,F,DCAL,ALPHA,BETA,DLEVEL,EMISS,AEMISS,OD,CT,
      *ET,AT,AMT,DIFFP,DIFFQ,LEVEL,RANGE,IU(10),pix,p1,p2,iamb,iatm,
      *IOMIN,T1,IOMAX,T2,TLD,TTL,IO1,IO,PIX1,P3,PIX2,T
      LOGICAL*2 MANIMAG,SNAPSHOT,DIFIMAG,UNDERF,OVERF,FLG,CLRFLG
C
C*****DATA IS READ INTO HEAD$ WHICH IS EAUVALENCED TO EACH OF THE****
C      INDIVIDUAL VARIABLES IN THE INPUT
C
C*****THE PICTURE DATA IS READ INTO PICTURE$ WHICH IS EQUVALENCED****
C      TO IPIX.
      EQUIVALENCE (head$(1:2),imgver),(HEAD$(3:8),PGMVER$),(HEAD$(9:10),
      *JORIGIN),(HEAD$(11:23),IMAGEID$),(HEAD$(24:24),NOTUSED$),(HEAD$(25
      *:26),IMAGEDR$),(HEAD$(27:62),MISSING$),(HEAD$(63:463),COMMENT$),(H
      *EAD$(464:465),KPREP),(HEAD$(466:473),FACTOR),(HEAD$(474:475),ISIGA
      *MP),(HEAD$(476:477),MANIMAG),(HEAD$(478:479),SNAPSHOT),(HEAD$(480:
      *481),DIFIMAG),(HEAD$(482:482),UNUSED$),(HEAD$(483:488),IDATE),(HEA
      *D$(489:496),ITIME),(HEAD$(497:542),TITLE$),(HEAD$(543:555),SCANNER
      *$),(HEAD$(556:556),NU$),(HEAD$(557:561),FOV$),(HEAD$(562:565),APER
      *$),(HEAD$(566:569),FILTER$),(HEAD$(570:570),NU2$)
      *,(HEAD$(571:578),R),(HEAD$(579:586),B),(HEAD$(587:594),F)
      EQUIVALENCE (HEAD$(595:602),DCAL),(HEAD$(603:610),ALPHA),(HEAD$(61
      *1:618),BETA),(HEAD$(619:626),DLEVEL),(HEAD$(627:634),EMISS),(HEAD$
      *(635:642),AEMISS),(HEAD$(643:650),OD),(HEAD$(651:658),CT),(HEAD$(6
      *59:666),ET),(HEAD$(667:674),AT),(HEAD$(675:682),AMT),(HEAD$(683:69
      *0),DIFFP),(HEAD$(691:698),DIFFQ),(HEAD$(699:762),NU3$),(HEAD$(763:
      *770),LEVEL),(HEAD$(771:778),RANGE),(HEAD$(779:780),UNDERF),(HEAD$(
      *781:782),OVERF),(HEAD$(783:846),NU4$)

```

```

EQUIVALENCE (PICTURE$,IPIX)
namelist /list1/DLEVEL,CT,EMISS,OD,AT,AMT,AEMISS

C
C
C*****CHECK FOR THE EXISTANCE OF MOUSE AND MOUSE DRIVER*****
C
      m1=0
      call mouse1(m1,m2,m3,m4)
      IF(M1.EQ.0)STOP 'ERROR - YOU MUST LOAD THE MOUSE DRIVER FIRST '

C
C*****CHECK FOR AND LOAD THE FONT FILE*****
C
      if(REGISTERFONTS('D:\LIB\HELV.B.FON').LT.0)THEN
        IF(REGISTERFONTS('HELV.B.FON').LT.0)THEN
          WRITE(*,*)' ERROR CANNOT FIND FONT FILE'
          STOP' THE FONT FILE ''HELV.B.FON'' MUST BE ON THE DEFAULT DISK'
        END IF
      END IF
      IF(SETFONT(FON1$).NE.0)THEN
        WRITE(*,*)' ERROR cannot set font'
        STOP
      END IF

C
C*****OPEN THE DATA FILE*****
C
      CALL GETARG(INT2(1),filn$,lh)
      if(lh.le.1)then
        write(*,*) 'enter filename and path of data file'
        read(*, '(a)')filn$
      end if
1 close (2)
      open(2,file=filn$,form='BINARY',IOSTAT=IER,ERR=990,MODE='READ',
        *STATUS='OLD')

C
C*****OPEN THE PRINTER FILE*****
C
      OPEN(3,FILE='LPT1')

C
C
C*****READ IN THE DATA AND THE PICTURE ELEMENTS*****
C
      READ(2,END=991,ERR=992,IOSTAT=IER)HEAD$,PICTURE$

C
C*****PRINT OUT THE CONSTANTS TO THE PRINTER*****
C
2 write(*,*)' ENTER 1 FOR PRINTING OUT THE CONSTANTS'
  write(*,*)' ENTER 0 FOR NOT PRINTING OUT THE CONSTANTS'
  read(*,*) II
  WRITE(*,*)' DO YOU WISH TO CHANGE ANY OF THE VARIABLES? (Y/N)'
  READ(*, '(A1)')NU$
  IF(NU$.NE.'Y'.AND.NU$.NE.'y')GO TO 4
3 WRITE(*, '(' THE FOLLOWING IS A LIST OF VARIABLES THAT MAY BE CHAN
+GED.'/' TYPE &LIST1 <ENTER> TO IDENTIFY THE LIST OF VARIABLES.'
+/'/' TYPE THE VARIABLE NAME FOLLOWED BY - THEN TYPE THE NEW VALUE.'
+/'/' AFTER THE LAST ENTRY TYPE / <ENTER> TO END THE ENTRIES.'')
  WRITE(*, '(' DLEVEL (THE LEVEL OFFSET) = ',1PD10.3')DLEVEL
  WRITE(*, '(' EMISS (THE EMISSIVITY OF TARGET) = ',1PD10.3')EMISS
  WRITE(*, '(' AEMISS (AREA EMISSIVITY) = ',1PD10.3')AEMISS
  WRITE(*, '(' OD (OBJECT DISTANCE) = ',1PD10.3')OD
  WRITE(*, '(' CT (ESTIMATED TRANSMISSION) = ',1PD10.3')CT

```

```

WRITE(*,'(' AT (ATMOSPHERIC TEMPERATURE) - ',' ,1PD10.3)')AT
WRITE(*,'(' ATM (AMBIENT TEMPERATURE) - ',' ,1PD10.3)')AMT
READ(*,LIST1)
WRITE(*,'(' DLEVEL (THE LEVEL OFFSET) - ',' ,1PD10.3)')DLEVEL
WRITE(*,'(' EMISS (THE EMISSIVITY OF TARGET) - ',' ,1PD10.3)')EMISS
WRITE(*,'(' AEMISS (AREA EMISSIVITY) - ',' ,1PD10.3)')AEMISS
WRITE(*,'(' OD (OBJECT DISTANCE) - ',' ,1PD10.3)')OD
WRITE(*,'(' CT (ESTIMATED TRANSMISSION) - ',' ,1PD10.3)')CT
WRITE(*,'(' AT (ATMOSPHERIC TEMPERATURE) - ',' ,1PD10.3)')AT
WRITE(*,'(' ATM (AMBIENT TEMPERATURE) - ',' ,1PD10.3)')AMT
4 IF(II.EQ.1) THEN
    WRITE(3,'(6X,' IMAGE VERSION - ',' ,I2)') IMGVER
    WRITE(3,'(6X,' PROGRAM VERSION$ - ',' ,A6)') PGMVER$
    WRITE(3,'(6X,' ORIGIN - ',' ,I2)') JORIGIN
    WRITE(3,'(6X,' IMAGE IDENTITY - ',' ,A13)') IMAGEID$
    WRITE(3,'(6X,' IMAGE DRIVE$ - ',' ,A2)') IMAGEDR$
    WRITE(3,'(6X,' MISSING BYTES - ',' ,A36)') MISSING$
    WRITE(3,'(6X,' COMMENTS - ',' ,A401)') COMMENT$
    WRITE(3,'(6X,' PREPROCESSOR - ',' ,I2)') KPREP
    WRITE(3,'(6X,' MAGNIFICATION FACTOR - ',' ,D11.4)') FACTOR
    WRITE(3,'(6X,' SIGNAL AMPLIFICATION - ',' ,I2)') ISIGAMP
    WRITE(3,'(6X,' MANIPULATED IMAGE - ',' ,L7)') MANIMAG
    WRITE(3,'(6X,' SNAPSHOT - ',' ,L7)') SNAPSHOT
    WRITE(3,'(6X,' DIFFERENCE IMAGE - ',' ,L7)') DIFIMAG
    WRITE(3,'(6X,' DATE - ',' ,3I3)') IDATE
    WRITE(3,'(6X,' TIME - ',' ,4I3)') ITIME
    WRITE(3,'(6X,' TITLE - ',' ,A46)') TITLE$
    WRITE(3,'(6X,' SCANNER - ',' ,A13)') SCANNER$
    WRITE(3,'(6X,' FIELD OF VIEW - ',' ,A5)') FOV$
    WRITE(3,'(6X,' APERTURE - ',' ,A4)') APER$
    WRITE(3,'(6X,' FILTER - ',' ,A4)') FILTER$
    WRITE(3,'(6X,' R - ',' ,D11.4)') R
    WRITE(3,'(6X,' B - ',' ,D11.4)') B
    WRITE(3,'(6X,' F - ',' ,D11.4)') F
    WRITE(3,'(6X,' DCAL - ',' ,D11.4)') DCAL
    WRITE(3,'(6X,' ALPHA - ',' ,D11.4)') ALPHA
    WRITE(3,'(6X,' BETA - ',' ,D11.4)') BETA
    WRITE(3,'(6X,' DLEVEL - ',' ,D11.4)') DLEVEL
    WRITE(3,'(6X,' EMISSIVITY - ',' ,D11.4)') EMISS
    WRITE(3,'(6X,' AREA EMISSIVITY - ',' ,D11.4)') AEMISS
    WRITE(3,'(6X,' OBJECT DISTANCE - ',' ,D11.4)') OD
    WRITE(3,'(6X,' COMPUTED TRANSMISSION - ',' ,D11.4)') CT
    WRITE(3,'(6X,' ESTIMATED TRANSMISSION - ',' ,D11.4)') ET
    WRITE(3,'(6X,' ATMOSPHERE TEMP - ',' ,D11.4)') AT
    WRITE(3,'(6X,' AMBIENT TEMP - ',' ,D11.4)') AMT
    WRITE(3,'(6X,' DIFFP - ',' ,D11.4)') DIFFP
    WRITE(3,'(6X,' DIFFQ - ',' ,D11.4)') DIFFQ
    WRITE(3,'(6X,' LEVEL - ',' ,D11.4)') LEVEL
    WRITE(3,'(6X,' RANGE - ',' ,D11.4)') RANGE
    WRITE(3,'(6X,' UNDERFLOW - ',' ,L7)') UNDERF
    WRITE(3,'(6X,' OVERFLOW - ',' ,L7)') OVERF
END IF

```

C

C\*\*\*\*\*CONVERT FROM BYTE FORMAT TO INTEGER FORMAT\*\*\*\*\*

C

```

MIN=512
MAX=0
DO I=1,19600
    J=2*((I-1)/140+1)
    IF(J.GT.140)J=J-141

```

```

      K=MOD((I-1),140)+1
      L=IPIX(I)
      IF(L.LT.0)L=L+256
      IF(L.LT.MIN)MIN=L
      IF(L.GT.MAX)MAX=L
      IMAGE(J,K)=L
    END DO
  C
  C*****FIND MAXIMUM AND MINIMUM TEMPERATURES*****
  C
    pix=range*(float(min)-128.)/254.0+level+dlevel
    PIX1=PIX
    P1=EMISS*CT
    P2=(1-EMISS)/EMISS
    IAMB=R/(EXP(B/AMT)-F)
    P3=1.0D0-CT
    IATM=R/(exp(B/AT)-F)
    IOMIN=PIX/P1-P2*IAMB-P3/P1*IATM
    t1=b/alog(abs((r/IOMIN+f)))-273.15
    pix=range*(float(max)-128.)/254.0+level+dlevel
    PIX2=PIX
    IOMAX=pix/P1-P2*IAMB-P3/P1*IATM
    t2=b/alog(abs((r/IOMAX+f)))-273.15
    IF(II.EQ.1)THEN
      WRITE(3,'(A)')' '
      WRITE(3,'(6X,'' P1                - ''',1PE11.3)')P1
      WRITE(3,'(6X,'' P2                - ''',1PE11.3)')P2
      WRITE(3,'(6X,'' P3                - ''',1PE11.3)')P3
      WRITE(3,'(6X,'' AMT              - ''',1PE11.3)')AMT
      WRITE(3,'(6X,'' AT                - ''',1PE11.3)')AT
      WRITE(3,'(6X,'' IAMB              - ''',1PE11.3)')IAMB
      WRITE(3,'(6X,'' IATM              - ''',1PE11.3)')IATM
      WRITE(3,'(6X,'' MINIMUM PIXEL VALUE - ''',I4)')MIN
      WRITE(3,'(6X,'' MAXIMUM PIXEL VALUE - ''',I4)')MAX
      WRITE(3,'(6X,'' IPIXMIN           - ''',1PE11.3)')PIX1
      WRITE(3,'(6X,'' IPIXMAX           - ''',1PE11.3)')PIX2
      WRITE(3,'(6X,'' IOMIN             - ''',1PE11.3)')IOMIN
      WRITE(3,'(6X,'' IOMAX             - ''',1PE11.3)')IOMAX
      WRITE(3,'(6X,'' MINIMUM TEMPERATURE - ''',F9.2)')T1
      WRITE(3,'(6X,'' MAXIMUM TEMPERATURE - ''',F9.2)')T2
      WRITE(3,'(A)')' '
      WRITE(3,'(A)')' '//CHAR(12)//' '
      CLOSE (3)
    ENDIF
    IF(OVERF)THEN
      WRITE(*,'('' MAX TEMP - ''',F9.2,'' OVERFLOW OCCURED'')')T2
    ELSE
      WRITE(*,'('' MAXIMUM TEMPERATURE - ''',F9.2)')T2
    ENDIF
    IF(UNDERF)THEN
      WRITE(*,'('' MIN TEMP - ''',F9.2,'' UNDERFLOW OCCURED'')')T1
    ELSE
      WRITE(*,'('' MINIMUM TEMPERATURE - ''',F9.2)')T1
    END IF
  C
  C*****INPUT TEMPERATURE THRESHOLD AND DIFFERENCE*****
  C
    31 WRITE(*,*)' ENTER TEMPERATURE THRESHOLD LEVEL (DEG. C)'
      write(*,*)' ENTER 1000 TO STOP'
      write(*,*)' ENTER 2000 TO READ IN A NEW FILE'

```

```

WRITE(*,*)' ENTER 3000 TO CHANGE VARIABLES'
READ(*, '(a)')ans$
if(ans$.eq.' ')then
    tLD=(T2-T1)/11.
    ttl=(t1 + tld)
else
    read(ans$, '(f6.0)')ttl
    IF(TTL.GT.2999.)GO TO 3
    IF(TTL.GT.2999.)GO TO 2
    IF(TTL.GE.1999.0)GO TO 993
    IF(TTL.GT.999.0) STOP
    WRITE(*, '( ' ENTER TEMPERATURE DIFFERENCE (DEG. C) ' )')
    READ(*,*)TLD
endif
flg=.false.

C
C*****GRAPHICS SECTION*****
C
    CALL GRAPHICSMODE(SCREEN, CLRFLG, MAXX, MAXY)
    DUMMY=SETCOLOR(int2(15))
    L0=150
    L1=50
    L2=576
    L3=335

C
C*****DRAW BORDER AROUND PICTURE AREA*****
C
    DUMMY=RECTANGLE($GBORDER, L0, L1, L2, L3)
    DO I=0,140,10
        DO J=1,4
            DUMMY= SETPIXEL(3*I+L0,L1-J)
            DUMMY= SETPIXEL(3*I+L0,L3+J)
        END DO
    END DO
    DO I=1,2
        DO J=0,140,10
            DUMMY= SETPIXEL(L0-I,2*J+L1)
            DUMMY= SETPIXEL(L2+I,2*J+L1)
        END DO
    END DO

C
C*****CALCULATE TEMPERATURES REPRESENTED BY DIFFERENT COLORS****
C
    L1=228
    do i = 1,10
        L4=5
        L1=L1-16
        CALL MOVETO(L4,L1,S)
        T=TTL+FLOAT(I-1)*TLD
        IF(I.EQ.1)THEN
            WRITE(LINE$, '( '<' ',F6.2)')T
        ELSEIF(I.EQ.10)THEN
            WRITE(LINE$, '( '>' ',F6.2)')T
        ELSE
            WRITE(LINE$, '( ' ' ',F6.2)')T
        ENDIF
        DUMMY = SETCOLOR(INT2(15))
        CALL OUTGTEXT(LINE$)
        L6=74
        L7=L1 - 6
    
```

```

      L8=L6+40
      L9=L1+4
      DUMMY = SETCOLOR(IC(I))
      DUMMY=RECTANGLE($GFILLINTERIOR,L6,L7,L8,L9)
      IU(I)=R/(EXP(B/(T+273.15))-F)

      END DO

C
C*****PRINT OUT HEADING INFORMATION*****
C
      call settextposition(int2(1),int2(10),s)
      call outtext(' IMAGE NUMBER = '//IMAGEID$)
      call settextposition(int2(2),int2(10),s)
      CALL OUTTEXT(' FOV = '//FOV$//'          APERTURE = '//APER$)
      CALL SETTEXTPOSITION(INT2(3),INT2(10),S)
      CALL OUTTEXT(' WAVELENGTH = '//SCANNER$//' FILTER = '//FILTER$)
      IF(OVERF)THEN
        CALL SETTEXTPOSITION(INT2(22),INT2(1),S)
        CALL OUTTEXT('OVERFLOW')
      ENDIF
      IF(UNDERF)THEN
        CALL SETTEXTPOSITION(INT2(23),INT2(1),S)
        CALL OUTTEXT('UNDERFLOW')
      ENDIF

C
C*****PLOT OUT PICTURE IN FALSE COLORS*****
C
      DO I=1,140
        DO J=1,140
          IOI=range*(image(i,j)-128.)/254.0+level+dlevel
          PIX=(IOI/P1-P2*IAMB-P3/P1*IATM)
          IF(PIX.LT.IU(1))THEN
            LC=0
          ELSE IF(PIX.LT.IU(2))THEN
            LC=1
          ELSE IF(PIX.LT.IU(3)) THEN
            LC=9
          ELSE IF(PIX.LT.IU(4))THEN
            LC=2
          ELSE IF(PIX.LT.IU(5)) THEN
            LC=10
          ELSE IF(PIX.LT.IU(6))THEN
            LC=5
          ELSE IF(PIX.LT.IU(7)) THEN
            LC=4
          ELSE IF(PIX.LT.IU(8))THEN
            LC=13
          ELSE IF(PIX.LT.IU(9)) THEN
            LC=6
          ELSE IF(PIX.LT.IU(10))THEN
            LC=14
          ELSE
            LC=15
          end if
          LO=50+2*I
          LI=LO+1
          L2=150+3*J
          L3=L2+2
          JPIX(J,I)=LC
          DUMMY=SETCOLOR(LC)
        
```

```

        DO IP=L0,L1
          DO JP=L2,L3
            DUMMY=SETPIXEL(JP,IP)
          END DO
        END DO
      END DO
    END DO
  END DO
C
C
C*****FIND TEMPERTURE AT A SELECTED POINT OR AVERAGED IN A BOX****
C      INITIALIZATION OF CROSS AND BOX
C
C
      j2=70
      i2=70
      FLG = .FALSE.
      CALL CROSS(FLG,I2,J2,I3,J3,JPIX)
      PIX=RANGE*(FLOAT(IMAGE(I2,J2))-128.)/254.+LEVEL + DLEVEL
      IO=PIX/P1-P2*IAMB-IATM*P3/P1
      T=B/ALOG(ABS(R/IO+F))-273.15
      CALL SETTEXTPOSITION(INT2(18),INT2(1),S)
      WRITE(TEXT$,'(''T = ''',F6.2)')T
      CALL OUTTEXT(TEXT$)
      J=1
      I=1
      L=140
      K=140
      FLG=.FALSE.
      CALL BOX(FLG,I,J,K,L,I1,J1,K1,L1,JPIX)
      ISUM=0
      JSUM=0
      DO KK=J,L
        DO LL = I,K
          JSUM=JSUM+1
          ISUM=ISUM+IMAGE(LL,KK)
        END DO
      END DO
      PIX=RANGE*(FLOAT(ISUM)/FLOAT(JSUM)-128.)/254.+LEVEL+DLEVEL
      IO=PIX/P1-P2*IAMB-IATM*P3/P1
      T=B/ALOG(ABS(R/IO+F))-273.15
      CALL SETTEXTPOSITION(INT2(20),int2(1),s)
      WRITE(TEXT$,'(''TA = ''',F6.2)')T
      CALL OUTTEXT(TEXT$)
      CALL SETTEXTPOSITION(INT2(21),int2(1),s)
      WRITE(FIL$,'(4I4)')J,I,L,K
      CALL OUTTEXT(FIL$)
      GO TO 61
C
C*****FIND TEMPERTURE AT A SELECTED POINT *****
C
      60 CALL WAIT(INT2(50))
      61 M1=11
      CALL MOUSEL(M1,M2,M3,M4)
      j2=j2+m3
      i2=i2+m4
      if(i2.lt.6)i2=6
      if(i2.gt.134)i2=134
      if(j2.lt.5)j2=5
      if(j2.gt.136)j2=136
      call settetxtposition(int2(19),int2(1),s)

```

```

write(LINE8$, '(214)')J2,12
CALL OUTTEXT(LINE8$)
CALL CROSS(FLG,I2,J2,I3,J3,JPIX)
PIX=RANGE*(FLOAT(IMAGE(I2,J2))-128.)/254.+LEVEL+DLEVEL
IO=PIX/P1-P2*IAMB-IATM*P3/P1
T=B/ALOG(ABS(R/IO+F))-273.15
CALL SETTEXTPOSITION(INT2(18),int2(1),s)
WRITE(TEXT$,'(''T - ''',F6.2)')T
CALL OUTTEXT(TEXT$)
m1=3
call mouse1(m1,m2,m3,m4)
m1=99
GOTO (61,70,80,90),M2+1
70 CALL WAIT(INT2(100))
71 M1=11
CALL MOUSEL(M1,M2,M3,M4)
I=I+M4
J=J+M3
IF(I.LT.1)I=1
IF(J.LT.1)J=1
IF(I.GE.K)I=K-1
IF(J.GE.L)J=L-1
CALL BOX(FLG,I,J,K,L,I1,J1,K1,L1,JPIX)
ISUM=0
JSUM=0
DO KK=J,L
  DO LL = I,K
    JSUM=JSUM+1
    ISUM=ISUM+IMAGE(LL,KK)
  END DO
END DO
PIX=RANGE*(FLOAT(ISUM)/FLOAT(JSUM)-128.)/254.+LEVEL+DLEVEL
IO=PIX/P1-P2*IAMB-IATM*P3/P1
T=B/ALOG(ABS(R/IO+F))-273.15
CALL SETTEXTPOSITION(INT2(20),int2(1),s)
WRITE(TEXT$,'(''TA - ''',F6.2)')T
CALL OUTTEXT(TEXT$)
CALL SETTEXTPOSITION(INT2(21),int2(1),s)
write(FIL$,'(4I4)')J,I,L,K
CALL OUTTEXT(FIL$)
M1=3
CALL MOUSEL(M1,M2,M3,M4)
M1=99
GO TO (71,60,80,90),M2+1
80 CALL WAIT(INT2(100))
81 M1=11
CALL MOUSEL(M1,M2,M3,M4)
K=K+M4
L=L+M3
IF(K.GT.140)K=140
IF(K.LE.1)K=I+1
IF(L.GT.140)L=140
IF(L.LE.J)L=J+1
CALL BOX(FLG,I,J,K,L,I1,J1,K1,L1,JPIX)
ISUM=0
JSUM=0
DO KK=J,L
  DO LL=I,K
    JSUM=JSUM+1
    ISUM=ISUM+IMAGE(LL,KK)
  END DO
END DO

```



```

        END DO
    END DO
    PIX-RANGE*(FLOAT(ISUM)/FLOAT(JSUM)-128.0)/254.0+LEVEL+DLEVEL
    IO=PIX/P1-P2*IAMB-IATM*P3/P1
    T=B/ALOG(ABS(R/IO+F))-273.15
    CALL SETTEXTPOSITION(INT2(20),INT2(1),S)
    WRITE(TEXT$,'('TA - ',F6.2)')T
    CALL OUTTEXT(TEXT$)
    CALL SETTEXTPOSITION(INT2(21),INT2(1),S)
    WRITE(FIL$,'(4I4)')J,I,L,K
    CALL OUTTEXT(FIL$)
    M1=3
    CALL MOUSEL(M1,M2,M3,M4)
    M1=99
    GO TO (81,60,70,90),M2+1

C
C
C*****CALL THE END OF PLOT AND GO BACK TO TEMPERATURE ENTRY*****
C
C
90  CALL ENDPLOTIT(CLRFLG)
    if(m1.eq.0)stop 'ERROR YOU MUST LOAD THE MOUSE DRIVER FIRST'
    GO TO 31

C
C
C*****ERROR RECOVERY SECTION*****
C
C
990  write(*,*)' CANNOT FIND '//FILN$
    GO TO 993
991  WRITE(*,*)' UNEXPECTED END OF FILE FOUND IN '//FILN$
    GO TO 993
992  WRITE(*,*)' CANNOT OPEN '//FILN$
993  WRITE(*,*)' ENTER NEW PATH AND FILE NAME. NULL ENTRY TO STOP'
    READ(*,'(A)')FILN$
    IF(FILN$.EQ.' ') STOP
    GO TO 1

C
C
C
C
    end

C
C*****GRAPHICS SUBROUTINE*****
C
C
    subroutine graphicsmode(screen,clrflg,maxx,maxy)
    include 'd:\include\fgraph.fd'
    record /videoconfig/ screen
    integer*2 dummy,maxx,maxy
    logical*2 clrflg
    clrflg = .true.
    call getvideoconfig(screen)
    select case(screen.adapter)
        case ($cga,$ocga)
            dummy = setvideomode($mres4color)
        case ($ega,$oega)
            dummy = setvideomode($erescolor)
        case ($vga,$ovga)
            dummy = setvideomode($vres16color)
    end select
end subroutine

```

```

case ($hgc)
  dummy = setvideomode($hercmono)
  clrflg=.false.
case default
  dummy = 0
end select
if(dummy.eq.0) then
  write(*,*) ' ERROR - - CANNOT SET GRAPHICS MODE!!'
  WRITE(*,*) ' If you have a Hercules mono card you must run the'
  write(*,*) ' MSHERC.COM program first.'
  stop
end if
call getvideoconfig(screen)
maxx = screen.numxpixels - 1
maxy = screen.numypixels - 1
return
end

```

C  
C  
C  
C

```

subroutine endplotit(clrflg)
include 'd:\INCLUDE\fgraph.fd'
integer*2 dummy
logical*2 clrflg
if(clrflg)then
  dummy = setvideomode($textc80)
else
  dummy = setvideomode($defaultmode)
end if
return
end

```

C  
C  
C  
C

C\*\*\*\*\*SUBROUTINE TO DRAW A CROSS ON THE SCREEN\*\*\*\*\*

```

SUBROUTINE CROSS(FLG,I,J,I1,J1,JPIX)
INCLUDE 'd:\include\FGRAPH.FD'
INTEGER*2 I,J,I1,J1,DUMMY,K,L0,L1,L2,J2,I2
INTEGER*2 JPIX(140,140)
LOGICAL*2 FLG
if(fl)then
  DO K=1,20
    L0=141 + 3*I1 + K
    L1=51 + 2*I1
    J2=(L0-150)/3
    DUMMY=SETCOLOR(JPIX(J2,I1))
    DUMMY=SETPIXEL(L0,L1)
    L0=151+3*I1
    L1=41+2*I1+K
    L2=L0+1
    I2=(L1-50)/2
    DUMMY=SETCOLOR(JPIX(J1,I2))
    DUMMY=SETPIXEL(L0,L1)
  END DO
END IF
DUMMY=SETCOLOR(INT2(7))
DO K=1,20
  L0=141+3*I+K

```

```

L1=51+2*I
L2=L1+1
DUMMY-SETPIXEL(LO,L1)
LO=151+3*J
L1=41+2*I+K
L2=LO+1
DUMMY-SETPIXEL(LO,L1)
END DO
FLG=.TRUE.
I1=I
J1=J
RETURN
END

```

C  
C  
C  
C

C\*\*\*\*\*SUBROUTINE TO DRAW A BOX OR RECTANGLE ON THE SCREEN\*\*\*\*\*

```

SUBROUTINE BOX(FLG,I,J,K,L,I1,J1,K1,L1,JPIX)
INCLUDE 'D:\INCLUDE\FGRAPH.FD'
INTEGER*2 I,J,K,L,M,N,I1,J1,K1,L1,LLO,LL1,LL2,J2,I2,DUMMY
INTEGER*2 JPIX(140,140)
LOGICAL*2 FLG
IF(FLG)THEN
  DO M=3*J1-2,3*L1-1
    LLO=153+M
    LL1=51+2*I1
    J2=(M+3)/3
    LL2=LL1+1
    DUMMY-SETCOLOR(JPIX(J2,I1))
    DUMMY-SETPIXEL(LLO,LL1)
    LL1=51+2*K1
    LL2=LL1+1
    DUMMY-SETCOLOR(JPIX(J2,K1))
    DUMMY-SETPIXEL(LLO,LL1)
  END DO
  DO N=2*I1,2*K1-3
    LLO=151+3*J1
    LL1=LLO+1
    I2=(N+3)/2
    LL2=53+N
    DUMMY-SETCOLOR(JPIX(J1,I2))
    DUMMY-SETPIXEL(LLO,LL2)
    LLO=151+3*L1
    LL1=LLO+1
    DUMMY-SETCOLOR(JPIX(L1,I2))
    DUMMY-SETPIXEL(LLO,LL2)
  END DO
END IF
DUMMY-SETCOLOR(INT2(7))
DO M=3*J-2,3*L-1
  LLO=153+M
  LL1=51+2*I
  LL2=LL1+1
  DUMMY-SETPIXEL(LLO,LL1)
  LL1=51+2*K
  LL2=LL1+1
  DUMMY-SETPIXEL(LLO,LL1)
END DO

```

```

DO N=2*I,2*K-3
  LLO=151+3*I
  LL1=LL0+1
  LL2=53+N
  DUMMY=SETPIXEL(LL0,LL2)
  LLO=151+3*L
  LL1=LL0+1
  DUMMY=SETPIXEL(LL0,LL2)
END DO
FLG=.TRUE.
I1=I
J1=J
K1=K
L1=L
RETURN
END

C
C
C SUBROUTINE TO WAIT OR KILL TIME
C
C
C SUBROUTINE WAIT(K)
C   INTEGER*2 I,J,K
C   REAL*4 X
C   DO I=1,K
C     DO J=1,100
C       X=SQRT(FLOAT(I)**2+FLOAT(J)**2)
C     END DO
C   END DO
C   RETURN
C
C
C
C
C   END

```

## **APPENDIX E**

### **EMISSIVITY MEASUREMENTS OF THE RESEARCH VESSEL *POINT SUR***

#### **A. INTRODUCTION**

In order to measure the emissivity of the paint surface of the R/V *Point Sur*, a series of calibrated thermistors were installed at various locations on the skin of the ship [Figure E.1]. The thermistors were connected to a portable COMPAQ-III computer that recorded voltage values converted to temperatures at 20-second intervals. On May 8, 1990, the ship was in port at the Moss Landing Research Station and the AGEMA Thermovision Camera was positioned approximately 10 yards away. A series of images were taken of the thermistor locations on the starboard side of the ship. The AGEMA thermal temperatures along with the thermistor temperatures are listed in Table E.1.

#### **B. TEMPERATURE MEASUREMENT**

The thermistors numbered 3.0, 1.0, and 1.1 are attached to the metal of the ship's hull and 4.1 is attached to the paint. They are held on to the ship by a conducting epoxy glue and covered with tape. The thermistor is very easy to pick out on the AGEMA thermal image [Figure E.2] and the average temperature value is read from the area closest to it which is the skin or paint of the ship.

The thermistors were calibrated at the Oceanography Department calibration bath which is accurate to  $\pm 5$  millidegrees. The calibrations are shown in Table E.2 along with linear regression formulas used to convert the thermistor values to actual temperatures.

### C. EMISSIVITY MEASUREMENT

The recently calibrated AGEMA camera has a default value of 1.00 for the emissivity input and all temperatures were recorded in this mode. In Table E.1, the actual thermistor temperatures are compared to the AGEMA thermal imaging temperatures. The temperatures measured with the AGEMA camera were lower than the skin temperature of the ship proving the emissivity was actually lower than 1.00. The still mode image function of the AGEMA camera, which allows the default values in the system to be changed, was used to lower the emissivity in steps of .01 until a temperature reading corresponded to the thermistor or actual skin temperature of the ship. The last column in Table E.2 shows that an emissivity of .97 is a very close approximation to the actual emissivity of the ship's surface.

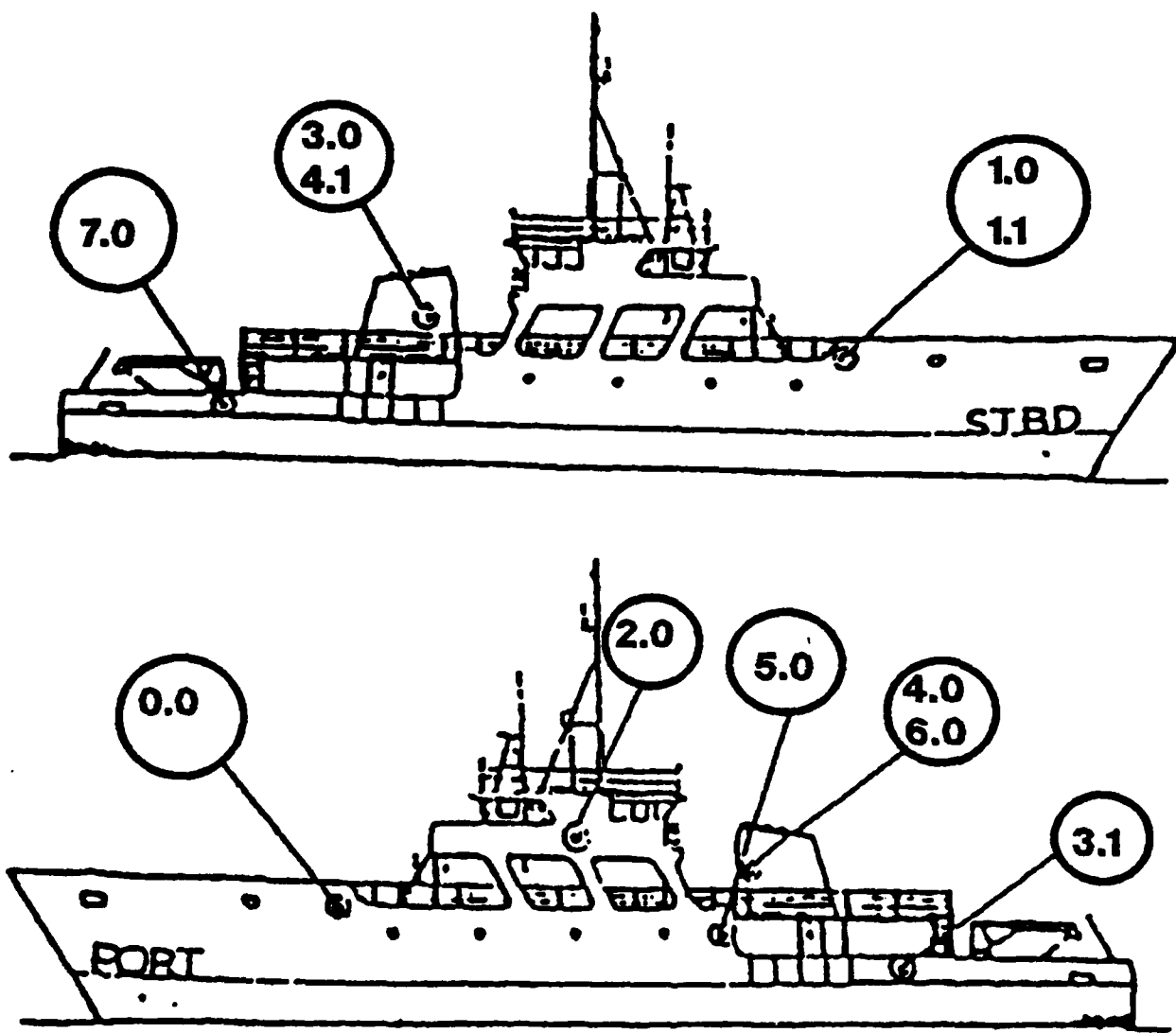


Figure E.1: May 1990 thermistor locations on the R/V *Point Sur*.

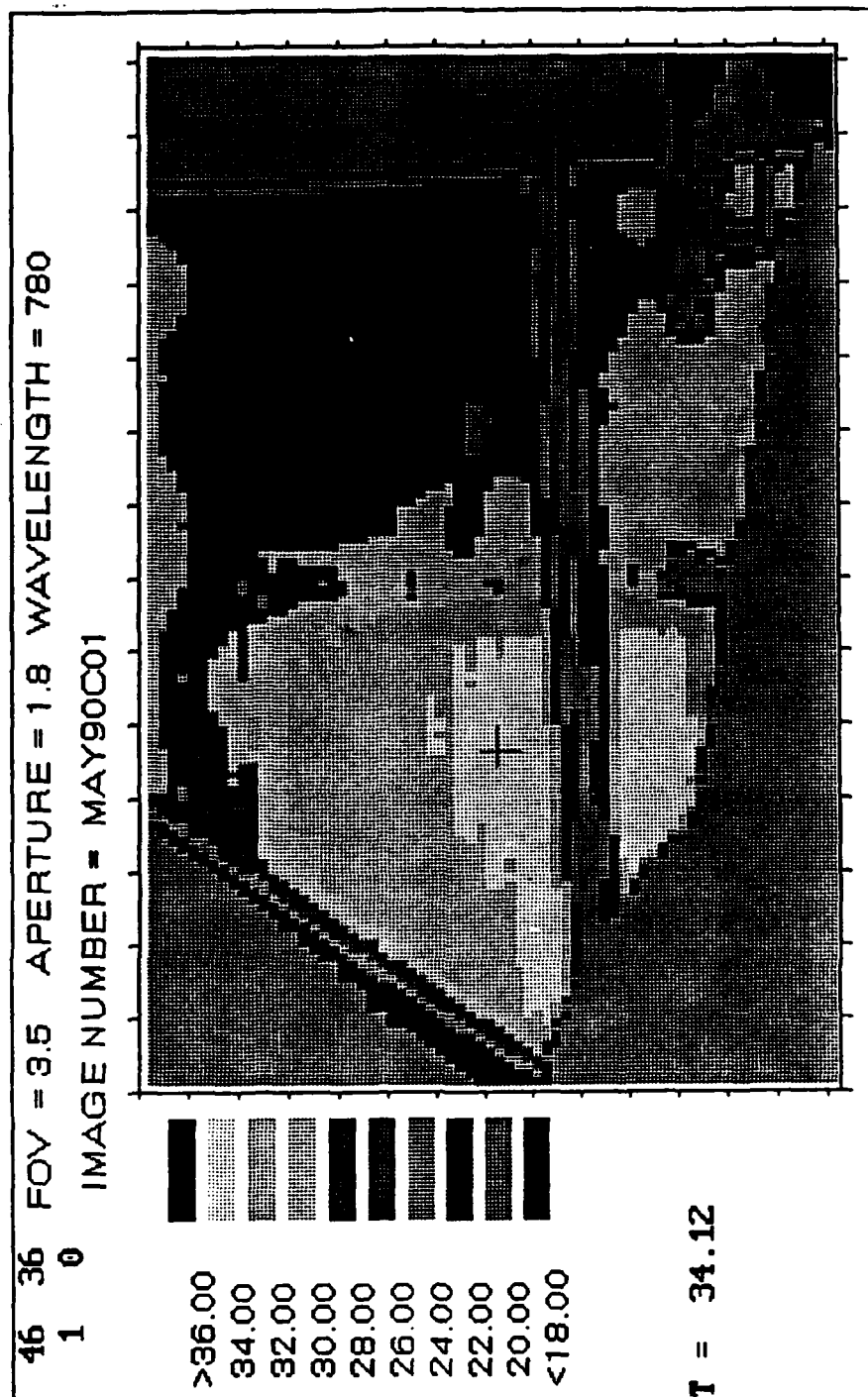


Figure E.2: AGACATS image showing location of Thermistor aboard the R/V *Point Sur*.



Table E.1

Thermistor Data From The R/V *Point Sur*, May 8, 1990

Time	Image No.	Sensor No.	Location	Temp. of Ship's Hull	Temp. of Thermistor	(Regression) Corrected Temp. of Thermistor	AGEMA Camera Temp. of Ship's Hull
				(°C) AGEMA camera	(°C) Ship's Hull	(°C) Ship's Hull	(Emissivity: .97)
17:12.11	2	(3.0)	stack	(22.0)	(21.414)	(22.11)	(22.1)
17:13.36	3	(3.0)	stack	(22.1)	(21.545)	(22.25)	(22.2)
17:22.04	9	(1.0)	starboard bow	(22.1)	(21.611)	(22.24)	(22.2)
17:25.19	10	(1.0, 1.1)	starboard bow	(22.2, 23.7)	(21.6767, 23.151)	(22.31, 23.84)	(22.3, 23.8)
17:26.21	11	(1.0, 1.1)	starboard bow	(22.1, 23.8)	(21.589, 23.217)	(22.31, 23.84)	(22.2, 23.9)
17:26.53	12	(1.0, 1.1)	starboard bow	(22.1, 23.7)	(21.524, 23.151)	(22.16, 23.84)	22.2, 23.8)
17:27.47	13	(1.0)	starboard bow	(22.1)	(21.655)	(22.29)	(22.2)
17:28.54	14	(3.0, 4.1)	stack	(22.1, 22.7)	(21.414, 22.073)	(22.11, 22.77)	(22.2, 22.8)
17:31.04	15	(3.0, 4.1)	stack	(22.3, 22.1)	(21.765, 21.501)	(22.46, 22.20)	(22.4, 22.2)
17:34.42	18	(1.0)	starboard bow	(22.4)	(21.874)	(22.51)	(22.5)
17:35.38	19	(1.0, 1.1)	starboard bow	(22.1, 22.2)	(21.545, 21.611)	(22.18, 22.31)	(22.2, 22.3)
17:36.11	20	(1.0, 1.1)	starboard bow	(22.1, 22.2)	(21.634, 21.699)	(22.27, 22.40)	(22.2, 22.3)

Table E.2

Thermistor Calibration Tables and Linear Regression Formulas for the  
May Cruise on the R/V *Point Sur*.

	ACTUAL TEMPERATURE (C)	THERMISTOR #1.0	THERMISTOR #3.0	THERMISTOR #1.1
1	4.0	4.718872	4.838959	4.759918
2	7.0	7.677216	7.788605	7.720429
3	10.0	10.650880	10.756960	10.684390
4	13.0	13.626250	13.725430	13.654450
5	16.0	16.609190	16.700900	16.634370
6	19.0	19.600280	19.688110	19.619140
7	22.0	22.592320	22.677090	22.605870
8	25.0	25.577760	25.659240	25.564060
9	28.0	28.630830	28.652410	28.589600
10	31.0	31.614230	31.650970	31.589050
11	34.0	34.632450	34.625400	34.592230
12	37.0	37.644010	37.658720	37.593510
13	40.0	40.630490	40.650420	40.588350

	THERMISTOR #4.1
1	4.947846
2	7.897949
3	10.848050
4	13.815520
5	16.794340
6	19.775090
7	22.751040
8	25.741670
9	28.731140
10	31.861150
11	34.992310
12	38.037930
13	40.872710

LINEAR REGRESSION FORMULAS

THERMISTOR # 1.0  $.99856(x) + .66278$

THERMISTOR # 3.0  $.99513(x) + .80496$

THERMISTOR # 1.1  $.99539(x) + .76550$

THERMISTOR # 4.1  $1.0014(x) + .81892$

## LIST OF REFERENCES

1. Naval Research Laboratory, Report 5816, *Emissivity as a Function of Surface Roughness: A Computer Model*, by I. B. Schwartz and D. Hon, 1986.
2. Naval Research Laboratory, Report 8311, *Fundamentals of Thermal Imaging Systems*, by G. L. Harvey and F. A. Rosell, 1979.
3. Ridgeway, M. G., *Evaluation and Application of a Sea Surface Emissivity Model for use in FLIR Tactical Decision Aids*, M.S. Thesis, Naval Postgraduate School, Monterey, CA, September 1988.
4. Psihogios, P. E., *Thermal Images of Sky and Sea-Surface Background Infrared Radiation*, M.S. Thesis, Naval Postgraduate School, Monterey, CA, December 1988.
5. Hudson, A. D., Jr., *Infrared Systems Engineering*, John Wiley and Sons, Inc., 1969.
6. Lloyd, J. M., *Thermal Imaging Systems*, Plenum Press, NY, 1975.
7. The AGA Thermovision 780 Operating Manual, AGEMA Corporation, Danderyd, Sweden.
8. AGEMA Infrared Systems, *CATS E 2.10 Operating Manual*, Pharos Company, NY, 1989.
9. Cox, C. and Munk, W., *Measurement and Roughness of the Sea Surface from Photographs of the Suns Glitter*, J. Optical Soc. Am., v. 44, 1954.
10. Shapiro, R., *Water Backgrounds in the Infrared (IR) and Visible (TV) Tactical Decision Aids*, ST Systems Corporation, August 31, 1987.
11. Sidran, M., *Broadband Reflectance and Emissivity of Specular and Rough Water Surfaces*, Applied Optics, v. 20, 15 September 1981.
12. Ontar Corporation, *PC-TRAN (Version 2)*, June 1987.
13. Integrated Sensors, Inc., *Blackbody Calculator V1.2*.
14. Chappell, A., *Optoelectronics, Theory and Practice*, McGraw-Hill Book Company, NY, 1978.

## INITIAL DISTRIBUTION LIST

	No. Copies
1. Defense Technical Information Center Cameron Station Alexandria, VA 22304-6145	2
2. Library, Code 52 Naval Postgraduate School Monterey, CA 93943-5002	2
3. Professor K. E. Woehler, Code PH Wh Chairman, Department of Physics Naval Postgraduate School Monterey, CA 93943-5000	2
4. Professor A. W. Cooper, Code PH Cr Department of Physics Naval Postgraduate School Monterey, CA 93943-5000	5
5. Commander, Naval Oceanographic & Atmospheric Research Laboratory (NOARL) Attn: John Cook & Mike Sierchio Naval Warfare Support Department Monterey, CA 93943-5006	1
6. The Johns Hopkins University Applied Physics Laboratory Attn: Dr. R. Steinberg Johns Hopkins Road Laurel, MD 20707	1
7. Georgia Tech Research Institute Georgia Institute of Technology Attn: K. R. Johnson & Morris Hetzler Electromagnetic Laboratory Atlanta, GA 30322	1

	No. Copies
8. Director, Research Administration, Code 012 Naval Postgraduate School Monterey, CA 93943	1
9. Superintendent Attn: Professor J. Sternberg, Code 73 Naval Postgraduate School Monterey, CA 93943-5000	2
10. Professor E. C. Crittenden, Jr., Code PH Ct Department of Physics Naval Postgraduate School Monterey, CA 93943-5000	1
11. Commander Attn: Mr. Herb Hughes, Code 543 Naval Ocean Systems Center San Diego, CA 95152	1
12. Commander, Naval Oceanographic & Atmospheric Research Laboratory (NOARL) Attn: Technical Library Naval Warfare Support Detachment Monterey, CA 93943-5000	1
13. Dr. P. L. Walker, Code PH Department of Physics Naval Postgraduate School Monterey, CA 93943-5000	1
14. Dr. E. Milne, Code PH Mn Department of Physics Naval Postgraduate School Monterey, CA 93943-5000	1

	No. Copies
15. Commander Naval Research Laboratory (NRL) Attn: Dr. I. B. Schwartz, Code 6522 Washington, DC 20375-5000	1
16. Commander Scott Air Force Base Attn: Captain Kim Carver (HQ AWS/DOZ) Belleville, IL 62225	1
17. AGEMA Infrared Systems Attn: Mr. Al Fudalli 108 Arena Street El Segundo, CA 90245	1
18. Commander COMPATWING 10 Attn: LCDR Coulter, Special Projects Asst. Code 311 Moffett Field, CA 94035	1
19. Commander Antisubmarine Warfare Operating Center (ASWOC) U. S. Naval Facility, Keflavik Iceland FPO NY 09751-0202	1
20. Commander Joint EW Center/SE Kelly Air Force Base San Antonio, TX 78243-5000	1
21. Gregory M. Lawler, LT/USN Fleet Air, Keflavik, Iceland Box 2, FPO New York 09751-0202	2